University of Alberta

A threshold model for development of the corpus callosum in normal and acallosal mice

by

Katherine Mary Bishop 

A thesis submitted to the Faculty of Graduate Studies and Research in partial fulfilment of the requirements for the degree of Doctor of Philosophy

Department of Psychology

Edmonton, Alberta

Fall 1997

University of Alberta

Library Release Form

Name of Author: Katherine Mary Bishop

Title of Thesis: A threshold model for development of the corpus callosum in normal and acallosal mice

Degree: Doctor of Philosophy

Year this Degree Granted: 1997

September 10/97

Katherine Bishop

Katherine Bishop
291 Cairnsmead Pl
Edmonton, AB T[illegible]

University of Alberta

Faculty of Graduate Studies and Research

The undersigned certify that they have read, and recommend to the Faculty of Graduate Studies and Research for acceptance, a thesis entitled "A threshold model for development of the corpus callosum in normal and acallosal mice" submitted by Katherine Mary Bishop in partial fulfilment of the requirements for the degree of Doctor of Philosophy.

Dr. D. Wahlsten (Supervisor)

Dr. D. Treit

Dr. A. Kingstone

Dr. J. Goldberg

Dr. F. Biddle (External)

Sept. 10/97

Date

ABSTRACT

Inbred mouse strains with defects of the cerebral commissures provide a useful model for investigation of the genetic and developmental mechanisms underlying normal and abnormal axon guidance across the telencephalic midline. Investigation of the critical events necessary for corpus callosum (CC) and hippocampal commissure (HC) formation and the relative timing of these events suggests a threshold model for development of the cerebral commissures.

The 129/ReJ and BALB/cWah1 inbred mouse strains and classical crosses between them were examined to establish thresholds for formation of the commissures. Recovery from retarded development of the commissures starts at about embryonic day 18 and is almost complete by the early postnatal period. However, there are thresholds of abnormality beyond which recovery does not occur. For the body weight range 0.5 to 1.0 g, an embryonic CC and HC index of .15 is the threshold for normal development of the CC and an index of 0 is the threshold for normal development of the HC. These thresholds magnify small variations in the embryo into macroscopic differences in the anatomy of the adult brain.

Recombinant inbred (RI) mouse strains formed from the 129 and BALB/c inbred strains that express more extreme forms of the callosal defect than either progenitor were examined to identify the critical events for commissure formation at the telencephalic midplane. Double labelling with lipophilic dyes indicated that timing of CC axon growth to midplane is normal. Severity of adult CC defects is related to HC formation. Extreme variability in certain strains in adult CC defects occurs when

HC formation is near threshold; delayed HC formation well beyond the threshold yields consistently abnormal commissures. Quantification of growth of the telencephalic midline in the coronal plane identified a severe defect in fusion of the longitudinal cerebral fissure that strongly correlated with the adult pattern of commissure defects in these strains. It is proposed that the floor of the interhemispheric fissure must rise to a critical level before HC and CC axons can cross midplane.

Therefore, agenesis of the CC and HC in inbred strains of mice results from an interaction between genetic influences, relative structural growth, and the inherently random nature of development.

ACKNOWLEDGEMENTS

This research was supported in part by Postgraduate Scholarships provided by the Natural Sciences and Engineering Research Council of Canada and a Dissertation Fellowship from the University of Alberta.

I would like to thank my supervisor, Dr. Doug Wahlsten, for his guidance and advice during the tenure of my graduate program. Doug provided laboratory facilities and equipment, plus all of the mice used in this study. His support is greatly appreciated.

Dr. Dallas Treit and Dr. Alan Kingstone were the other members of my supervisory committee. They provided valuable suggestions, support and a million letters of reference throughout the tenure of my program. Thank you both. I would like to thank Dr. Fred Biddle and Dr. Jeff Goldberg for agreeing to act as examiners in my thesis defense, and for making it such an enjoyable experience.

Violet Sparks has provided expert technical assistance over the years, for which I am greatly appreciative. I would also like to thank Dr. Dan Livy for showing me aspects of the lipophilic dye labelling procedure and Darwin Song for assistance with the sagittal measurements.

Most of all, I would like to thank my sister, Chris Bishop, and my mother, Margaret Bishop, for the enormous degree of support, encouragement and love they have given me throughout my life and especially in the past year and a half. It is their unfailing belief in me that is the source of my strength - a gift that I can never repay. I wish them success in attaining all that they dream of in their own lives.

Table of Contents

List of Tables

List of Figures

List of Abbreviations

AC - anterior commissure

ACA - anterior cerebral artery

BW - brain weight

CC - corpus callosum

CCHC - corpus callosum and hippocampal commissure

CCHCI - corpus callosum and hippocampal commissure index

CF - columns of the fornix

CNS - central nervous system

CPMB - crossing point to main bundle

DCF - dorsal comissure of the fornix

DSC - dorsal surface of the cortex

E - embryonic

F - fornix

HbC - habenular commissure

HC - hippocampal commissure

IG - indusium griseum

ISMB - injection site to main bundle

LF - longitudinal cerebral fissure

LFD - longitudinal cerebral fissure depth

LT - lamina terminalis

LV - lateral ventricle

MS - medial septum

NMDA - *N*-Methyl-D-aspartate

P - postnatal

PC - posterior commissure

PSFO - primordium of the subfornical organ

RI - recombinant inbred

VT - velum transversum

GENERAL INTRODUCTION

One primary issue in developmental neurobiology is the question of how precise patterns of axon growth are generated in the developing brain. Precision of growth of commissural axons that connect the two hemispheres of the brain is especially interesting because these axons typically travel long distances from their cells of origin in one hemisphere, traverse midline at a highly specific time and location, and then continue growing through the contralateral hemisphere to specified target locations. Examination of inbred mouse strains with defects of the corpus callosum (CC) provides a useful model for investigation of the genetic and developmental mechanisms underlying normal and abnormal axon guidance across the telencephalic midplane.

The corpus callosum is of special interest because it is by far the largest brain structure connecting the two cerebral hemispheres through the midline, containing an estimated 200 million nerve fibres in humans (Tomasch, 1954; Aboitiz et al., 1992). It contains primarily homotopic, reciprocal and topographically organized connections but has some heterotopic connections and is thus both a decussation as well as a commissure. Although the corpus callosum appears as an anatomically unitary structure, it is in fact functionally diverse. The anterior portion (genu) contains primarily fibres from the motor cortex, the posterior portion (splenium) contains mainly visual system fibres, and the remaining large body of the callosum includes mixed areas of auditory, somatosensory, and limbic connections (Lomber et al.,

1994). The CC also contains fibres of the claustrum and many fibres that connect the cerebral cortex with the ipsilateral thalamus, caudate nucleus, septum, and hypothalamus. What is referred to as the corpus callosum is, in fact, a collection of highly diverse and dynamic axon tracts. Formation of the corpus callosum is therefore especially interesting because axons from diverse regions of the cerebral cortex converge in a small area at the midsagittal plane where they traverse the telencephalic midline.

Normal postnatal development of the corpus callosum has been studied extensively in animals and is characterized by flexible developmental processes. Although synaptic terminals of CC axons are widely and diffusely distributed in the cerebral cortex at birth, many of these axons perish postnatally and eventually there are very few zones with CC connections interspersed among regions without callosal output (Innocenti et al., 1977; Ivy and Killacky, 1982; LaMantia and Rakic, 1990; Elberger, 1994a; Elberger 1994b). At least 70% of the axons originally produced are eliminated from the corpus callosum in development, in both monkeys and cats (LaMantia and Rakic, 1990; Aggoun and Innocenti, 1994), and the early postnatal restriction is thought to be due to elimination of axon collaterals rather than the death of callosally projecting neurons themselves (O'Leary et al., 1981). Callosally projecting neurons also undergo a striking dendritic remodelling during development (Koester and O'Leary, 1992). Gross anatomical parameters of the corpus callosum are known to be modifiable by early prenatal and postnatal environmental influences, such as hormone levels (Fitch et al., 1990) and environmental stimulation (Berrebi et

al., 1988). In addition, the response properties of neurons to their callosal input can be modified by experience even in adult animals (Milleret and Buser, 1993), although the structural bases for these changes, if any, remains unknown. About 90 to 95% of the callosal fibres are myelinated in adult humans, about 50% in the adult rat and cat, and about 86% in the adult monkey (Lent and Schmidt, 1993) and myelination of callosal axons from distinct cortical regions is thought to occur in a mosaic-like manner without following a continuous gradient (LaMantia and Rakic, 1990). Myelination of this axon tract is one of the last processes to be completed in brain development and may take place until about age 20 in humans (Cowell et al., 1992; Pujol et al., 1993). Overall, the normal postnatal development of the callosal phenotype is not narrowly pre-programmed but is instead a result of interactions between cortical neurons, the cellular environment, and signals from the sensory periphery.

At present, the normal functions of the CC are virtually unknown, although it is commonly thought that the corpus callosum acts in both specific functions such as coordination of hand movements and general abilities like the allocation of attention across modalities. Functional theories proposed may be classified into four groups. The homotopic excitatory theory states that homotopic modules primarily synchronize neuronal activity in the two hemispheres by conveying topographically bound information to the other side. The diffuse inhibitory theory suggests that widespread contralateral suppression of neuronal activity occurs in the corpus callosum. The nonspecific excitatory, or transcallosal "arousal theory", suggests that the corpus

callosum excites homotopic modules not for conveying specific information, but rather to "alert" them. Finally, the topographical inhibitory theory assumes contralateral inhibition of cortical modules, resulting in topographically organized complementary specialization of homotopic regions. It is also believed by some that the corpus callosum is responsible for or involved in cerebral lateralization through the inhibition of cortical regions during development (Lassonde et al., 1990). The diffuse inhibitory theory proposes that lateralization originates from rather subtle functional and morphological symmetries that are shaped and reinforced by callosal activity, the hemisphere better suited for a given task inhibiting large regions of the other in order to handle a given task without interference. The topographical inhibitory theory, on the other hand, attributes lateralization predominantly to callosal fibres that shape small, genuine functional symmetries of the hemispheres.

The large majority of callosal axons exerts direct excitatory actions on neurons of the contralateral hemisphere. Most neurons are pyramidal, most callosal axons make synapses of the asymmetric type, the majority of callosal axons use glutamate as their neurotransmitter and exert their postsynaptic effects by acting on both NMDA and non-NMDA receptors, and monosynaptic excitatory postsynaptic potentials are the most frequent responses elicited by callosal activation (as reviewed by Conti and Manzoni, 1994). However, recent evidence suggests that the callosal system is more complex than previously conceived and there is some evidence for the existence of a population of callosally projecting neurons whose effects may be inhibitory (as reviewed by Conti and Manzoni, 1994). Heterogeneity of the callosal system would

account for the excitatory and inhibitory functions of this system proposed from neuropsychological research.

In the animal world, lack of a corpus callosum does not necessarily mean abnormality. Among the vertebrates, only placental mammals typically possess a CC. In animals such as the platypus, the opossum, and the spiny anteater, direct communication between the hemispheres is possible through other commissural pathways such as the anterior commissure (AC). However, in mammals that normally possess a corpus callosum, agenesis of the corpus callosum is considered an abnormality. It is among one of the most common brain malformations observed in humans, with an estimated incidence of 0.0005 to 0.7% in the general population (Wisniewski and Jeret, 1994), but the actual frequency may be greater because of unnoticed asymptomatic cases. Agenesis of the CC occurs in a large number of human neurological syndromes and its incidence among the developmentally disabled population ranges between 2 and 3% (Wisnewski and Jeret, 1994). It is highly unlikely that these syndromes share a common etiology but is more probable that processes at the cerebral midline are more prone to disruption by a variety of influences such as genetic mutations, prenatal environmental influences, and abnormal timing of embryonic events. Four well established syndromes in humans for which at least partial absence of the CC is typical are Andermann syndrome, Aicardi syndrome, acrocallosal syndrome and Shapiro's syndrome. Fetal alcohol syndrome, Arnold-Chiari syndrome, West's syndrome and the oral-facial-digital syndrome have also been associated with agenesis of the CC beyond chance level and isolated cases

of agenesis have been found in many other human neurological syndromes (Geoffrey, 1994; Lassonde and Jeeves, 1994; Wisnewski and Jeret, 1994).

Neurologically, mental retardation and/or retarded development, brain malformations, and seizures are frequently associated with callosal agenesis. Among 705 patients with partial or complete absence of the CC, Jeret et al. (1987) found 73% with mental retardation. Although this number is high, it is not surprising considering the large number of associated syndromes involved. Gupta and Lilford (1995) have found that apparently isolated agenesis of the corpus callosum appears to carry an excellent prognosis, with an 85% chance of normal mental and motor development. In addition, a few asymptomatic cases of corpus callosum agenesis have been reported, most found after autopsy. Subtle cognitive impairments due to agenesis of the CC can not be ruled out by these findings, however.

Callosal Agenesis in the Mouse

The mouse is the only available non-human source of hereditary CC absence. Four strains of mice (BALB/c, 129, I/LnJ and ddN) frequently exhibit agenesis of the corpus callosum to varying degrees. Examination of agenesis in this species may be useful for several reasons. Because the corpus callosum develops prenatally in humans, nothing is known about the sequence of events that result in absence of the CC in this species. The low incidence of corpus callosum agenesis in the human population makes gathering adequate sample sizes for examination of the

developmental or functional correlates of CC agenesis difficult and time consuming. In addition, agenesis of the corpus callosum in the mouse apparently occurs without associated neurological problems, allowing the isolated examination of this nervous system defect. With recent advances in mouse genetics, the mouse is also the preferred subject for studying the genetic bases of neural and behavioral variability because it can be inbred and technologies now exist for mapping and identifying associated genes. Because of the advantages the mouse provides for studying congenital agenesis of the corpus callosum, much work has been done examining the genetic, developmental, anatomical and behavioral correlates of this mouse brain defect.

Genetics

Congenital absence of the mouse corpus callosum was first reported by Keeler in 1933, who asserted that this defect was caused by a single locus that followed an autosomal recessive pattern of inheritance, which he named 'ac' (Keeler, 1933). However, linkage of the gene was never determined and King (1936) expressed doubts about its mode of inheritance. Agenesis of the corpus callosum has since been rediscovered in four mouse strains. Richard Wimer reported in 1965 that strains BALB/cJ and 129/J strains have absent CC (Wimer, 1965) and later discovered, in a systematic survey of over 60 other strains, that I/LnJ mice also exhibit this neurological defect. Ozaki and his colleagues in Japan have also observed CC agenesis in their ddN strain (Ozaki et al., 1984). These four strains exhibit agenesis

of the corpus callosum to varying degrees, however. Adult I/Ln mice are most severely afflicted because the corpus callosum is always completely absent and in addition the hippocampal commissure (HC) is small or absent in about 50% of cases (Wahlsten and Ozaki, 1994). I/LnJ mice are also extremely poor breeders, which makes studying them difficult. BALB/cWah1 and 129/J or ReJ mice exhibit incomplete penetrance of the CC with about 55% of cases having a small or absent CC and about 20% a completely absent callosum (Wahlsten and Ozaki, 1994). Penetrance of the callosal defect is much lower in ddN mice, where only about 8% of mice show a defect (Ozaki et al., 1984) and very large sample sizes of this strain are required to generate enough mice with the callosal defect.

Crosses of BALB/cWah1, 129 or I/Ln mice with normal strains such as C57BL/6J show that inheritance is autosomal, recessive and polygenic (Lipp and Waanders, 1990; Wahlsten, 1982b). When these four strains are crossed to form hybrids, only the BALB/cWah1 x 129 group yields completely normal offspring (Livy and Wahlsten, 1991), demonstrating that mice of different strains can suffer from the same anatomical defect for genetically different reasons and confirming that inheritance of this defect involves a difference of more than one locus between these two strains.

Wahlsten and Schaloman (1994) proposed a three locus model of inheritance for congenital agenesis of the corpus callosum in the mouse. A mouse must be homozygous recessive at two or more loci to suffer a defect in the CC, whereas homozygosity at three loci causes a more severe form of the defect than homozygosity

at two loci. Under this model I/Ln mice are homozygous recessive at three loci (a/a, b/b, c/c), BALB/cWah1 mice at two loci (a/a, b/b, +/+) and 129 mice at two loci (a/a, +/+, c/c) with a two locus difference between BALB/cWah1 and 129 mice (at the b and c loci). This model was confirmed in a sample of F_2 hybrids between BALB/c and 129, which showed the expected distribution of callosal defects (Wahlsten and Schalomon, 1994).

However, results of experiments that can be explained by a two-locus model can also be accommodated by a polygenic threshold model with duplicate epistasis that stipulates an animal homozygous recessive at half or more of the relevant loci will suffer a severe defect (i.e.: Fraser, 1980; Juriloff, 1995). Wahlsten et al. (1997) have recently bred recombinant inbred (RI) lines from a cross between BALB/cWah1 and 129/ReJ to test these competing models. If an anomalous phenotype seen in certain progenitor strains exhibits recessive inheritance and allelic differences at only a few loci, extreme phenotypic forms should reappear and fix quickly in certain of the RI lines. According to the two-locus model, about 25% of the RI lines produced from a BALB/cWah1 x 129/ReJ cross should have a phenotype like I/Ln and be more extreme than either progenitor, whereas about 25% of the strains should become phenotypically normal within a few generations of inbreeding. This is what was observed: at generation seven about 30% of the lines had the most extreme phenotype of total CC absence and a small HC. Once these lines had fixed for this extreme phenotype, a complementation test was then performed in which they were crossed with each other to rule out the polygenic threshold model. When the extreme lines

are crossed with each other, a two-locus model would predict no reduction in the severity of the brain malformation, whereas a polygenic threshold model would predict a substantial reduction in severity of the CC defect in the hybrids. When the three lines that had fixed for the I/Ln phenotype at generation seven were crossed with each other, all of the hybrid offspring lacked a CC and almost all showed reduction in HC size, thus ruling out the polygenic threshold model. However, according to the two-locus model of inheritance, 5.4% of the F_2 hybrids should have an abnormally small hippocampal commissure. In fact, the HC was abnormally small in 14% of the F_2, indicating that more severely afflicted animals than expected were observed. The two-locus model would fit the data better if the recessive alleles possessed by I/Ln at one or more loci are less deleterious than those in BALB/cWah1 and 129 and are dominant over them while being recessive with respect to the wild-type alleles.

Several recent studies using the transgenic knockout method in mice have also reported a high frequency of absent corpus callosum. A knockout of the *Emx-1* homeobox gene normally expressed in mouse embryo forebrain yields completely acallosal mice like I/LnJ (Qiu et al., 1996). Nonviable animals lacking the CC, HC and the anterior commissure (AC) and exhibiting failure of the midline hemispheres to fuse normally during development results from a knockout of the *Macs* gene (Stumpo et al., 1995). *Netrin-1* deficient mice exhibit complete absence of the corpus callosum and hippocampal commissure and retain a small remnant of the anterior commissure in only a few cases (Serafini et al., 1996). The receptor protein-tyrosine

kinases Nuk and Sek4 interact with a set of cell-surface ligands that are implicated in axon guidance and fasciculation. While *Nuk* deficient mice exhibit defects in pathfinding of anterior commissure axons (Henkemeyer et al., 1996), *Sek4* mutants have defects in corpus callosum formation (Orioli et al. , 1996). The phenotype of both axon tracts is markedly more severe in *Sek4/Nuk*^{1} double mutants who also die at an early age because of defects in palate formation (Orioli et al., 1996). In addition, mice with a point mutation at the Small eye *(Sey)-Pax-6* locus often exhibit agenesis or hypoplasia of the corpus callosum (Schmahl et al., 1993). Embryonic formation and growth of the forebrain commissures is a complicated process and probably involves hundreds of genes, mutations of many of which might abolish the CC. Whether the abnormal gene knockouts in mice involve the same loci that give rise to functionally viable mice with agenesis of the corpus callosum in the BALB/c, 129, I/Ln, or ddN inbred strains remains to be established.

Development

The corpus callosum normally develops prenatally in the mouse, reaching a size within the adult range at about six days after birth but continuing to grow and become myelinated until several weeks of age (Sturrock, 1980). In the normal $B6D2F_2$ mouse embryo the earliest callosal axons grow out of their cortical cells of origin at about embryonic day 15.5 (E15.5) and then grow through the external sagittal striatum and the intermediate zone (Ozaki and Wahlsten, 1992). The axons from the frontal cortex grow most rapidly and reach midline first, at about E16.2,

resulting in a rostral-caudal gradient of formation of the CC (Ozaki and Wahlsten, 1992). After 20.5 days, growth of the CC in a posterior direction becomes apparent and the structure becomes thicker throughout its length (Wahlsten, 1984).

In the acallosal embryo, tract tracing studies with lipophilic dyes have shown that the emergence and growth of callosal axons are evidently normal until the axons reach midplane (Ozaki and Wahlsten, 1993). The problem occurs in the substrates of axon guidance at the midplane, not in the cells of origin or axons themselves (Wahlsten, 1987). It had previously been thought that the cells of the subventricular layer emanating from the lateral ventricles may play an important role in directing callosal axons across midplane (Silver et al., 1982). Evidence suggested that when these subventricular cells do not extend across the midline region, the CC may fail to form (Silver et al., 1982; Wahlsten, 1987). This sling, which normally forms a continuous band between the hemispheres, is abnormal in BALB/c embryos where the glial elements do not migrate far enough or in sufficient numbers to form a cohesive structure (Silver et al., 1982). However, recent evidence has called this "sling" hypothesis into question. Livy and Wahlsten (1997) have clearly observed the earliest CC axons to cross midline fasciculating along and between existing hippocampal axons at the dorsal surface of the hippocampal commissure. In addition, no cell bodies of the sling were seen close to the midsagittal plane until 0.68 g, when they were located rostral to the HC and ventral to a well-formed corpus callosum. Therefore, it is not yet clear whether the sling cells actually guide the first callosal axons across midplane.

Retarded growth of the anterodorsal portion of the medial septum is also implicated in callosal agenesis (Wahlsten and Bulman-Fleming, 1994). In I/Ln embryos at 0.5 g, there is a distinct cleft between the hemispheres. In BALB/c there is a similar gap at this stage and at 0.8 g this narrow gap has sometimes become a wide chasm (Wahlsten and Ozaki, 1994). The 129 strain does not exhibit the same defect in the medial septum (Wahlsten and Bulman-Fleming, 1994) but may exhibit agenesis of the corpus callosum for other reasons. Examination of the medial septum defect in embryos suggests that it may be due to a single recessive gene (Wahlsten and Bulman-Fleming, 1994). However, the mechanism behind this defect is as yet unknown. It is unclear whether normal, steady growth of the medial septum is due to genuine fusion of the cerebral hemispheres or to enlargement by migration of cells into the region which then pushes the meninges further anteriorly, or both.

The HC normally forms before the CC and may serve as a bridge by which the axons of the CC traverse a fissure at the middle of the forebrain (Wahlsten, 1987). In BALB/cWah1 and 129 embryos HC formation itself is retarded (Livy and Wahlsten, 1997) and the degree of embryonic HC retardation is correlated with the degree of callosal defect observed in adults in a number of inbred strains (Livy and Wahlsten, 1997). The precise timing of growth of the HC bridge relative to the arrival of the CC axons at midplane varies among mice having the same genotype (Ozaki and Wahlsten, 1993). If the HC is only mildly retarded, many embryos will have the CC axons still at the bridgehead when the HC bridge finally forms and these will develop a CC that may even look normal in the adult, despite the gross

retardation of the process prenatally. More severe retardation of the HC results in an increased frequency of CC absence and even more severe retardation will lead to a diminution of the adult HC, as in the I/Ln strain.

Evidence also suggests that there may be thresholds for normal development of the corpus callosum and hippocampal commissure. Small variations in the timing of events in the embryo may lead to a large difference in anatomy of the adult commissures if developmental thresholds exist. It is known that CC axons that arrive at midline on schedule, but before the substrates for crossing midline have formed, turn back and grow into the cerebral hemispheres from whence they originated (Ozaki and Wahlsten, 1993). Hence, there may be a narrow window of time during which the CC and HC axons may successfully cross to the contralateral hemisphere.

Although genetic and developmental threshold models have been proposed for the mechanisms underlying agenesis of the corpus callosum, a distinction between these two types of models should be made. In general, a threshold model hypothesizes that the difference between classes of the phenotype of interest is determined by a threshold imposed upon a continuously varying trait. For a genetic threshold model, qualitative differences between phenotypes are determined by the genotype at a required fraction of a large number of relevant genetic loci. For example, a genetic threshold model for agenesis of the corpus callosum has been proposed in which many relevant loci differ between the inbred strains BALB/cWah1 and 129/ReJ and an animal homozygous recessive at more than half of those loci will express severe defects in the CC and HC (Wahlsten et al., 1997). For a

developmental threshold model, quantitative differences between phenotypes are determined by a threshold value of a quantitative primary developmental abnormality. For example, a developmental threshold model for agenesis of the corpus callosum has been proposed in which mice with an embryonic CC and HC size at least 5.5 standard deviations below the mean exhibit an abnormally small corpus callosum as adults (Wahlsten and Ozaki, 1994). It is important to note that although threshold models may be proposed at the genetic and developmental levels for the same quantitative trait, there need not be a relationship between the two types of thresholds.

Anatomy

In adult mice with agenesis of the corpus callosum, a variety of midline defects is seen (Wahlsten and Schalomon, 1994) and the severity of the defect corresponds to the degree of retarded formation of the hippocampal commissure in the embryo (Livy and Wahlsten, 1997). The various types of defects are illustrated in Figure 1. The least severe form of callosal defect occurs in cases in which the CC is reduced in size and the dorsal commissures of the fornix (DCF) and HC are normal (Figure 1B). In rare cases a tiny patch of CC axons is observed dorsal to the HC and the DCF is found above the HC (Figure 1C). In a more severe form of the defect, the CC is completely absent and the HC and DCF are of normal size, with the DCF found directly above the HC (Figure 1D). Cases in which the CC and DCF are absent but the HC is of normal size may also be observed (Figure 1E). And, finally, in the most severe form of the midline defect observed, the HC itself can be greatly

Figure 1: Commissural defects in the adult mouse. Midsagittal plane of the adult mouse brain showing the variety of commissural defects found in acallosal mouse strains. Sketches are of 129XC recombinant inbred adult mouse brains (8 weeks of age and older) stained with gold chloride. A) A normal brain with large corpus callosum (CC), including the splenium (s) and genu (g). B) The CC is small but the hippocampal commissure (HC) is normal. The area of the CC does not include the dorsal commissure of the fornix (DCF). C) The CC is extremely small and the DCF is found directly on top of the HC. D) An acallosal brain in which the CC is absent but the HC and DCF are of normal size. E) The HC is of normal size but the DCF is absent. F) The HC is abnormally small. In all six brains the anterior commissure (AC), habenular commissure (HbC) and posterior commissure (PC) are of normal size.

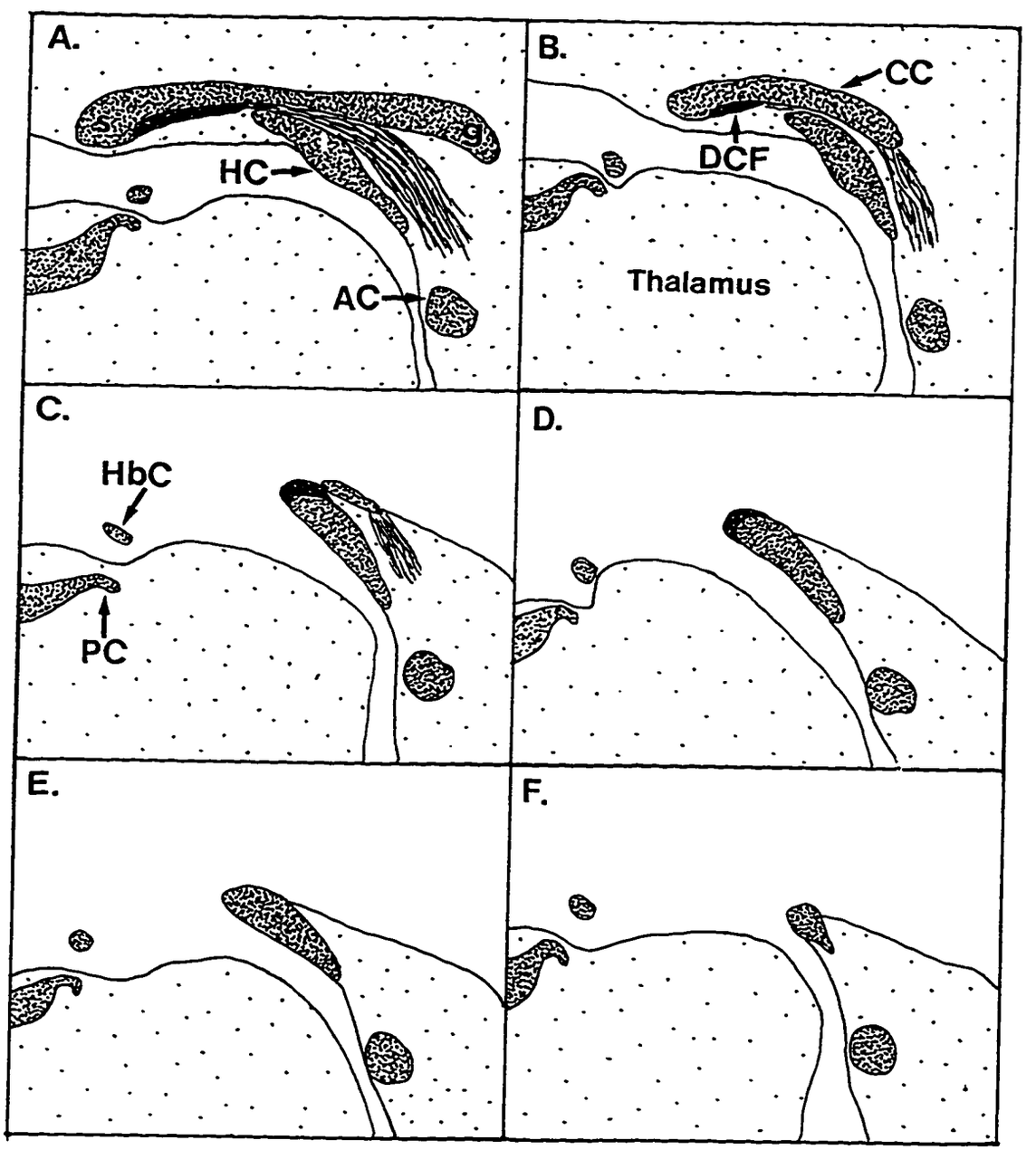
A.
HC
AC
B.
CC
DCF
Thalamus
C.
HbC
PC
D.
E.
F.

reduced (Figure 1F).

In cases of partial agenesis, the existing CC fibres still originate from and terminate in all major areas of the cortex and are distributed according to the normal topographic plan (Olavarria et al., 1988). When no CC axons have crossed, almost all of the CC axons are seen to enter the Probst bundle and then leave it within a few hours to course ipsilaterally into the white matter and never to return towards midline (Ozaki and Wahlsten, 1993). In adult acallosal animals these fibres are electrically functional (Lefkowitz et al., 1991) and are known to form ipsilateral corticocortical connections eventually in a similar topographical arrangement as the intrinsic association fibres (Ozaki et al., 1987). The function of this "extra association system" remains unknown.

The anterior commissure (AC) is not enlarged in size when the CC is reduced or absent in BALB/c mice (Wahlsten & Jones, 1983; Schmidt and Caparelli-Daquer, 1989) and CC axons do not reroute via the AC when they fail to cross (Wahlsten & Jones, 1983; Olavarria et al., 1988; Ozaki et al., 1987). However, a recent study has found that there are approximately 70,000 more unmyelinated AC axons with narrow diameter in acallosal mice than in normal controls (Livy et al., 1997). Therefore, it is possible that connectivity between the hemispheres may be increased in cases of agenesis through increased number and density of AC axons without rerouting of CC axons.

Behavior

Few behavioral correlates of agenesis of the corpus callosum have been found in mice, but relatively little work has been done examining this issue. Tests of bilateral motor coordination suggest subtle problems in limb coordination. I/LnJ mice, which always exhibit complete CC agenesis, have been observed circling during swimming navigation (Lipp and Waanders, 1990; Lipp and Wahlsten, 1992). I/Ln animals are known for their high activity (McClearn et al., 1970) and fast moving animals often show bouts of uncontrolled circling which alternate with straight running. On a task requiring a mouse to walk along a notched bar, a clear strain correlation was found between size of the CC and the number of hind-paw slips, the acallosal I/Ln mice having the greatest mean number of slips (Lipp and Wahlsten, 1992). However, no correlation between CC size and platform slips was observed within strains (129/J, BALB/c, (C57BL/6 x I/Ln) x I/Ln backcrosses: Lipp and Wahlsten, 1992) or in a recent study by Schalomon and Wahlsten (1997). In a study examining running wheel performance of recombinant inbred mice with varying degrees of congenital CC deficits (from a cross between BALB/cWah1 x 129/ReJ), the mice became more proficient at running with experience over seven days, but no significant correlates of CC agenesis were detected in their motor performance (Bishop et al., 1996).

Completely acallosal I/Ln mice are relatively ambilateral compared to strains with normal CCs and strong paw preferences (Gruber et al., 1991). However, in a sample of backcrossed hybrids [(C57BL/6 x I/Ln) x I/Ln] no correlation between CC size and degree of paw lateralization was observed (Lipp et al., 1991). Although a

significant correlation was reported in a small sample of 129/J mice but not in a sample of BALB/c mice (Ward et al., 1987), larger studies have confirmed the lack of relationship between CC size and degree of paw preference lateralization in BALB/c mice (Schmidt et al., 1991; Bulman-Fleming et al., 1992). Biddle and Eales (1996) also failed to find a significant relationship between the degree of lateralization of paw preference and the size of the corpus callosum in three strains of mice that show significantly different degrees of lateralization (CDS/Lay, SWV, C57BL/6J).

It is intriguing, in light of the fact that the CC is often surgically bisected in the treatment of severe epilepsy, that an inbred epilepsy-prone substrain derived in part from BALB/c mice shows absence of the corpus callosum (Morin et al., 1994). In addition, acallosal ddN mice show reduced bilateral interhemispheric synchrony of cortical EEG and require fewer days to reach stage 3 kindling seizures compared to normal ddN mice (Usuki et al., 1992). Other strains of epilepsy-prone mice (ddY; El) show genetic relations to acallosal mice (to ddN and 129, respectively) (Wayne Frankel, personal communication). However, Seyfried (Wahlsten, personal communication) has recently found no relationship between agenesis of the corpus callosum and seizure susceptibility in recombinant inbred lines of mice derived from a cross between the 129/ReJ and BALB/cWah1 inbred strains.

Difficulty detecting behavioral correlates of CC agenesis is not surprising in cases of incomplete agenesis because the anatomical studies of Olavarria et al. (1988) show that in mice with even a small CC the pattern of cortical connections through the CC is normal, only reduced in density. Absence of behavioral consequences in

complete CC absence may indicate that the CC is not functionally equivalent in mice and humans. Neural plasticity may also compensate more completely for the CC absence in mice than humans. It is also possible that the behavioral methods utilized have been inadequate to detect the subtle behavioral phenotype associated with callosal agenesis.

Overall, studies of congenitally acallosal mice have indicated that the genetic basis for this defect most likely involves three major genetic loci, that there is a close temporal and spatial relationship between development of the corpus callosum and hippocampal commissure, and that a developmental threshold model may account for the range of commissural defects observed in adults from the 129 and BALB/cWah1 inbred strains. However, much about the genetic and developmental causes and the behavioral and anatomical consequences of this brain defect remains unknown. In particular, the identification and characterization of the genes involved would do much to elucidate the genetic, developmental and anatomical mechanisms underlying agenesis of the corpus callosum and hippocampal commissure in the mouse.

The mouse as a model for human agenesis?

Mice with congenital agenesis of the corpus callosum are excellent subjects for for studying the genetic, developmental and behavioral aspects of this neurological defect and much work has been done in these areas. But does congenital agenesis of the corpus callosum in the mouse provide a valid model for agenesis in humans?

When reviewing the literature on human agenesis of the corpus callosum, the most striking fact is the enormous heterogeneity of this brain malformation in the human population (Rubenstein et al., 1994). The basis for this extreme heterogeneity is thought to lie in the complicated and fragile embryological development of this structure. Several different mechanisms can result in agenesis of the commissures and plasticity in development may result in compensation for abnormalities in some instances. Two primary or "true" types of CC agenesis and two secondary types of callosal anomalies have been recognized for humans (Dobyns, 1996). The first type of true agenesis includes cases in which the callosal axons form and travel to midline normally but are unable to cross to the contralateral hemisphere because of a defect in the substrates for crossing. In these cases Probst's bundles are evident. The second type of "true" agenesis includes those cases in which the commissural axons or their parent cell bodies fail to form in the cerebral hemispheres (Sidman and Rakic, 1982). In this case Probst's bundles are not evident. In addition, other defects that can be mistaken for "true" agenesis include defects in which absence of the CC is secondary to a major malformation of the embryonic forebrain that occurs prior to formation of the corpus callosum (i.e.: forebrain exencephaly or holocephaly) and defects in which axonal degeneration or atrophy result in a thinning but not foreshortening of the corpus callosum (i.e: Lyon syndrome; Lyon et al., 1990).

As expected, evaluation of the genetic basis of human agenesis is complicated enormously by the heterogeneity of this brain malformation, but this area of research has recently gathered much attention, primarily because of the large number of human

neurological syndromes that involve agenesis of the corpus callosum. The first cytogenetic map of human callosal agenesis based on associated chromosomal abnormalities was presented by Muenke in 1991 at the Birth Defects Conference in Vancouver. A recent review by Dobyns (1996) lists the current status of the cytogenetic and syndrome maps. Agenesis of the corpus callosum has now been associated with over 60 different chromosomal rearrangements (deletions, translocations, duplications and trisomies) in published reports. Isolated agenesis of the corpus callosum has been observed in families with autosomal dominant, autosomal recessive, and X-linked inheritance, but none of these loci have been mapped. In addition, callosal agenesis is associated with 17 X-linked malformation syndromes and the genes have been mapped for nine of these. Agenesis of the corpus callosum has also been reported in more than 20 autosomal malformation syndromes and genes have now been mapped for eight of these. One syndrome, Andermann syndrome (or peripheral neuropathy with or without agenesis of the corpus callosum), has recently been mapped to a 5-cM region on chromosome 15q13-q15, based on a study of 14 French Canadian families (Casaubon et al., 1996). This syndrome is one case in which true total agenesis of the corpus callosum with longitudinal Probst bundles has been seen (Carpenter, 1994).

Most of the data regarding the cognitive or behavioral performance of humans with agenesis is conflicting, probably because of the large variability in functioning in these individuals, the small samples used in this type of research, differences in the tasks used between studies, differences in the control group used, and disparity in the

extent of associated central nervous system deficits in these patients. However, several clear conclusions can be reached about humans with callosal agenesis compared to IQ-matched controls. Language is quite normal in almost every respect, perhaps with deficits in syntactic comprehension and rhyming (Dennis, 1981; Temple et al., 1989). The most consistent functional finding is that acallosals are often comparatively slow and clumsy on "simple tasks requiring bilateral motor coordination under speed stress" (Jeeves, 1989). Also undisputed is the observation that callosal agenesis does not produce the same cognitive deficits that callosotomy, the surgical transection of the CC, does (Sperry, 1982; Sauerwein and Lassonde, 1994). Unlike callosotomy patients, acallosals can transfer information from one hemisphere to another, suggesting that plasticity exists in the development of forebrain cortical connections.

Overall, because of the large degree of heterogeneity in human cases of agenesis of the corpus callosum, a mouse model of this brain defect may be more or less valid for certain cases and syndromes than others. It is evident that information regarding the embryological determinants of this disorder in the two species is essential for making comparisons. Congenital agenesis of the corpus callosum in the mouse strains mentioned in this thesis arises because of a defect in the midline substrates for crossing of the callosal axons and not because of a problem with the callosal cells or axons themselves. Therefore, this model would be applicable only to human syndromes, such as Andermann syndrome, that include this type of "true" agenesis. In contrast, those syndromes such as CRASH syndrome, due to a mutation

in the L1 gene which codes for a neural cell adhesion molecule (Fransen et a., 1995), in which agenesis is a result of faulty axon guidance to midplane, do not apply to the congenital mouse model.

With that caveat in mind, the mouse provides excellent genetic material for mapping and identifying genes involved in callosal development and agenesis of the corpus callosum. Because of the high degree of homology between the mouse and human genomes (Nadeau, 1992) it is expected that mouse genes involved in agenesis of the corpus callosum will have homologous counterparts in the human genome that are mutated in one or more of the human acallosal syndromes. The mouse also provides excellent material for studies of the molecular, cellular, and anatomical roles of these gene products in corpus callosum development and function, studies that are not possible with human subjects. For example, the portion of chromosome 15 to which Andermann syndrome has been recently mapped corresponds to mouse chromosome 7 and provides a likely candidate region for mapping of the loci involved in congenital agenesis in our RI strains. Mapping and cloning this putative gene in the mouse would then provide material to examine the structure and expression of the encoded protein and its role in the development and functioning of the brain.

In addition, the mouse is the only available species for studying the genetically influenced events in embryological development responsible for normal or abnormal corpus callosum morphology in the adult. Because developmental mechanisms are not accessible in human fetuses whose later callosal phenotype would be known, study of mouse embryos provides important insights into the mechanisms underlying normal

and abnormal development of the corpus callosum that may apply across species.

The research described herein examines the development of the telencephalic midline region in acallosal and normal mouse strains in order to further elucidate the genetic and development mechanisms responsible for formation of the corpus callosum. This work provides a useful model of mechanisms of normal commissural axon guidance and may be relevant to agenesis of the corpus callosum in humans. This research is divided into several parts as described below:

Experiment 1. ***Development of the corpus callosum in acallosal and normal inbred strains and classical crosses of mice: Developmental thresholds for axonal crossing of the telencephalic midline.*** Inbred strains of mice raised in controlled environments exhibit a variety of defects of the corpus callosum, ranging from completely normal commissures to complete absence of the corpus callosum with a diminutive hippocampal commissure. How can this extreme phenotypic variability be explained when genetic and environmental variability are negligible? It is proposed that relatively small differences in the timing of events at the telencephalic midline may result in a very large range of defects in the adult because of abrupt thresholds for CC and HC axon growth across midline. Although genes of the embryo may determine the relative timing of these critical events, stochastic (or probabilistic) development produces variability in their occurrence and thus contributes a "third source" of individual differences (Grobstein, 1988; Wahlsten, 1987). This study examines large samples of the 129 and BALB/cWah1 inbred strains and crosses between them in

order to identify and quantify developmental thresholds that may account for the incomplete penetrance of the commissural defects. It is expected that embryonic development of the corpus callosum and hippocampal commissure is highly correlated with the degree of commissural defect observed in adults. Two thresholds, one for normal development of the corpus callosum and another for normal development of the hippocampal commissure, should be identified. It is also expected that F_1 embryos will exhibit delayed formation of the commissures, even though adults from this cross are normal.

In addition, these crosses are used to investigate the genetics and development of a previously identified defect in the dorsal medial septal region (Wahlsten and Bulman-Fleming, 1994). Previous research has suggested that BALB/cWah1 and 129 mice likely differ at two loci relevant to callosal development (Livy and Wahlsten, 1991; Wahlsten and Schalomon, 1994). It is therefore possible that two anatomically distinct developmental processes may be identified and that one of these loci may be related to the septal notch defect (Wahlsten and Bulman-Fleming, 1994). If so, then classical crosses should show evidence of bimodality in the backcross to BALB/cWah1 for the septal notch defect but not for embryonic CC and HC size. Neonates from these classical crosses are examined in order to determine the time-course for recovery of the CC and HC and whether recovery occurs before or after the septal notch closes.

Experiment 2. ***Development of the corpus callosum in acallosal and normal***

recombinant inbred lines derived from 129/ReJ and BALB/c mice: Genetic effects on events at the cerebral midline. It has been proposed that the relative timing of cerebral fusion, HC formation and CC axon arrival at midplane establishes rather abrupt thresholds for normal development of the corpus callosum. In this study, newly derived recombinant inbred strains of mice (the 9XC strains) are used to quantify the timing and structural growth of events in the telencephalic midline region. Recombinant inbred mice are good for this purpose because extreme acallosal and normal strains with complete penetrance for the callosal defect have been bred from the same original parents, thus providing ideal experimental and control groups.

This study contains three parts. In part one, lipophilic dyes are used to examine the relative timing of CC axon growth towards midline and the formation of the hippocampal commissure, a possible substrate for CC axon crossing. It is hypothesized that CC axons in all of the RI strains arrive at midplane on schedule (Ozaki and Wahlsten, 1993) but that formation of the hippocampal commissure is retarded in acallosal strains (Livy and Wahlsten, 1997). In part two, growth of the corpus callosum, hippocampal commissure and dorsal medial septal region are examined in the midsagittal plane in order to quantify the relative timing of these events and defects in them. It is proposed that the extreme acallosal strains will all exhibit a defect in the dorsal medial septum (Wahlsten and Bulman-Fleming, 1994). In addition, the results from the recombinant inbred strains will be used to confirm the developmental thresholds proposed for development of the corpus callosum and hippocampal commissure. The last part of this experiment examines growth of the

telencephalic midline region in the coronal plane in order to investigate the role delayed fusion of the interhemispheric fissure may play in delayed growth of CC and HC axons across the midline and to determine whether the extreme strains are anatomically the same. Therefore, embryos of normal, acallosal and variable recombinant inbred strains are examined and compared in order to determine why the nerve fibres cannot cross a fissure between the two halves of the brain. Quantification of midline development is used to further qualify the developmental threshold model for agenesis of the corpus callosum.

Experiment 1: Development of the corpus callosum in acallosal and normal inbred strains and classical crosses of mice: Developmental thresholds for axonal crossing of the telencephalic midline

Introduction

In most cases of genetically-induced callosal agenesis, whether in inbred strains or transgenic mice, the telencephalic defect occurs with varying degrees of penetrance. Penetrance refers to the proportion of animals having a particular genotype that also displays a particular phenotype (Wahlsten, 1982). Strains of mice that have been inbred for over 60 generations through brother by sister matings are genetically homozygous at every locus (Green, 1981); each individual of an inbred strain should therefore be genetically identical. Even when raised in a highly controlled environment, however, individual mice of certain inbred strains exhibit a variety of CC and HC sizes in adulthood. In addition, differences within an inbred strain do not result from residual hereditary variation; there is no correlation between the phenotype of an offspring and its two parents (Wahlsten, 1989). Environmental differences within the uterine environment also do not contribute to the alteration in callosal size in any consistent manner (Bulman-Fleming and Wahlsten, 1991). This pattern suggests that developmental thresholds may occur for crossing of the midline by axons of the corpus callosum and hippocampal commissure. The stochastic or probabilistic nature of development produces small individual differences in the timing

of critical events at the midline. A sharp developmental threshold for these critical events will magnify small differences into large differences in adult anatomy of the cerebral commissures. Testing this developmental threshold model, quantifying the developmental thresholds and attempting to identify the time and location of the events involved is important for a full understanding of normal development of the cerebral commissures.

Four inbred stains of mice exhibit agenesis of the corpus callosum and differ greatly in the degree of penetrance as adults. The I/Ln strain has 100% total absence of the corpus callosum and often suffers from defects in the hippocampal commissure as well (Livy and Wahlsten, 1991). The Japanese strain ddN has low frequency of total CC absence (about 8%) and normal HC anatomy (Ozaki et al., 1984). The BALB/c and 129 strains both show incomplete penetrance for CC formation in the adult. The BALB/cWah1 strain has about 20% total absence of the CC and another 25% partial absence (Wahlsten, 1987). Strains 129/J and 129/ReJ have about 20 to 30% total absence and another 30% of mice with abnormally small CC (Lipp and Wahlsten, 1992; Wahlsten et al., 1997). The hippocampal commissure is almost always normal in adult mice of these strains. Adults of the F_1 hybrid cross between BALB/c and 129 are almost always normal, suggesting that two or more loci are involved in the callosal defect in these strains (Livy and Wahlsten, 1991; Wahlsten et al., 1997). The F_2 hybrid cross between BALB/cWah1 and 129/ReJ strains yields about 23% of mice with total absence of the CC, another 25% with an abnormally small CC and 7% with an unquestionably small HC (Wahlsten and Schalomon, 1994).

These results are consistent with a two-locus difference between the BALB and 129 strains. Because of the moderate degree of penetrance and the range of callosal defects observed in the 129 and BALB/cWah1 inbred strains and crosses between them, they make an excellent model system to study the thresholds important for CC and HC development.

In addition, embryos of these strains may be used to evaluate the development and genetics of one possible critical event for commissural development, growth of the dorsal medial septal (MS) region. Wahlsten and Bulman-Fleming (1994) demonstrated that growth of the dorsal region of the MS is delayed in inbred BALB/cWah1 mice but not those from the 129 strain and results in a "septal notch" defect. Results from BALB/cByJ, normal C57BL/6J, and recombinant inbreds derived from these two parental strains suggest that the septal notch defect may have a single-gene mode of inheritance. Proper growth of the dorsal medial septal region may be implicated in commissure formation because the axons of the hippocampal commissure first cross the cerebral midplane at this location (Livy and Wahlsten, 1997).

This study examines development of the telencephalic midline region in large samples of embryos and neonates of the BALB/cWah1 and 129 inbred strains and crosses between them. Embryos are examined in the time period during which axons of the CC first and most rapidly cross midplane and during which the MS defect first becomes evident (0.5 to 1.0 g body weight; approximately E16-18). One to three day old neonates are examined in order to determine how quickly the animals recover

from early defects in commissural and medial septal development. Developmental thresholds are proposed and tested for commissural development. In addition, growth of the dorsal medial septal region is quantified and the single-gene model for the notch defect tested. Finally, the possibility of a relationship between development of the dorsal medial septal region and crossing of the midline by axons of the corpus callosum and hippocampal commissure is explored.

Methods

Mice and matings

The strains and sample sizes used in this study are given in Table 1. Mice of the acallosal strain 129/ReJ were purchased from Jackson Laboratories (Bar Harbor, Maine) and BALB/cWah1 acallosal mice were from the colony of D. Wahlsten, where they have been maintained by full-sib inbreeding for over 100 generations, originally at the University of Waterloo and presently at the University of Alberta. Reciprocal crosses were carried out, except in the backcrosses where the female was always a F_1, but because no significant differences were found for the results of the two crosses, the data for each combination were pooled. All mice were housed in 29 x 18 x 13-cm opaque plastic mouse cages with Aspen-Chip bedding (Northeastern Products Corp., Warrenburg, NY) and a few sheets of toilet tissue added. Pregnant females were provided with a Nestlet for improved nest construction and all breeding

Table 1: Sample sizes and body weights of mice used in experiment 1

	Embryos		Neonates	
Group	N	Body Weights (g)	N	Body Weights (g)
BALB/cWah1	27	.509-.803	26	0.931-1.647
129	28	.503-.928	18	1.305-1.852
$C129F_1$	21	.521-.660	18	1.346-2.008
$C129F_1$ x BALB	44	.527-.875	57	0.978-2.133
$C129F_1$ x 129	91	.507-.946	91	0.925-1.986
$C129F_2$	61	.548-.930	74	1.077-2.202

mice were given free access to breeder food (PMI Foods Rodent Blox 5015) and Edmonton tap water. Mice were maintained under 12 hours light - 12 hours dark illumination (lights on at 6 a.m.).

Collection of embryos and newborns

Embryos were extracted between gestational days 16 and 18 (E16 and E18) to obtain body weights between 0.50 and 1.00 g, the period in development when the majority of corpus callosum and hippocampal commissure axons cross midplane. As proposed by Kaufman (1992), all mice studied prenatally are referred to as embryos, even though some have completed organogenesis and might be regarded as fetuses. One to three females were mated with one male for four hours or overnight, after which the females were checked for vaginal plugs. If a plug was detected, the female was weighed and then housed alone for the duration of gestation. Time of conception (0.0 days) was calculated to be the midpoint between detection of a plug and the previous check without a plug. At the appropriate time, pregnant females were anaesthetized with an overdose of sodium pentobarbital (120 mg/kg, intraperitoneal injections) and their uteri were removed and rinsed in a 0.9% solution of saline in ice. The uteri were cut open and each embryo was separated from its placenta by cauterizing the umbilical artery. Embryos were rinsed in ice-cold 0.9% physiological saline, carefully blotted to remove excess fluid and weighed to the nearest mg. Immediately after weighing, each whole mouse was immersed in Bouin-Duboscq

fixative for 48 h and then transferred to several changes of 70% ethanol. Shortly after being placed in the fixative, the animal had the scalp removed and small slits cut in the skull lateral to midline to aid penetration of the fixative.

Newborns were collected on postnatal days 0 to 2 (P0, P1, and P2). Newborns were anaesthetized by hypothermia and perfused through the left ventricle with 3-5 ml of 0.9% physiological saline followed by 5-10 ml of Bouin-Duboscq fixative by means of a peristaltic perfusion pump, micropipettes and a stereomicroscope. Heads were immersed in fresh fixative for 48 h. At this time the brain was extracted and weighed and then transferred to several changes of 70% ethanol.

Histology and correction for artifacts

Whole heads (embryos) or brains (neonates) were embedded in paraffin for sectioning in the sagittal plane, then serial sections were cut at 10 μm and stained with haematoxylin and eosin. Tracings were made with a Leitz tracing device and measurements were made with a Numonics 2200 graphics tablet and the Sigma Scan program from Jandel.

Dehydration shrinks neural tissue substantially and slicing the paraffin block dorsal to ventral compresses the section to some degree, which necessarily affects measures of area and thickness. The magnitudes of these artifacts were determined for a subset of the neonatal brains by piercing each midbrain region with a square

array of four tungsten needles set 1.0 mm apart before processing. The distances between holes in the processed tissue averaged .88 mm in the anterior-posterior direction affected only by shrinkage and .66 mm in the dorsal-ventral direction affected by both shrinkage and compression. Distance measures were corrected by multiplying the raw measure by the appropriate correction factor and area measures were corrected by multiplying by 1.74 (1/.88 x 1/.66).

The desired plane of sectioning was sagittal, but a perfectly sagittal alignment was rare. When the actual plane of sectioning deviates from the true sagittal plane, area and distance measurements may be distorted. Deviation from the true plane of sectioning was calculated and measurements corrected as previously described (Wahlsten and Bulman-Fleming, 1994). In all cases the corrections for shrinkage and compression were much greater than for angle of sectioning.

Sagittal reconstruction

In prenatal and early postnatal development the cerebral hemispheres are separated by a deep interhemispheric fissure, the bottom of which demarcates the surface of the medial septum. Errors in the angle of cutting may cause the dorsal and ventral portions of the septum to be at midplane in different sections (see Figure 2). To obtain a valid representation of the midplane portion of the medial septum, that section was reconstructed from serial sections, each of which contains a portion of the true midplane (Wahlsten and Bulman-Fleming, 1994; see Figure 2). The medial

Figure 2. Midsagittal reconstruction for B6D2F$_2$ neonate brain. Numerals 1 to 8 represent the section number where the anterior cerebral artery (ACA) is exactly at midplane. The dashed lines represent the limit of contiguous septal tissue in each section. Letters b to f represent the zones of the dorsal medial septum (MS) where the thickness was measured. Each line is perpendicular to a line joining the anterior aspects of the velum transversum (VT) and lamina terminalis (LT). Abbreviations: CC = corpus callosum; HC = hippocampal commissure; PSFO = primordium of the sufornical organ. Dorsal is at the top of the page and anterior/rostral is to the left.

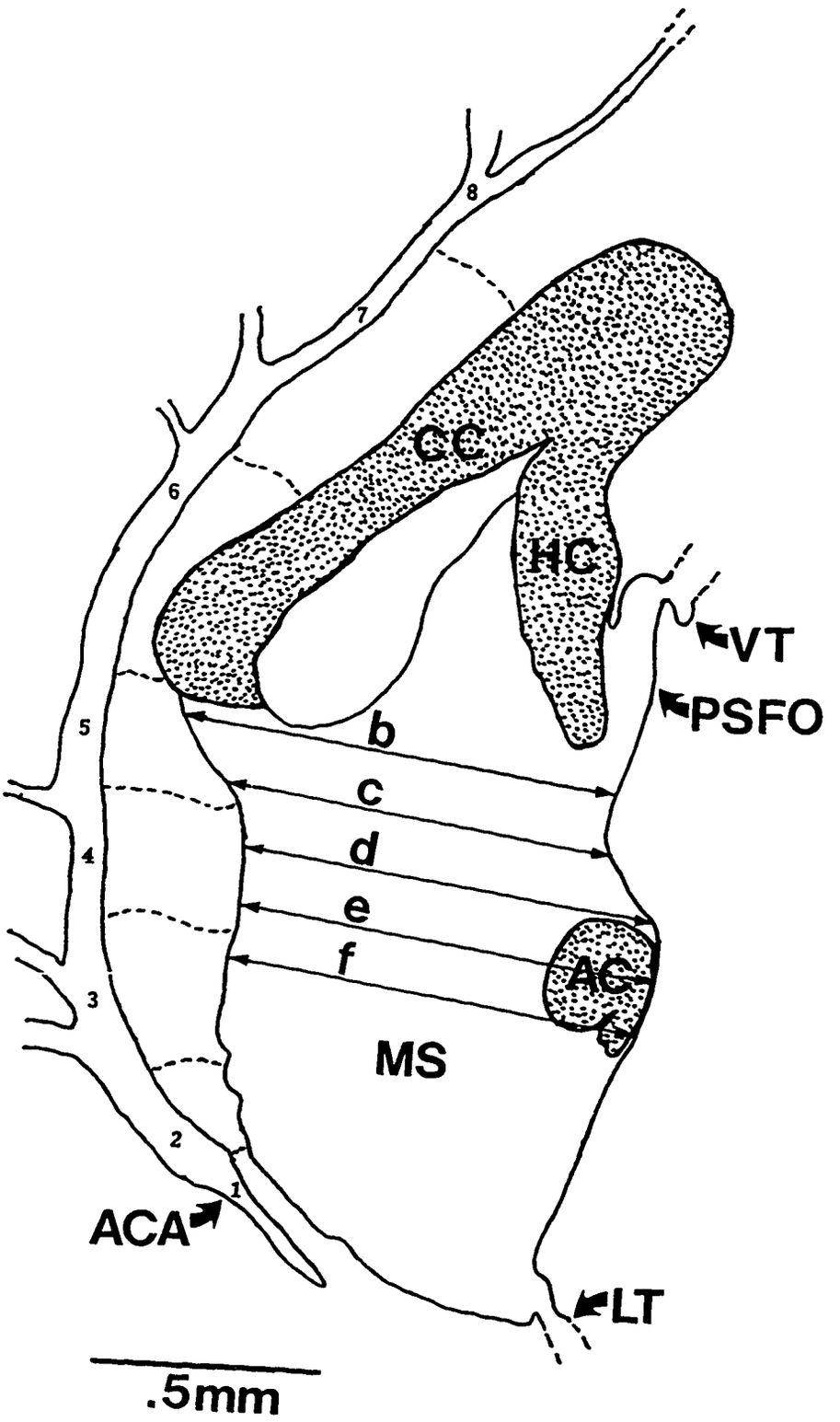
8
7
6
5
4
3
2
1
CC
HC
VT
PSFO
b
c
d
e
f
AC
MS
ACA
LT
.5mm

septum was defined in this study as the contiguous, closely packed neural tissue composed of neurons, glia, their precursor cells and cells of the neurepithelium lining the third ventricle. The region of the fissure instead clearly contains meninges and blood vessels and a line can be drawn to demarcate the limit between these regions. The true midplane region of the medial septum was reconstructed for each tracing using a) the anterior commissure, b) the lamina terminalis (LT) at the ventral limit of the MS, and c) the velum transversum (VT) as stable landmarks. The outlines of the CC, HC and the AC were not reconstructed but were traced from the section passing through each commissure at midplane. All brains were coded so that tracings, reconstructions and measurements were done without knowledge of the animals' age or pedigree.

Measurements

Cross-sectional areas were measured for the CC and HC combined (CCHC), the AC, the PSFO, and the MS (see Figure 2). The dividing line between the PSFO and MS was defined as the place where the HC was closest to the third ventricle or where this would be if no were HC present. The thickness of the MS was recorded at 6 sites which were the most dorsal of 11 widths equally spaced along a line from the most dorsal LT to the PSFO boundary and perpendicular to that line (see Figure 2). These widths correspond to the dorsal region of the medial septum where the notch defect is evident (Wahlsten and Bulman-Fleming, 1994).

Results

Chronological age and stage of development

It is conventional in neuroscience research to describe the developmental stage of a mouse using chronological age (e.g. embryonic day 17 - E17). However, embryos of the same age may show enormous individual variability in developmental rate due to intrauterine factors (McLaren and Mitchie, 1960; Barr, Jensh, and Brent, 1972) or parental genotype (Wahlsten and Wainwright, 1977; Wahlsten, 1981; Wainwright and Deeks, 1984). Comparisons between embryos of the same age may be confounded by individual differences in overall development and thus morphological differences detected in parts of the brain may be because of a smaller brain overall. Confounding of specific morphological defects by overall developmental differences may be avoided by using a more accurate individual metric for level of maturity. Staging schemes have been worked out for many aspects of early embryonic development (i.e.: counting the number of tail somites). However, for the ages examined in this study, body or brain weight provides a more practical estimate. Brain weight would be the preferred measure for neuroscience studies but is inaccurate at most prenatal ages because the fragile prenatal brain is often damaged during extraction from the skull. Body weight has been shown to be a reasonable estimate of maturity for studies of prenatal brain development (Wahlsten and Wainwright, 1977; Wahlsten and Bulman-Fleming, 1994; Livy and Wahlsten, 1997).

Therefore, growth of neural structures was assessed in relation to body weight prenatally and brain weight in the early post-natal period in this study.

Normal growth in hybrid mice

B6D2F_2 hybrid mice provide a good standard for normal development of the corpus callosum and structures related to development of the CC. Being F_2 hybrid, they show large variability in brain morphology and development. And, critically, they consistently exhibit normal development of the corpus callosum and hippocampal commissures. Hybrid B6D2F_2 mice have been used to provide a standard for normal development in previous studies of callosal development (Ozaki and Wahlsten, 1992; Wahlsten and Bulman-Fleming, 1994; Livy and Wahlsten, 1997).

Prenatal growth

Normal growth of structures in the septal region at the midsagittal plane has previously been investigated for the late prenatal period (see Wahlsten and Smith, 1989; Wahlsten and Bulman-Fleming, 1994). The following description is largely based on those findings. Some portions of this region grow very rapidly whereas others change very little during this period of time. But, in all cases the relationship with body size is strong, validating the use of body size as an indicator of level of maturity. The axons of the HC first cross midplane at about .40 g body weight, crossing between the dorsal surface of the septum and the ventral surface of the pial

membrane lining the bottom of the longitudinal cerebral fissure (Livy and Wahlsten, 1997). HC growth occurs rapidly in the dorsal direction such that by .60 g the HC is about 0.2 mm thick (Livy and Wahlsten, 1997). Axons of the corpus callosum from the frontal cortex are evident at midplane at about .62 g and cross between the dorsal surface of the HC and the ventral surface of the pial membrane lining the bottom of the longitudinal cerebral fissure (Ozaki and Wahlsten, 1992). There is evidence, however, that axons from the cingulate cortex are the first to pioneer the CC at about .45 g body weight (Koester and O'Leary, 1990). The corpus callosum and hippocampal commissure are indistinguishable at the midsagittal plane using general purpose stains until later in development (see Figure 3A). Growth of the CC and HC area is rapid and nonlinear prior to birth. Axons of the AC arrive at midplane at about .30 g and the area of the AC also shows positively accelerated growth during this period. Growth of the area and width of the medial septum is rapid and linear prenatally. The dorsal width of the MS grows at about 150 μm/day and growth in the dorsal-ventral direction between the LT and the ventral limit of the PFSO exceeds 230 μm/day. In general, individuals differ primarily in the shape of the MS region between the relatively stable thickness of the dorsal LT and ventral PFSO.

Postnatal growth

Observations of B6D2F$_2$ brains in the early postnatal period (P0-P2) provide a standard for normal growth of the CC and associated midplane structures during the period when recovery from earlier defects is thought to occur in acallosal embryos.

The following description is based on findings from an original sample of B6D2F_2 neonates examined in this study. In normal hybrid neonates the CC, HC, AC and MS are all clearly evident at midplane at birth and the midsagittal region has assumed an approximate adult structure but is smaller than the adult size (see Figure 3A). During the first few days after birth the areas of the CC and HC continue to show very rapid growth (Figure 4A), most probably due to the addition of new axons across the midsagittal region rather than myelination of existing connections. Although growth in this restricted weight range (.07 to .13 g brain weight) appears linear, overall growth in the postnatal period is most likely asymptotic. The CC increases in size primarily along the rostral-caudal axis (Figure 3) with the majority of axons being added to the posterior end so that by P2 the CC extends well beyond the posterior edge of the HC. Thickening of the CC in the dorsal-ventral direction is also apparent; however, it is much less than growth of the CC along the rostral-caudal axis (Figure 3). The hippocampal commissure elongates appreciably and the CC and HC are evident as distinct structures at about .80 g body weight when they become separated by a thin band of cell bodies and their distinctly different shapes. By the third day after birth (approximately 1.2 g body weight) the CC and HC are both within the adult range of sizes (approximately .610 mm^2 and .230 mm^2 for the CC and HC respectively, for 21-day old B6D2F_2/J mice; Bishop and Wahlsten, 1997). The area of the anterior commissure also continues to grow rapidly after birth, reaching a size of about .10 mm^2 by 1.3 g body weight (Figure 4B), close to the .103 mm^2 observed in 21 day old hybrid mice. Therefore, although MS growth over this

Figure 3: Neonatal development of the midsagittal region in B6D2F$_2$ mice. A) At .08 g brain weight a substantial corpus callosum (CC) and hippocampal commissure (HC) are evident and the dorsal medial septal (MS) region has fused. The anterior portion of the CC extends far beyond the HC. B) At .10 g brain weight the posterior portion of the CC has grown substantially. C) By .12 g brain weight the HC and AC have reached near adult size and the corpus callosum has more than doubled in size from .08 g brain weight. The dorsal region of the medial septum is now in contact with the anterior portion of the CC, fully enclosing the cavum septi (CS; Hankin et al., 1988). Dorsal is to the top and anterior to the left in these photos. Scale bar = .5 mm.

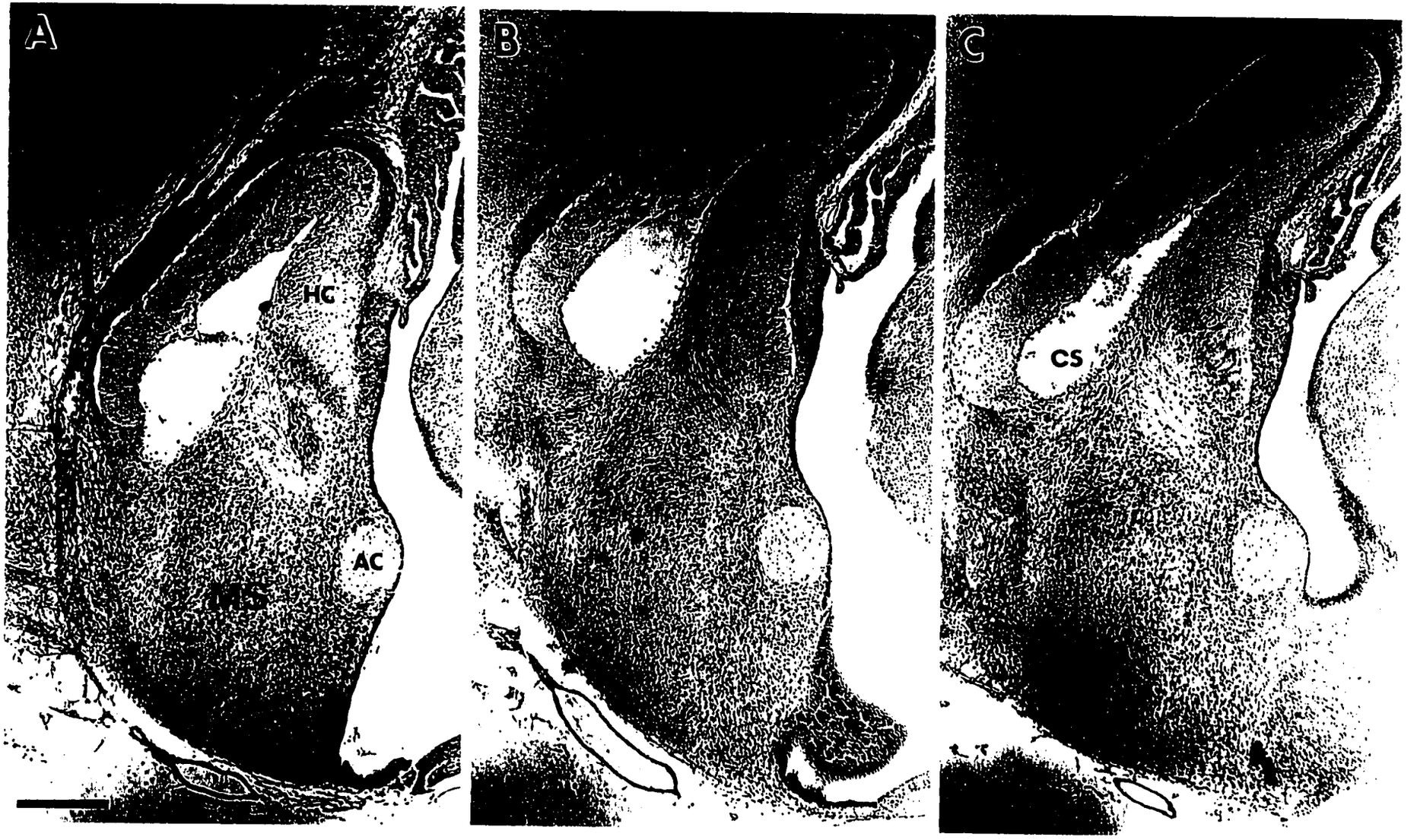
A
HC
AC
B
C
CS

Figure 4: Growth of midplane structures in hybrid B6D2F$_2$ neonates. Normal neonatal growth of A) CCHC area; B) AC area; C) MS area in relation to body weight. Equations give the line of best fit for the regression relationship with brain weight for this restricted weight range. Although growth of the corpus callosum, hippocampal commissure and anterior commissure is linear in relation to brain weight, it is expected that an asymptote would be realized if slightly older mice were examined, reflecting the underlying logistic growth in the postnatal period.

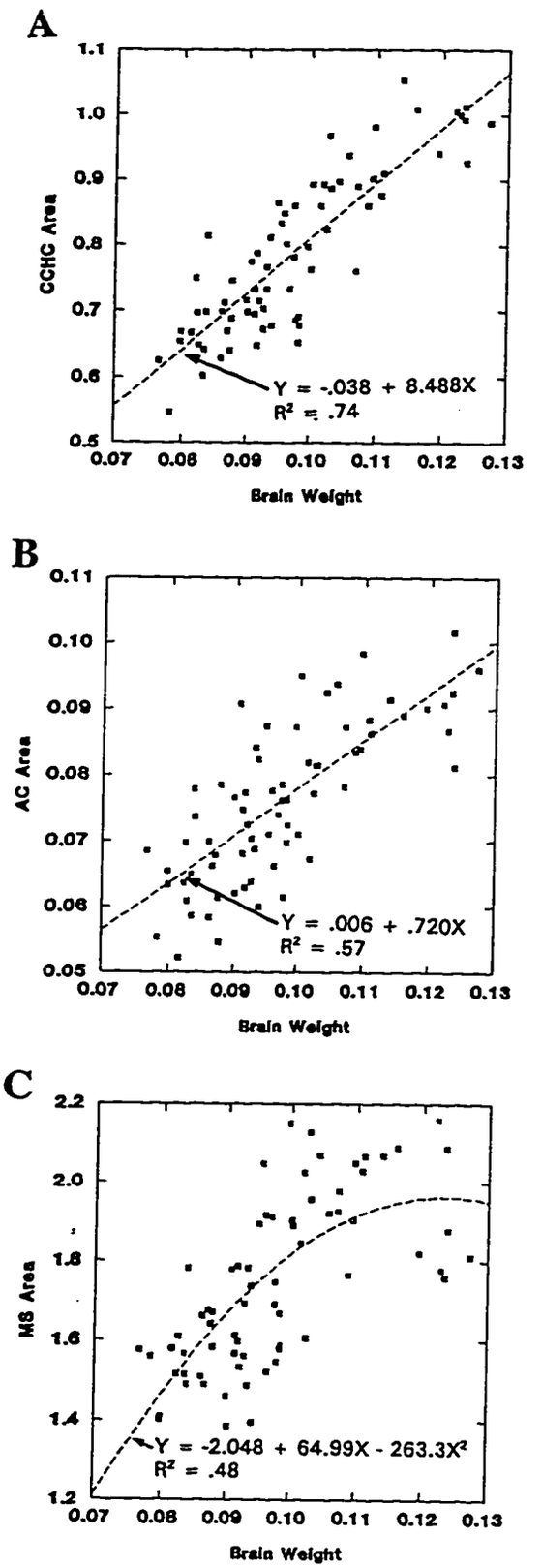
A
CCHC Area
Brain Weight
Y = -.038 + 8.488X
R² = .74
B
AC Area
Brain Weight
Y = .006 + .720X
R² = .57
C
MS Area
Brain Weight
Y = -2.048 + 64.99X - 263.3X²
R² = .48

restricted weight range appears linear, extension of the weight range would most likely reveal an asymptote at about .10 mm^2. No change in shape of the AC is evident during this period (see Figure 3). In contrast to the linear growth of the CC, HC and AC in this restricted weight range, growth of the medial septum clearly levels off appreciably in the early post-natal period (Figure 4C) such that the MS reaches a maximum area of about 2.0 mm^2 at about 0.11 g brain weight. Growth of the thickness of the MS has slowed to about 100 μm/day in the dorsal region and the dorsal-ventral growth of the MS has also slowed to under 85 μm/day. A closer examination of the shape of the MS indicates that at this age in all of the $B6D2F_2$ brains fusion of the hemispheres is complete and the posterior edge of the dorsal medial septum is consistently full and rounded (see Figure 3). It is interesting that in the majority of brains heavier than .09 g (but not in those below this weight) the posterior edge of the dorsal medial septal region lies directly ventral to the most posterior end of the CC, forming a thin band of tissue attaching the two structure at this point and sealing off the cavum septi (see Figure 3C).

Growth of the commissures in acallosal mice

CCHC index vs z-score

When examining brain morphology for defects it is important to be able to distinguish between structures that are small because of a delay in overall growth of the brain and structures that are small because of a genetic abnormality specific to that

structure. This distinction can be made by quantifying normal growth of a structure of interest and then calculating an index that represents the deviation from normal. Two indices were calculated for each brain, a z-score that represents the number of standard deviations by which a CCHC area deviates from the mean for normal mice of the same body weight and an index of abnormality that represents the ratio of the actual CCHC size to the size expected for a given body weight on a scale from 0 to 1. By representing CCHC size differences using unit-free indices, data from embryos, newborns and even adults can be also be compared directly.

Data from B6D2F$_2$/J and C57BL/6J embryos with normal corpus callosum formation (Wahlsten and Smith, 1989) were used to derive an equation for normal CC and HC growth in relation to body weight (BW). The quadratic equation CCHC = -.05 -.323*BW + .633*BW^2 fit the data best (R^2 = .94) over the weight range .5 to 1.0 g body weight. This equation was used to calculate a z-score for each embryo to represent the number of standard deviations by which a CCHC area deviates from the mean for normal embryos of the same body weight. The z-score equation takes into account the observation that dispersion of points around the line predicting CCHC from body weight was greater for heavier fetuses. Embryo CC and HC areas were converted to z- scores using the equation:

$$z=\frac{(CCHC)-(-.05-.323BW+.633BW^2)}{\sqrt{(.00231-.00920BW+.00940BW^2)}}$$

An index of abnormality (CCHCI) was also calculated for each embryo to represent

the ratio of the actual CCHC size to that expected for an embryo of a given body weight. Index values are expected to range from 0 (no CC or HC) to 1.0 or a little larger (normal CC and HC size). An index value was calculated for each embryo using the equation:

$$CCHCI = \frac{observedCCHC}{-.05 - .323BW + .633BW^2}$$

Data from $B6D2F_2$ neonates with normal CCs were used to derive an equation for normal CC and HC growth in relation to brain weight (BR). The linear equation CCHC = -.038 + 8.488*BR fit the data best (R^2 = .74; see Figure 4A). Dispersion of points around this line did not vary with brain weight and the expected standard deviation of the difference between observed and expected CCHC was calculated to be the square root of .004. Neonatal CCHC areas were then converted to z-scores using the equation:

$$z = \frac{CCHC - (-.038 + 8.488BR)}{\sqrt{.004}}$$

and to index values using the equation:

$$CCHCI = \frac{observedCCHC}{-.038 + 8.488BR}$$

CC and HC sizes for embryos and newborns with varying degrees of callosal

retardation are illustrated in Figure 5, along with the z-scores and CCHC indices that represent the degree of defect. Comparison of the individual z-scores and CCHC indices for embryos (A) and newborns (B) are made in Figure 6. In general, there is good correspondence between the two indices. However, the z-score exhibits more variability for more retarded or acallosal brains than the CCHC index does, especially in neonatal brains. This is because for brains that are completely acallosal the CCHC index will always be 0 whereas the z-score will vary because of the imperfect relationship between CCHC size and body weight.

Prenatal growth of commissures

CC and HC areas for the BALB/cWah1 and 129/ReJ embryos and the crosses between them are plotted against body weight in Figure 7A. Retarded development of the commissures is evident in most embryos because CCHC sizes generally fall well below the values expected from the analysis of normal hybrid B6D2F_2 brains. Table 2 presents the mean and standard deviation of the CCHC z-scores and index values for each cross between BALB/cWah1 and 129 mice. z-scores have been calculated so that the distribution of values in a normal population has a mean of zero and a standard deviation of one. t-tests of the mean z-score for each group indicate that all of the mean values are significantly below 0 ($p < .05$; one-tailed). CCHC development is retarded prenatally in all groups, even in F_1 embryos that exhibit normal commissures as adults. CCHC index values are lowest for the BALB/cWah1 and 129 inbred strains which show about 50% penetrance for the callosal defect as

Figure 5: Embryos and neonates with varying degrees of midplane defects. Examples of 129XCF$_2$ embryos and neonates with varying degrees of CCHC development, as expressed by z-scores and CCHC indices. The dorsal medial septum (MS) appears notched in both of the embryos displaying retarded development of the CCHC while all of the neonates exhibit a fully rounded septum (see arrows).

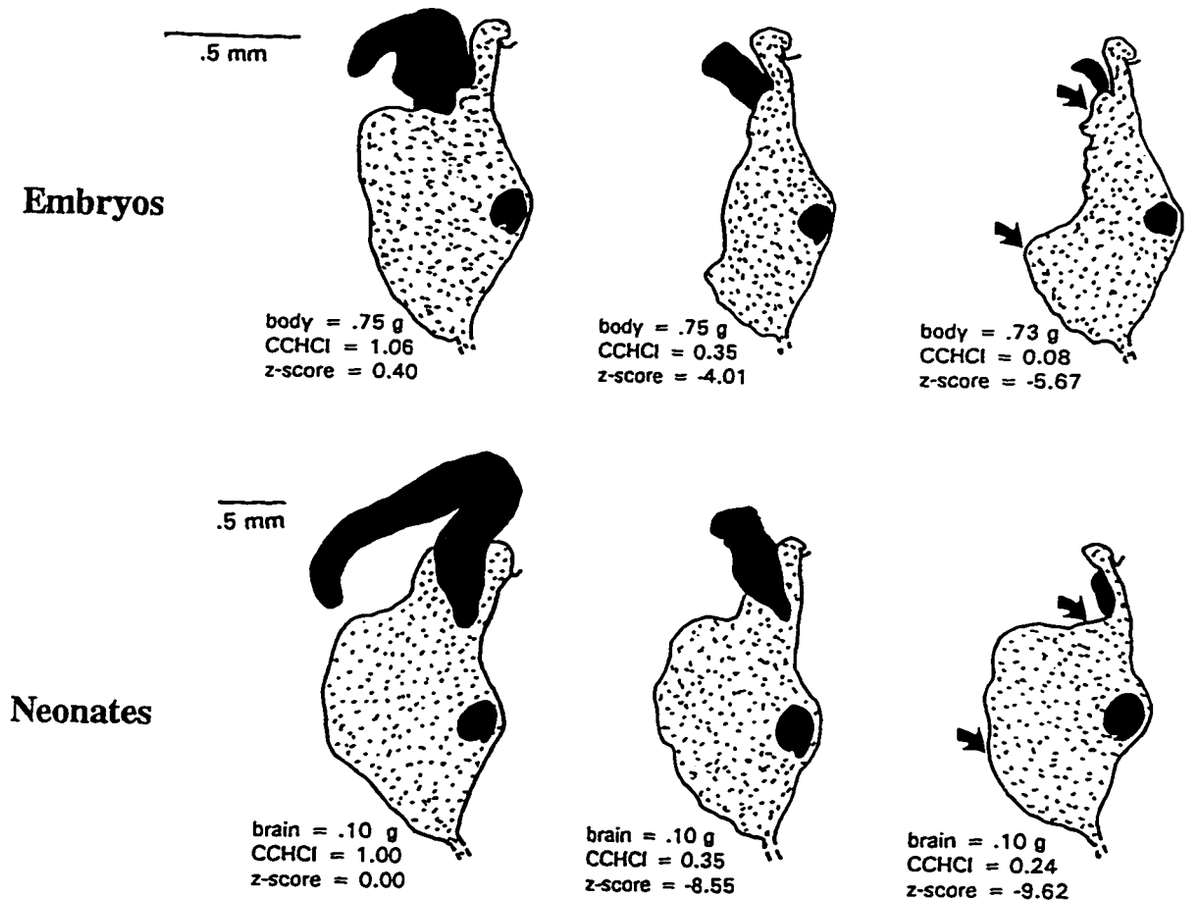
.5 mm
Embryos
body = .75 g
CCHCl = 1.06
z-score = 0.40
body = .75 g
CCHCl = 0.35
z-score = -4.01
body = .73 g
CCHCl = 0.08
z-score = -5.67
.5 mm
Neonates
brain = .10 g
CCHCl = 1.00
z-score = 0.00
brain = .10 g
CCHCl = 0.35
z-score = -8.55
brain = .10 g
CCHCl = 0.24
z-score = -9.62

Figure 6: Comparison of CCHC indices. Plot of CCHC z-score vs CCHC index for A) embryos and B) neonates. Dashed lines of x = 1.0 and y = 0 indicate the index values expected if CCHC size is normal.

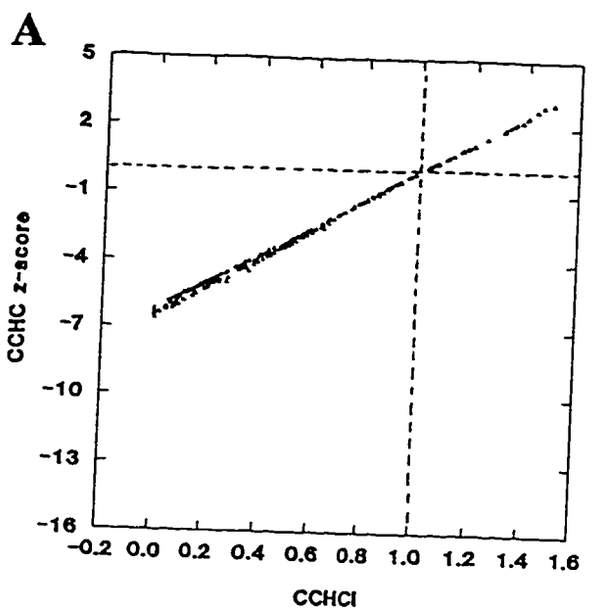
A
5
2
-1
-4
-7
-10
-13
-16
CCHC z-score
-0.2 0.0 0.2 0.4 0.6 0.8 1.0 1.2 1.4 1.6
CCHCl

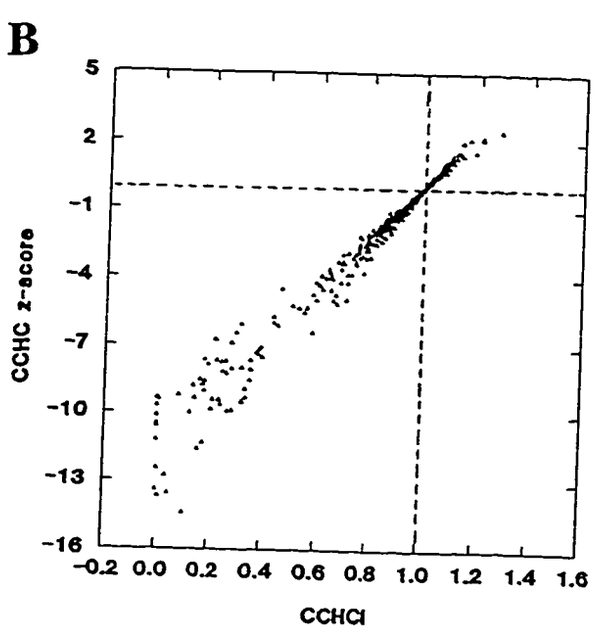
B
5
2
-1
-4
-7
-10
-13
-16
CCHC z-score
-0.2 0.0 0.2 0.4 0.6 0.8 1.0 1.2 1.4 1.6
CCHCl

Table 2: Mean and SD of CCHC index and z-scores for embryonic mice

	CCHC Index		CCHC z-score		
Group	Mean	SD	Mean	SD	t
BALB/Cwah1	0.218	0.179	-4.935	1.104	-23.23*
129	0.230	0.145	-4.849	0.926	-27.71*
$C129F_1$	0.590	0.248	-2.637	1.580	- 7.65*
$C129F_1$ x BALB	0.435	0.291	-3.604	1.865	-12.82*
$C129F_1$ x 129	0.587	0.435	-2.645	2.763	- 9.13*
$C129F_2$	0.708	0.350	-1.831	2.203	- 6.41*

* one-tailed $p < .05$, test of the difference between the mean z-score and the expected value of 0 for normal CCHC development.

Figure 7: Prenatal development of the midsagittal region in inbred strains and classical crosses. Plot of A) CCHC area B) AC area C) MS area against body weight for the BALB/cWah1 and 129 embryos and crosses between them. Dashed lines indicate values expected from B6D2F_2 hybrid embryos.

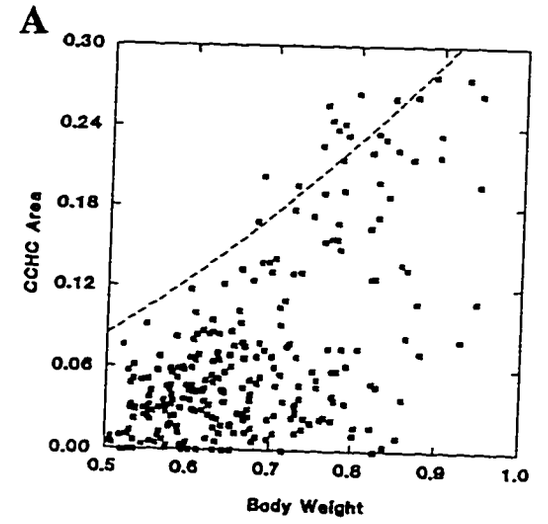
A
0.30
0.24
0.18
0.12
0.06
0.00
CCHC Area
0.5
0.6
0.7
0.8
0.9
1.0
Body Weight

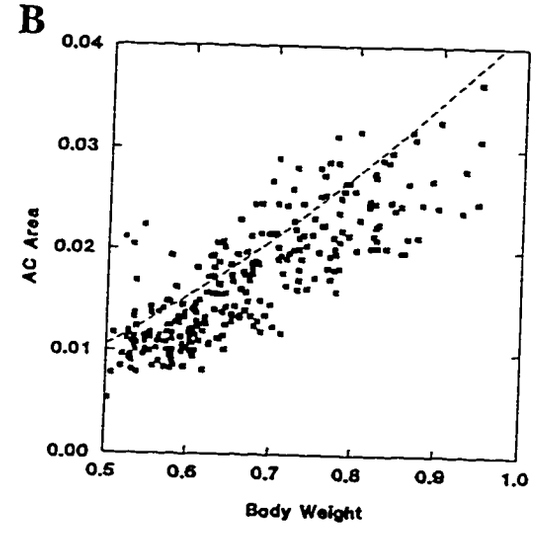
B
0.04
0.03
0.02
0.01
0.00
AC Area
0.5
0.6
0.7
0.8
0.9
1.0
Body Weight

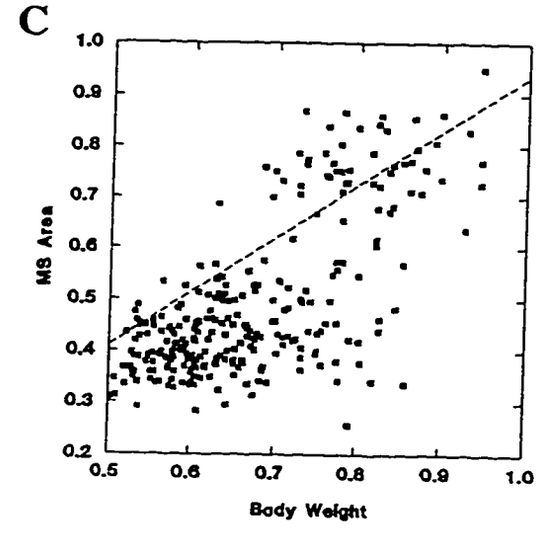
C
1.0
0.9
0.8
0.7
0.6
0.5
0.4
0.3
0.2
MS Area
0.5
0.6
0.7
0.8
0.9
1.0
Body Weight

adults, highest for the F_2 group and the backcrosses, with the F_1s falling between. The standard deviations for the 129 and BALB z-scores are close to 1.0, indicating complete penetrance for the CCHC defect prenatally in these strains. The variation in CC and HC index values within each group can be seen in Figure 8A, where frequercy distributions of the individual index values are presented separately for each group of embryos. It is clear that the majority of embryos exhibit retarded development of the commissures prenatally, most with index values more than two standard deviations below the mean for normal embryos. As previously suggested, the inbred strains BALB and 129 show complete penetrance for the commissural defect as embryos, being normally distributed with a mean well within the abnormal range of sizes. Although F_1s almost always exhibit normal commissures as adults, many embryos exhibit retarded development of the commissures as embryos, indicating that there must be a rapid period of recovery in these animals later in development. The distributions for the F_1 backcrosses appear to be slightly skewed to the right and resemble the distribution expected from the three-locus model which predicts that half of the embryos will be like the F_1s and half will be abnormal like BALB or 129. Wide variability in embryonic commissure sizes are exhibited by the F_2 embryos, as would be expected from the three-gene model as well. The distribution of CCHC sizes for the F_2 and backcross groups provides clear evidence of genetic segregation by virtue of increased variability. For the inbred strains and classical crosses, the anterior commissure (AC) exhibits slightly retarded growth compared to B6D2F_2 hybrid animals ($t = -11.8$, $p < .001$; see Figure 7B), although

the average difference is very small (.003 mm^2).

Postnatal growth of the commissures

Figure 9A presents CCHC sizes plotted against brain weight for the inbred BALB/cWah1 and 129 neonatal mice and the crosses derived from these strains. Many commissures are very small (<.3 mm^2) and fall well below the range expected for their brain weight, but not nearly as many animals fall into in this category as for the embryonic period. An analysis of the data for individual groups shows that all of the mean CCHC z-scores are significantly less than 0 except for the F_1 cross (Table 3). The F_1 neonates have recovered from an earlier defect but recovery appears incomplete as yet. This group now exhibits CCHC z-scores close to the normal range of -2.4 to 2.2 for $B6D2F_2$ embryos for this stage of development. The standard deviations of the z-scores for the BALB/cWah1 and 129 inbred strains are much greater than 1 (2.631 and 3.282, respectively), indicating that incomplete penetrance for the CCHC defect is now evident. It seems likely that compensation for the earlier defect in CCHC size (which showed complete penetrance) has occurred in some but not all of the brains of the mice in these inbred strains. Frequency distributions of the CCHC index (Figure 8) for the 129 and BALB/cWah1 neonates confirms that about half of these inbred animals have recovered from the prenatal defect and the distributions resemble those seen for adults of these strains. Almost all of the F_1 values are in the normal range of .82 to 1.21 found for the $B6D2F_2$ neonates, consistent with the adult pattern for this strain, although there is one animal that has a

Figure 8: Distribution of CCHC sizes in inbred strains and classical crosses. Frequency distributions of CCHC index values are plotted separately by groups for embryos and neonates.

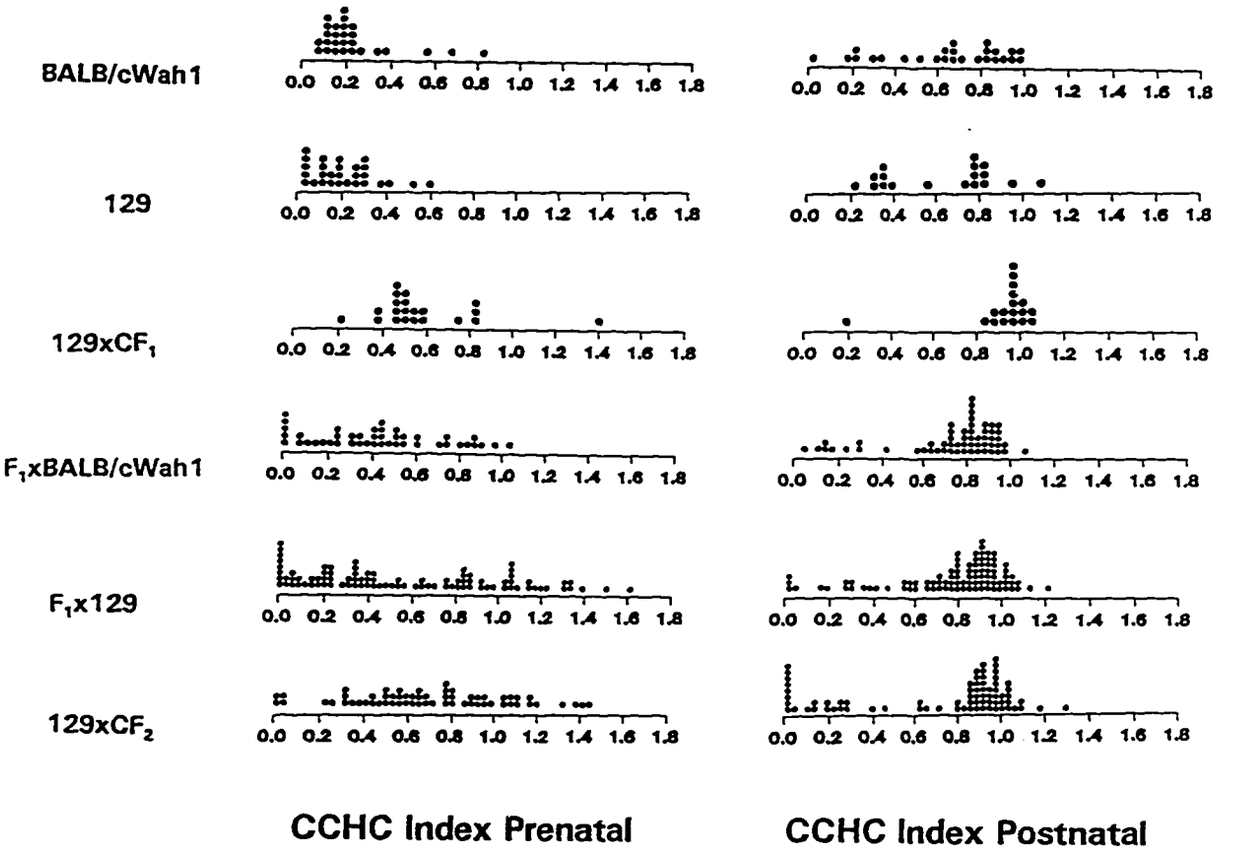
BALB/cWah1
129
129xCF1
F1xBALB/cWah1
F1x129
129xCF2
0.0 0.2 0.4 0.6 0.8 1.0 1.2 1.4 1.6 1.8
CCHC Index Prenatal
CCHC Index Postnatal

Figure 9: Postnatal development of the midsagittal region in inbred strains and classical crosses. Plot of A) CCHC area B) AC area C) MS area against body weight for the BALB/cWah1 and 129 neonates and crosses between them. Dashed lines indicate values expected from B6D2F_2 hybrid neonates.

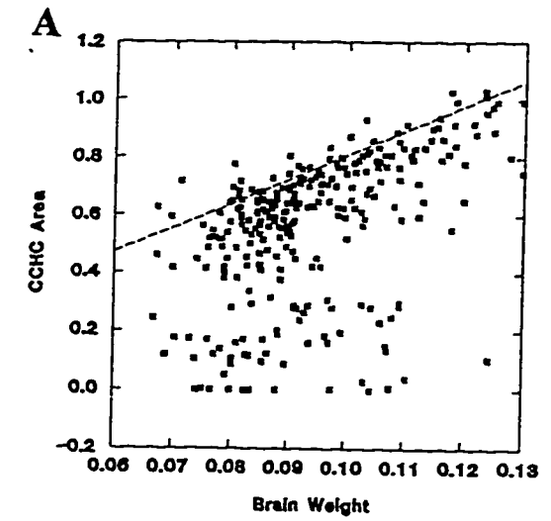
A
CCHC Area
1.2
1.0
0.8
0.6
0.4
0.2
0.0
-0.2
0.06 0.07 0.08 0.09 0.10 0.11 0.12 0.13
Brain Weight

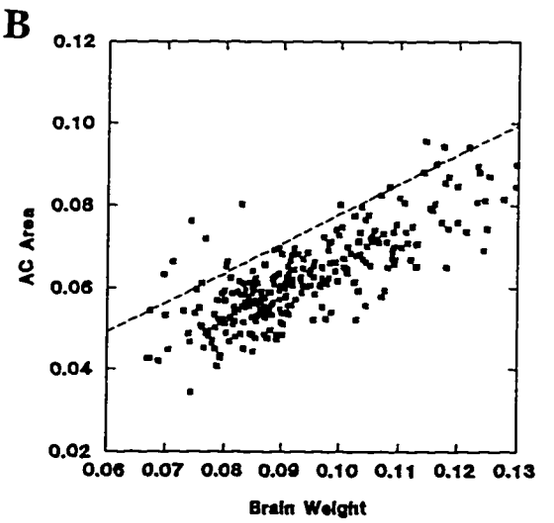
B
AC Area
0.12
0.10
0.08
0.06
0.04
0.02
0.06 0.07 0.08 0.09 0.10 0.11 0.12 0.13
Brain Weight

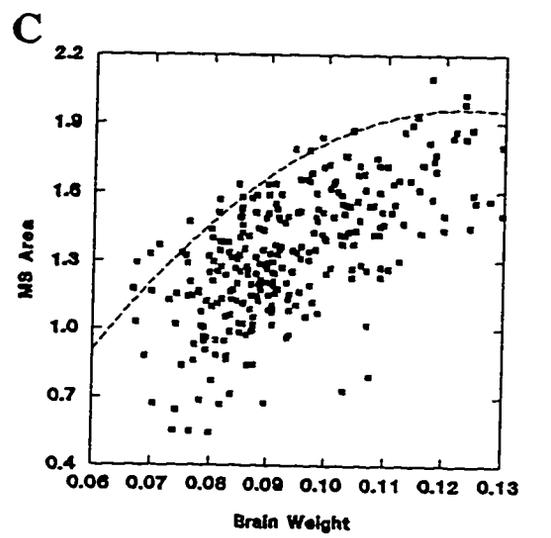
C
MB Area
2.2
1.9
1.6
1.3
1.0
0.7
0.4
0.06 0.07 0.08 0.09 0.10 0.11 0.12 0.13
Brain Weight

Table 3: Mean and SD of CCHC index scores for neonatal mice

	CCHC Index		CCHC z-score		
Group	Mean	SD	Mean	SD	t
BALB/cWah1	0.633	0.283	-3.643	2.631	- 7.06*
129	0.636	0.265	-4.402	3.282	- 5.69*
$C129F_1$	0.926	0.191	-0.929	2.390	- 1.65
$C129F_1$ x BALB	0.754	0.251	-2.942	2.985	- 7.44*
$C129F_1$ x 129	0.760	0.271	-2.915	3.370	- 8.25*
$C129F_2$	0.702	0.379	-3.420	4.233	- 6.95*

* one-tailed $p < .05$, test of the difference between the mean z-score and the expected value of 0 for normal CCHC development.

very abnormally small CCHC area. The distributions for the backcrosses are no longer bimodal, but are consistent with the prediction from the three-locus model that half of the neonates will be normal and half will show incomplete penetrance like BALB and 129. The distribution for the F_2 neonates also resembles that seen for adult F_2 animals (Wahlsten and Schalomon, 1994). Under the three-gene model, it is expected that 44.15% of CCHC sizes are normal, 37.5% show incomplete penetrance like the 129 and BALB/cWah1 strains, and 6.25% are severely affected like the inbred strain I/LnJ: a test of the frequency of defects in the F_2 group shows greater defects than the expected pattern ($\chi^2 = 12.2$, $p < .05$). A plot of the median index values for neonates versus those for fetuses (Figure 10) illustrates that there is a general recovery in commissure sizes after the late prenatal period so that by the time of birth (approximately E19 or 20) the majority of animals have recovered from an earlier defect in formation of the commissures.

Growth of the anterior commissure in inbred BALB/cWah1, 129 and intercross neonates is slightly retarded in comparison to normal hybrid B6D2F_2 mice at this age ($t = -27.1$, $p < .001$; see Figure 9B), but the average difference is very small (.011 mm^2). Growth is rapid and the AC area approaches adult size by about .13 grams body weight even though adult brains are much heavier (approximately .45 grams) in these animals.

Thresholds for CC and HC formation

Figure 10: Comparison of prenatal and postnatal CCHC development. Plot of median CCHC index of embryos versus neonates for each crossing group. The line represents the line of best fit from a regression analysis ($R^2 = .63$). Notice that the neonatal median values are consistently considerably greater than those for the embryos, indicative of substantial recovery from retardation of growth of the CC and HC prenatally. Abbreviations: BALBBX = backcross to BALB/cWah1; 129BX = backcross to 129.

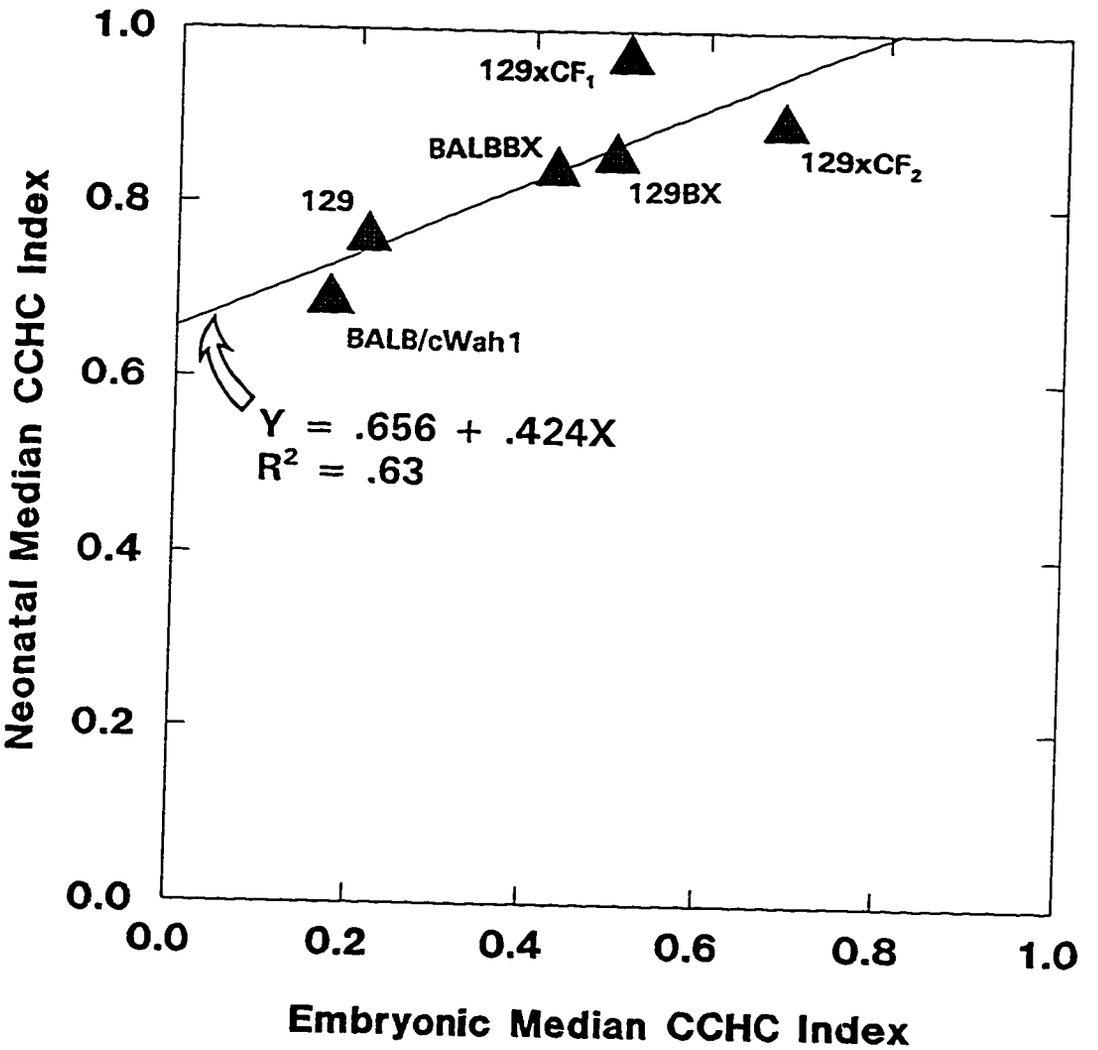
1.0
0.8
0.6
0.4
0.2
0.0
0.0
0.2
0.4
0.6
0.8
1.0
Neonatal Median CCHC Index
Embryonic Median CCHC Index
129xCF1
BALBBX
129BX
129xCF2
129
BALB/cWah1
Y = .656 + .424X
R2 = .63

A comparison of CC and HC sizes in embryos and neonates suggests that there are thresholds for formation of the commissures and a very short period just before birth during which recovery from an earlier defect may occur. Separate thresholds can be hypothesized for CC and HC development based on the known trimodal distribution of adult commissure defects (Wahlsten et al., 1997) and neonatal commissural defects (see Figure 11). Examination of the embryonic frequency distributions suggests that thresholds of CCHCI = 0.15 and 0.00 are reasonable (Figure 11A). To test this model, the proportion of embryos with indices below .15 was compared to the proportion of newborns with abnormal CC size (CCHCI < .50) and the proportion of embryos with an index equal to 0 was compared to the proportion of newborns with abnormal HC size (CCHCI < .10). The newborn CCHCI values of .5 and .1 for abnormality were chosen based on the cut-offs evident in the frequency distribution of newborn CC and HC sizes (Figure 11B). These values are slightly less than the cut-offs for normal adult morphology previously used (Wahlsten et al., 1997) because of the incomplete recovery evident in the neonates. The model was validated by correctly predicting CCHC defects in almost all groups of neonates (Table 4). The exception to this was the data from the F_2 animals, where more neonates exhibited defects of both the CC and HC than expected from the embryonic commissure sizes. Otherwise, the threshold model nicely accounts for the transition from a uniform distribution of commissure sizes prenatally to a trimodal distribution postnatally in the acallosal strains (Figure 11). When the thresholds are expressed as embryonic z-scores, values of -5.0 and -6.5 correctly predict the

Figure 11: Thresholds for development of the corpus callosum and hippocampal commissure. Frequency distributions of CCHC index sizes for A) embryos and B) neonates for mice from the BALB/cWah1 and 129 inbred strains and crosses derived from them. Note that the distribution for embryos is slightly skewed to the right while that for the neonates is trimodal, indicating that thresholds for development of the CC and HC occur prenatally. Shaded regions on the embryo distribution indicate the position of hypothesized thresholds i) for normal CC and HC sizes (CCHC index > .15) and ii) normal HC size with abnormally small CC (.15 > CCHC index > 0).

A

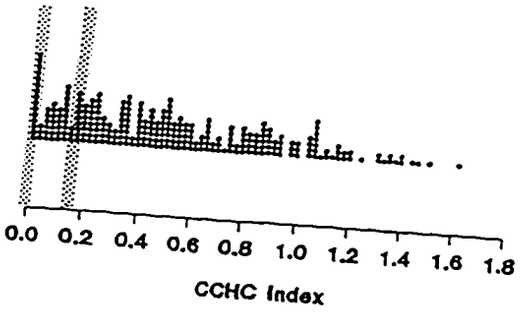
0.0 0.2 0.4 0.6 0.8 1.0 1.2 1.4 1.6 1.8
CCHC Index

B

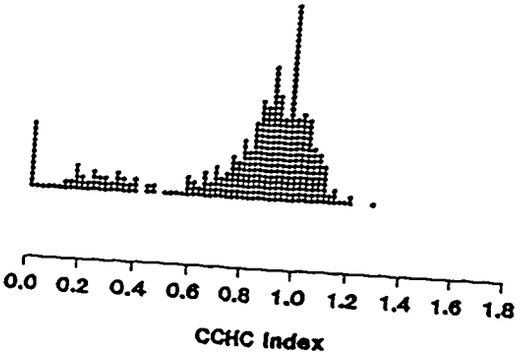
0.0 0.2 0.4 0.6 0.8 1.0 1.2 1.4 1.6 1.8
CCHC Index

Table 4: A) Proportion of neonates with abnormal CC predicted by embryo threshold of CCHCI = .15.

Cross	Embryo CCHCI < .15	Neonate CCHCI < .50
BALB/cWah1	40%	27%
129	41%	39%
$C129F_1$	0%	4%
$C129F_1$ x BALB	18%	16%
$C129F_1$ x 129	19%	15%
$C129F_2$	7%	28%*

B) Proportion of neonates with abnormal HC predicted by embryo threshold of CCHCI = 0.

Cross	Embryo CCHCI = 0	Neonate CCHCI < .1
BALB/cWah1	0%	4%
129	0%	0%
$C129F_1$	0%	0%
$C129F_1$ x BALB	9%	2%
$C129F_1$ x 129	9%	4%
$C129F_2$	2%	12%*

* $p < .05$, chi-squared test

neonatal pattern of defects. An embryo with a CCHC size 5 or more standard deviations below the mean for $B6D2F_2$ hybrid embryos will not develop a normal corpus callosum. This threshold is close to the value of -5.5 suggested by Wahlsten and Ozaki (1994).

Growth of the dorsal medial septum in acallosal mice

The septum is the area of grey matter lying between the anterior horns of the lateral ventricles, and the "medial septal nucleus" is the portion of this area along the dorsal midline. The medial septum contains primarily projections that descend to the diencephalon and brainstem and ascend to the hippocampal formation (Swanson and Cowan, 1979). Axons of both the corpus callosum and hippocampal commissure first cross midplane over the dorsal septal region, suggesting that morphology of the medial septum may be important in commissural formation. During early development, bilateral evaginations in the telencephalon produce the two telencephalic vesicles which are surrounded by the meninges and are separated by the interhemispheric fissure. It is presently not known whether the medial septal region is then formed by migration of cells from the lateral ventricles, cell division within the septal area or genuine fusion of the hemispheres. Glas (1975) proposed that cells migrate from the third ventricle rostrally and the lateral ventricles medially to form the septal region immediately ventral to the fissure. As the septal region then expands, the interhemispheric fissure fuses: the medial walls of the fissure contract,

interrupting the meninges, which causes the region dorsal to the contracting area to reform the floor of the fissure. In this way, the fissure is moved both rostrally and dorsally by the migrating septal cells. In contrast to this scenario, Silver et al. (1982) proposed that the primary event is a "zippering" of the hemispheres themselves, which then allows the septal cells to occupy the midplane region. In any event, growth of the medial septum and fusion of the hemispheres are intimately related and their spatial location suggests that these events may be implicated in the traverse of midline by commissural axons.

Prenatal growth

Growth of the area of the MS is rapid and linear in the prenatal phase of development (Figure 7C; see also Wahlsten and Bulman-Fleming, 1994). Examination of the distribution of areas of the medial septum suggests that there is an abrupt transition at about .8 g body weight where the MS suddenly doubles in size. A detailed examination of the shape of the MS at this age suggests that are two distinct forms of this part of the septum and that development occurs primarily through an abrupt transition in shape of the dorsal half of the caudal edge of the septum. In this way the dorsal portion of the medial septum abruptly goes from appearing "notched" to "rounded" (see Figure 5 for examples). Examination of serial sections on either side of midplane provides a better understanding of how this transition occurs: the dorsal edge of the septum fuses with a rapidly expanding cell mass that lies just caudal to the edge of the notched septum. Early in development,

this cell mass is evident in sections on either side of midplane but is not continuous between the hemispheres. It then grows laterally and is eventually evident in the midplane section, but is not yet fused with the dorsal edge of the septum at midplane. At this stage the cell mass appears as a distinct oval structure lying just caudal to the notched portion of the septum. The cell mass then expands, its rostral edge eventually touches the caudal edge of the septal region, at which point the two structures fuse and a rounded dorsal medial septum results.

Previous research has identified a "septal notch" defect in BALB/cWah1 mice - a possible single gene effect on delayed development of the dorsal thickness of the MS, the area that is seen to undergo a transition from notched to rounded. Measurement of the mean thickness of this region provides the best indication of this transition (Figure 12). Frequency distributions for the mean thickness of the dorsal medial septum for the acallosal crosses are presented in Figure 13. BALB/cWah1 mice all show the septal notch and have a mean width of only .3 mm at this age. In contrast, the distribution for 129 mice is bimodal and two distinct forms are evident: the notched (mean width = .3 mm) and the rounded (mean width = .6 mm) shapes. The pattern of septal thicknesses in the crosses between these two inbred strains supports a single gene mode of inheritance of this defect, such that the BALB notched allele is recessive to the 129 wild-type allele. Several observations are consistent with this genetic model: the backcross to BALB animals are mostly notched with only a few rounded septa; the backcross to 129 is bimodal like the 129 distribution; and the F_2 animals are 3/4 notched and 1/4 rounded. The results would fit the model better if

Figure 12: Growth of the dorsal medial septal region. Plot of the mean thickness of the dorsal region of the medial septum for A) embryos and B) neonates of the BALB/cWah1 and 129 inbred strains and crosses derived from them. Note the distinct gap in sizes at about .45 mm^2 for embryos and .70 mm^2 for neonates, indicating that fusion of the hemispheres in this region is a punctate event rather than a continuous one.

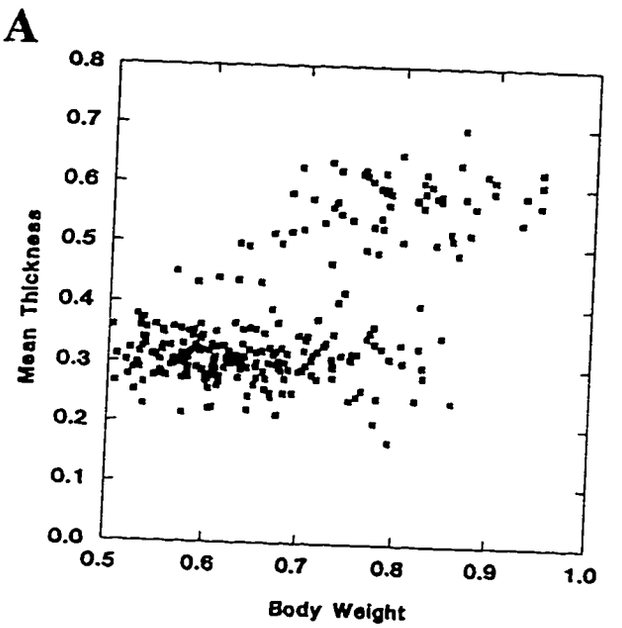
A
0.8
0.7
0.6
0.5
0.4
0.3
0.2
0.1
0.0
Mean Thickness
0.5
0.6
0.7
0.8
0.9
1.0
Body Weight

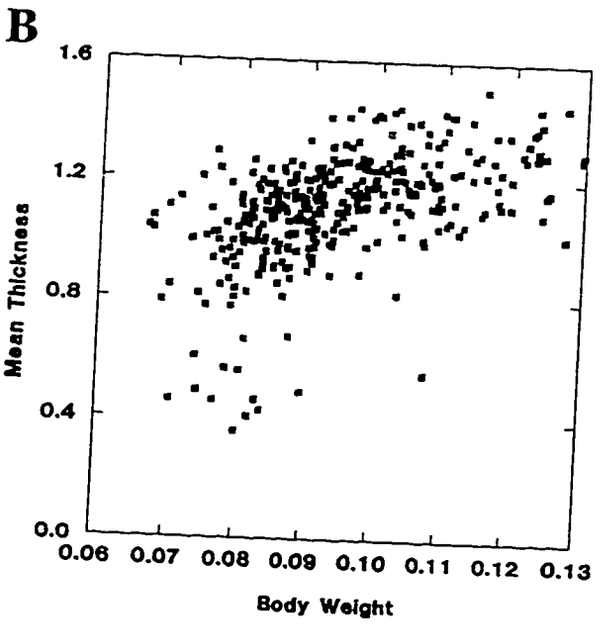
B
1.6
1.2
0.8
0.4
0.0
Mean Thickness
0.06
0.07
0.08
0.09
0.10
0.11
0.12
0.13
Body Weight

Figure 13: Distribution of medial septum thicknesses for inbred strains and classical crosses. Frequency distributions of the mean thickness of the dorsal region of the medial septum plotted separately by groups. A) Index values for individual embryos; B) Index values for individual neonates.

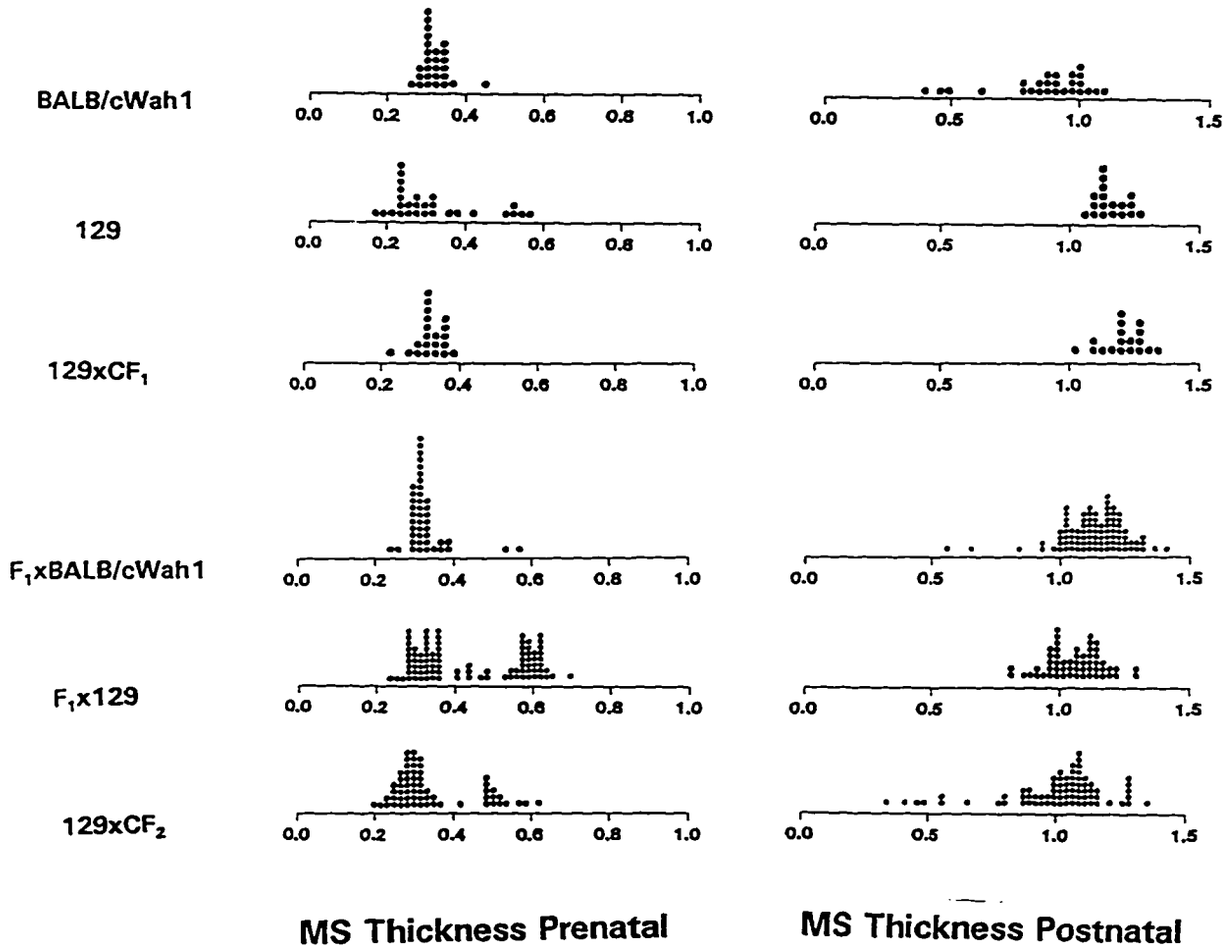
BALB/cWah1
129
129xCF1
F1xBALB/cWah1
F1x129
129xCF2
0.0
0.2
0.4
0.6
0.8
1.0
0.5
1.5
MS Thickness Prenatal
MS Thickness Postnatal

the distribution for the F_1s showed a few rounded septa. Surprisingly, when the morphologies of the dorsal medial septa are categorized as notched or rounded by an unbiased observer (V. Sparks), 7 of the 21 F_1 embryos are found to be rounded. Thus, examination of the shape of the dorsal medial septal region may provide a more accurate measure of the development of this region than quantification of dorsal widths. The fact that the individual distributions for the crossing groups are all uni- or bimodal confirms the suggestion that there is a sharp transition in MS development between the notched and rounded forms, even within a genotype.

Postnatal growth

Plotting MS area by brain weight for neonates suggests that growth continues to be rapid and almost linear up to about 1.9 mm^2 at .9 g brain weight, when the MS stops growing. An examination of the septum shapes for the individual brains suggests that the transition from notched to filled out form is normally complete at birth and that postnatal growth is due primarily to an overall increase in size that correlates with overall growth of the brain. However, an examination of the frequency distributions of the mean septal thickness for the acallosal groups of mice shows that there are a few brains which retain the notched form at this stage (Figure 13). These postnatal notched septa are all in the BALB/cWah1, the backcross to BALB and the F_2 groups, consistent with the genetic model proposed for the septal defect. It is hypothesized that these severely retarded animals are homozygous for the BALB/cWah1 notch allele. The postnatal notch phenotype does not occur in any of

the groups that have a 129 allele.

Relationship with commissure development

Examination of the morphology of the area of the medial septum suggests that the dorsal portion of the septum normally undergoes an abrupt transition in shape at about embryonic day 17, going from a notched form to a rounded form. Although the septal notch occurs in BALB/cWah1 mice who also exhibit agenesis of the corpus callosum, it is difficult to determine whether the two defects are causally related in these mice. The spatial relationship between the two structures suggests that they may be related, but several possibilities are suggested: 1) delayed fusion of the hemispheres in the dorsal septum may make it more difficult for commissural axons to cross midline; 2) delayed formation of the CC and HC may cause the hemispheres to remain separated by a wide gap; 3) a third developmental factor or factors at the cellular or molecular level may cause both delayed fusion of the hemispheres and a defect in the substrate for the commissural axons to cross midplane; or, 4) there may be no relationship between the two genetic defects. Examination of prenatal and postnatal plots of dorsal MS thickness versus CCHC area (Figure 14) suggests that there is some kind of relationship because almost all of the brains that exhibit normal septal development also exhibit normal CCHC sizes, and most of the brains with the notched form of the septum exhibit retarded formation of the CCHC, but not vice-versa. Fusion of the hemispheres in the medial septal region may be a permissive condition for axons of the CC and HC to cross midplane on schedule. However, it is

Figure 14: Relationship between CCHC and MS development. Plot of the mean thickness of the dorsal region of the medial septum versus CCHC area for A) embryos and B) neonates of the BALB/cWah1 and 129 inbred strains and crosses derived from them.

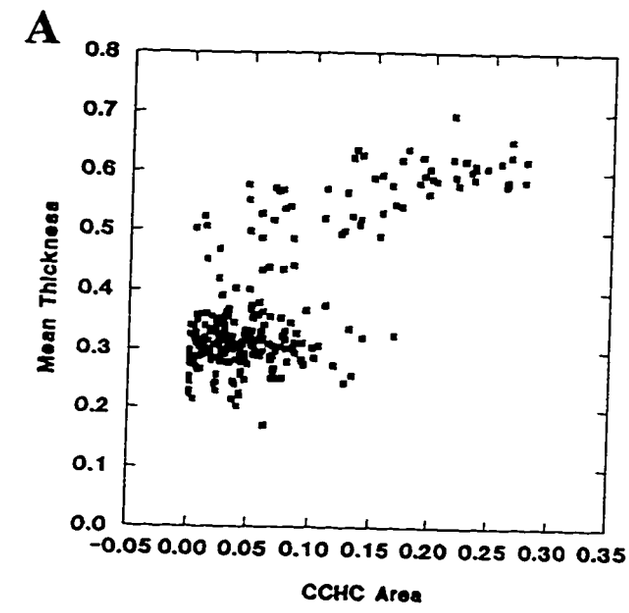
A
0.8
0.7
0.6
0.5
0.4
0.3
0.2
0.1
0.0
Mean Thickness
-0.05 0.00 0.05 0.10 0.15 0.20 0.25 0.30 0.35
CCHC Area

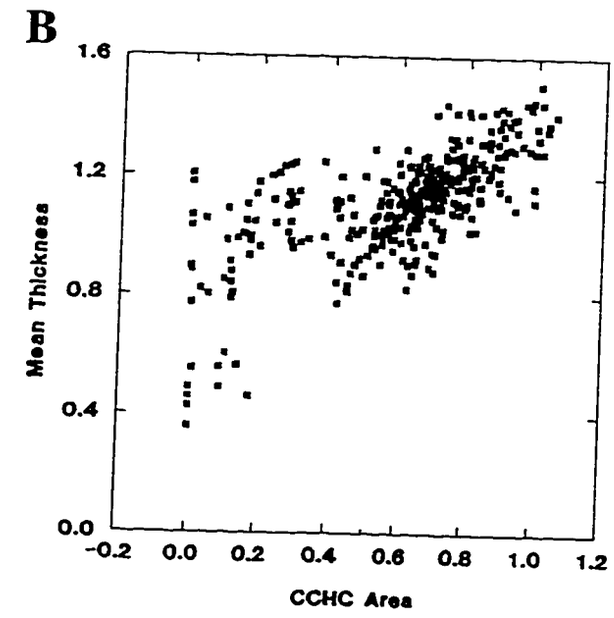
B
1.6
1.2
0.8
0.4
0.0
Mean Thickness
-0.2 0.0 0.2 0.4 0.6 0.8 1.0 1.2
CCHC Area

not a sufficient condition because there are brains in which the dorsal septal region has fused but development of the corpus callosum and hippocampal commissure is delayed.

Discussion

The results indicate that there is substantial developmental plasticity in the formation of the corpus callosum and hippocampal commissure. Recovery from prenatal retarded development of the commissures starts at about embryonic day 18 and is almost complete by the time of birth (approximately E20) in mice. However, there are thresholds of abnormality in embryos beyond which recovery does not occur. Results suggest that for the body weight range .5 to 1.0 g, an embryonic CCHC index of .15 is the threshold for normal development of the corpus callosum and an index of 0 is the threshold for normal development of the hippocampal commissure. Therefore, if no axons of the hippocampal commissure have crossed midplane by about .9 g body weight the HC will never attain a normal adult size and the corpus callosum will be completely absent. If the area of the CCHC has not grown to about .005 mm^2 by about .9 g body weight, then the hippocampal commissure will appear normal but the corpus callosum will be abnormally small. The abrupt thresholds for normal development of the corpus callosum and hippocampal commissure mean that small variations in the embryo are magnified into macroscopic differences in the anatomy of the adult brain.

Results from neonates and embryos produced by classical crosses between BALB/cWah1 and 129/ReJ mice also provide additional support for a two-gene model for agenesis of the corpus callosum in these strains. Support for the model is provided by the observations that: a) the distributions of the CCHC index for backcrosses to BALB/cWah1 and 129 are bimodal; b) the F_1 neonates have normal CCHC indices, like adult mice from this group; and c) the distribution of CCHC defects for newborn F_2 animals is as expected under the two-gene model. Previous studies on adult mice have provided strong evidence for the two-gene model (Wahlsten and Schalomon, 1994; Wahlsten, Sparks and Bishop, 1997) but this is the first study to support the model for embryonic development of the commissures. However, the embryonic results are also consistent with a polygenic threshold model and therefore can not provide definitive proof of the two-gene model.

A one-gene model for delayed development of the dorsal medial septum was also supported by the results of this experiment. Growth of the dorsal medial septum occurs by an abrupt transition in form from a notched shape to a fully rounded one. This transition corresponds with fusion between the dorsal region of the septum and a mass of cells lying caudal to this region in the midsagittal plane. The mechanism of the transition is somewhat surprising, as it had previously been thought that the dorsal region of the medial septum grew through gradual growth of the septal area itself because of cell proliferation or cell migration. Inbred strain 129 embryos exhibit both the notched and rounded forms at this stage in development of the dorsal medial septum region. In BALB/cWah1 mice the transition is delayed further and only the

notched form is evident prenatally. By birth this transition is complete in most animals, except a few mice from the BALB/cWah1 and BALB/cWah1 backcross groups that still exhibit the notch defect. It is hypothesized that a single gene is responsible for the delay in dorsal medial septal development, that the BALB/cWah1 and 129 inbred strains possess different alleles of this gene, and that the 129 allele is dominant over the BALB/cWah1 allele. There is some evidence that growth of the medial septal region is slightly delayed in the 129 strain compared to the C57BL/6J strain (Wahlsten and Bulman-Fleming, 1994), although less so than in the BALB/cWah1 strain. Therefore, it is likely that the 129 and C57BL/6 strains are also fixed for different alleles at the hypothesized genetic locus. However, although results of this experiment provide support for a single-gene model for delayed growth of the dorsal medial septal region, these results can also be explained by a polygenic threshold model. Therefore, while results support the single gene hypothesis, proof has not been provided.

The first axons of the hippocampal commissure to cross midline do so over the dorsal medial septal region (Livy and Wahlsten, 1997). Thus, it is possible that the septal notch defect plays a role in retardation of the cerebral commissures. However, both the 129 and BALB/cWah1 inbred strains exhibit agenesis of the corpus callosum but only the BALB/cWah1 strain has a severe delay in development of the dorsal septum (Wahlsten and Bulman-Fleming, 1994). Results from this study provide weak support for a relationship between these two midline defects. The area of the CC and HC grew normally only in embryos and neonates that exhibited the rounded

morphology of the dorsal septum. Development of the CC and HC was retarded in all embryos and neonates that exhibited the notched defect, but some axons were able to cross midplane in these brains.

It is proposed that agenesis of the corpus callosum and hippocampal commissure results from an interaction between genetic influences, relative structural growth, and chance. Genetic differences between inbred strains determine the location of the mean of each strain on the developmental scale. The spatial and temporal relationship between critical structures and events determines the location and nature of developmental thresholds. And stochastic (or probabilistic) events determine the numbers and types of classes that are found in each genotype. A complete developmental threshold model for development of the corpus callosum must take into consideration each of these types of influences.

Normal embryonic development is inherently random. Embryonic events depend on a long sequence of steps that begins at conception: each step has a high probability of occurring, but development is so complicated that the number of steps required is also extremely high. Randomness devolves from sensitive dependence on early conditions and events, maybe as far back as the third cleavage stage (Gärtner and Baunack, 1981), or even before fertilization, originating in ooplasmic differences (Gärtner, 1990). Random influences apply to any event in which small numbers of units interact, in a probabilistic fashion, in a way that influences later masses involving larger aggregates.

However, in genetic models of developmental defects this "3rd source of

variability" is often overlooked. This occurs despite ample experimental evidence that more than genes and environment influence development. Stochastic models can explain a number of developmental phenomenon at the cellular level, including cell differentiation (Gusella et al., 1976; Coleclough, 1983), growth (Smith and Martin, 1973), aging (Smith and Whitney, 1979), haemopoiesis (Kurnit et al. 1985), and oncogenesis (Knudson, 1971). Kurnit et al. (1987) have used stochastic models to simulate phenotypic variability of cardiac defects among individuals having identical genes and environments. In these simulations, stochastic variability was detected very early in development. The inherently random nature of development may account for why monozygotic twin mice are more similar than genetically identical dizygotic twin mice. Gärtner and Baunack (1981) propose that the differences in dizygotic twins may be due in part to non-genetic influences. It may also explain why attempts to decrease the variability in quantitative and qualitative traits in lab animals by controlling the genes and environment have been of limited success (Gärtner, 1990). The use of inbred strains and controlled environments did not substantially decrease variability in these traits, nor did a tremendous increase in environmental variability substantially increase it. Chance may also play a major role in many common malformations that cluster in families but occur less frequently than expected from simple Mendelian genetics (Kurnit, 1987).

Individual variability occurs because of the inherently random nature of developmental processes. When sharp thresholds are imposed on this variability, incomplete penetrance for many genetic defects results. Developmental threshold

models have been used to explain the incomplete penetrance of genetically determined traits, including ventricular septal defects (Newman, 1985), cleft lip (Wang et al., 1995) and cleft palate (Biddle, 1980; Vekemans and Biddle, 1984), and variation in the azygous vein (Biddle et al., 1991). In all of these models, genetic effects are thought to shift the timing of events in the embryo such that the window for successful development is narrowed and the liability to defect is increased. However, individual differences in development mean that while the liability to the defect is increased, it is not complete.

In a similar manner, a developmental threshold model for agenesis of the corpus callosum and hippocampal commissure has been proposed. The inherently random nature of development means that individual differences will exist in axon growth and development of the telencephalic midline, even in embryos from inbred strains raised in a controlled environment. Genetic defects shift the timing of critical events such that the period during which the axons may successfully traverse midline is altered. Thresholds for midline crossing by axons of the hippocampal commissure and corpus callosum are determined by the finite time during which the CC and HC axons remain at midplane waiting to cross. In support of this, Ozaki and Wahlsten (1993) have shown that axons of the corpus callosum leave the Probst bundle after only a few hours to reenter the ipsilateral cortex and never return to midplane. Although the developmental threshold model is useful for explaining the etiology of agenesis of the cerebral commissures, the genes and developmental defects that are critical for commissural formation in these mice remain to be identified.

Experiment 2: Development of the corpus callosum in acallosal and normal recombinant inbred lines derived from 129 and BALB/c mice: Genetic effects on events at the telencephalic midline

Introduction

The generation of recombinant inbred (RI) strains provides an elegant experiment in which the genes of two individuals are "mixed up" and recombined in several different configurations: examination of the resulting phenotypes may reveal something about the genetic nature of the trait under investigation. Recombinant inbred strains have traditionally been used for genetic mapping (Neumann and Collins, 1991; Crabbe et al., 1994) and the study of genetically correlated characters (Payloor and Seyfried, 1984). Wahlsten, Sparks and Bishop (1997; see also Wahlsten and Sparks, 1996) have generated recombinant inbred strains from BALB/cWah1 and 129/ReJ progenitors (the 9XC recombinant inbred strains) for the purpose of confirming the genetic model for transmission of agenesis of the corpus callosum and physically mapping and identifying the genes involved in this trait. However, the existence of consistently acallosal and normal strains provides good experimental and control groups to investigate events related to callosal agenesis in the embryo. Normal strains can serve as a control for comparison with abnormal strains because they are all derived from the same two parents and studies are facilitated by strains that have complete penetrance for commissural defects.

The standard protocol for generating recombinant inbred strains is to perform a cross between mice from the two inbred lines of interest, mate the resulting progeny to produce a number of F_2 animals, mate a large number (50 pairs or more) of randomly chosen pairs of the F_2 mice, and then inbreed these lines by brother-sister matings for at least 20 generations, by which time they can be considered to be isogenic (Green, 1981). Because of genetic recombination due to cross-over events during meiosis in the F_1, a set of combinations of alleles from the two inbred strain is produced.

Recombinant inbred strains have been generated from the BALB/cWah1 and 129/ReJ strains for the purpose of studying the genetics of commissural defects (Wahlsten, Sparks and Bishop, 1997). Within a few generations of inbreeding, three lines (RI-1, RI-3 and RI-4) showed the most extreme phenotype of absence of the CC and greatly reduced HC in almost every adult, a more extreme defect than observed in I/LnJ mice (Livy and Wahlsten, 1991). These lines are hypothesized to be homozygous recessive for the alleles at the two loci that together cause severe retardation of embryonic commissure formation. In addition, several other lines of mice (RI-21 and RI-23) quickly showed almost consistently normal commissures (CC and HC) in the adult. These lines are hypothesized to be homozygous recessive at the putative loci. The breeding results are consistent with the hypothesized two-gene model for callosal agenesis (Wahlsten and Schalomon, 1994). Conclusive evidence for the genetic model was provided by a variation on the recombinant inbred method in which the most extreme acallosal lines were intercrossed. None of the offspring

showed a lessening of the commissural defect, as would be expected under the competing polygenic threshold model.

Table 5 presents the frequency of commissural defects observed in recent generations of seven of the RI strains. While certain strains may be classified as normal or acallosal, it is obvious that a degree of phenotypic variability exists and that strains within a classification may differ somewhat. Acallosal strain 4 is the only one with a completely consistent developmental outcome, having no CC and a small HC in all cases. Strains 1 and 3 have been classified as acallosal, although occasionally a normal HC is seen in these strains and sometimes even a small CC is observed in strain 3 mice. Strains 21 and 23 have been classified as normal, but the CC is sometimes reduced or absent in these mice and this defect occurs more often in strain 23 than 21. Strains 14 and 15 have been classified as variable, however they exhibit different patterns of commissures and strain 15 is generally more defective than strain 14. Therefore, although the RI strains are referred to as normal, acallosal, and variable, these are only general classifications used to describe the usual adult anatomy of mice within a group.

The anomalous results observed in the extreme strains, the differences in frequency of commissural defects between strains within a grouping, and the greater than expected frequency of defects in the F_2 generation (Experiment 1; Wahlsten et al., 1997) can not be accounted for by a simple two-gene model. Several alternative explanations have been suggested to account for these anomalies. There may be one or more modifier loci that shift the distributions of events in the embryonic brain by

Table 5: Frequency of commissural defects in adult recombinant inbred mice

RI Strain	N	Generations of Inbreeding	Normal CC and HC	Small CC, Normal HC	No CC, Normal HC	No CC, Small HC
1	30	9 to 13	0%	0%	7%	93%
3	32	9 to 14	0%	9%	25%	66%
4	60	9 to 15	0%	0%	0%	100%
14	27	9 to 13	22%	41%	11%	26%
15	36	9 to 15	0%	39%	56%	5%
21	20	9 to 15	90%	0%	10%	0%
23	16	9 to 13	62%	19%	19%	0%

small amounts; the genotype, including the genetic background, may influence not only the mean of a distribution but its variance as well; or the mode of inheritance at one major locus may not be completely recessive when the other major locus is homozygous (i.e. Juriloff, 1995). A final test of the two-locus model and variations upon it will best be made by identifying the genes themselves.

However, these RI strains provide an excellent opportunity to examine genetically determined events in the embryonic brain that may be implicated in development of the corpus callosum and hippocampal commissure. Comparison of observations in embryos with the adult pattern of defects for these strains will help to elucidate the development and genetic mechanisms of defective development of the cerebral commissures. Examination of the RI strains as embryos may also help to refine further the genetic model for agenesis of the corpus callosum by eliminating or supporting suggested variations on the two-gene model. Examination of embryonic development of the commissures in the RI strains will also aid in interpretation of the functions of the genes involved, once they are identified.

In part I of this experiment, differential labelling with lipophilic dyes is used to examine development of the hippocampal commissure and corpus callosum at midplane and to examine the relative timing of the formation of these two midline structures. General purpose stains (i.e. haematoxylin and eosin, silver nitrate) do not distinguish between axons of the corpus callosum and the hippocampal commissure prenatally. The lipophilic dyes DiI and DiA are ideally suited for this purpose (Godement et al., 1987; Honig and Hume, 1989). These fluorescent tracers can be

used with fixed tissue, provide precise labelling of individual axons, and their passive transport within the lipid bilayer of membranes makes them particularity suited for prenatal research (Elberger, 1993). Most importantly, the use of dyes with different emission spectra (i.e. DiI and DiA) permits the differentiation of axons from different origins.

Normal, acallosal and variable 129XC recombinant inbred lines are examined in order to relate the development of these structures in the embryo to the known pattern of commissural defects in the adult. A narrow range of ages is examined in the period extending from after the HC is expected to have formed (.50 g) and before the first CC axons are expected to have crossed midplane (.68 g) in normal embryos. Because such a small range of ages is used, small sample sizes are used (5-6 animals per strain). Ozaki and Wahlsten (1993) found that the timing of axon emergence and axon growth rate is normal in acallosal embryos from the BALB/c and 129 inbred strains. Callosal axons arrive at midplane on schedule but then loop back to form a Probst bundle and often reenter the ipsilateral cortex. Livy and Wahlsten (1997) used lipophilic dyes to examine development of the hippocampal commissure in normal and acallosal mice, and results suggested that presence of the HC is important for formation of the corpus callosum and that absent CC may be a consequence of a defect that affects formation of the HC prior to arrival of the CC axons at midplane. Therefore, it is hypothesized that axons arrive at midplane on schedule in the RI embryos and that there are no differences in timing or variability of axon growth between the lines. It is also expected that formation of the HC in the embryo is

related to CC absence in the adult in these strains: HC development should be more advanced in the normal strains compared to the acallosal strains. In addition, a few older embryos (> 1.0 g) are double-labelled in order to examine formation of the Probst bundles and rerouting of HC axons in severely defective brains.

In part II of this experiment, the anatomy of the midline region is examined in the midsagittal plane and measurements taken of the size of the CC and HC, the AC, the MS and the thickness of the dorsal medial septum in normal, acallosal and variable RI embryos. Wahlsten and Bulman-Fleming (1994) found evidence for a single gene defect in the dorsal region of the medial septum in BALB/c but not 129 mice. Results from Experiment 1 supported the single gene hypothesis for this defect and suggested that development of the CCHC and dorsal medial septal region may be related. In addition, Experiment 1 identified developmental thresholds for normal development of the corpus callosum and hippocampal commissure in inbred strains and classical crosses of mice. For the RI strains, it is hypothesized that the embryonic CCHC defect is more extreme in the acallosal lines than in BALB/cWah1 and 129/ReJ inbred strains, that the normal RI strains show retarded prenatal commissure development but recover from this defect by birth, and that the extreme RI lines exhibit the septal notch defect. It is also proposed that genetic differences between the normal and acallosal RI strains produce a shift in the mean of the CCHC size distribution prenatally and that thresholds imposed on this distribution produce the large strain differences observed as adults.

Finally, in order to further examine possible defects in the midline substrates

for axon growth, part III of this study compares the anatomy of the midline region in the coronal plane in the same 129XC RI strains. The coronal plane is especially good for examining the relationship between development of the CC, HC, closure of the interhemispheric fissure and fusion of the hemispheres. Structures in the coronal plane are first quantified in a sample of B6D2F_2 hybrid embryos in order to provide a standard for normal development. Then samples of normal, acallosal and variable 129XC RI strains are examined and compared to each other and to the standard for midline development. It is especially interesting whether the interhemispheric fissure is abnormally deep or wide in acallosal brains and what the spatial and temporal relationship is between the fissure and the developing corpus callosum and hippocampal commissure. Results from embryonic observations of midplane structural development are correlated with the observed frequencies of callosal defects in adults of the RI strains in order to examine the relationship between putative defects in the substrates for guidance across the midplane and formation of the commissures.

Methods

Mice, matings and fetuses

Subjects were mice from 7 recombinant inbred strains that have been formed from pairs of 129 x BALB F_2 mice (Wahlsten, Sparks and Bishop, 1997). The lines

were generated from hybrid crosses of a 129/ReJ female x BALB/cWah1 male. In the F_2 generation, pairs of parents were chosen randomly and their offspring were then inbred by full-sib mating. This study used three strains of acallosal mice (RI-1, RI-3, RI-4) between the 11th and 16th generations of inbreeding, two strains of normal mice (RI-21 and RI-23) at the 15th generation of inbreeding, and two strains of variable mice (RI-14 and RI-15) at the 13th, 14th, and 15th generations of inbreeding.

One adult male and one to five adult females were placed together in a cage for four hours or overnight, after which the females were checked for vaginal plugs. When a plug was detected, the female was weighed and then housed singly for the duration of gestation. Conception (0.0 days) was considered to be the midpoint between plug detection and the previous plug check. All mice were housed in a common room with 12 hours light - 12 hours dark illumination (lights on at 6 a.m.) and maintained at about 23° C. They were housed in 29 x 18 x 13-cm opaque plastic mouse cages with Aspen-Chip bedding (Northeastern Products Corp., Warrenburg, NY) and a few sheets of toilet tissue added. Pregnant females were provided with a Nestlet for improved nest construction and all mice were given free access to breeder food (PMI Feeds Rodent Blox 5015) and Edmonton tap water.

Embryos were extracted between gestational days 16 and 18 (E16 and E18) to obtain mice at the appropriate stage of development, as measured by body weight. As proposed by Kaufman (1992), all mice studied prenatally are referred to as embryos, even though some have completed organogenesis and might be regarded as

fetuses. To extract the embryos, pregnant females were anaesthetized with an overdose of sodium pentobarbital (120 mg/kg, intraperitoneal injections) and their uteri were removed and rinsed in a 0.9% solution of saline in ice. The uteri were cut open and each embryo was separated from its placenta by cauterizing the umbilical artery. Embryos were rinsed in ice-cold 0.9% physiological saline, carefully blotted to remove excess fluid and weighed to the nearest mg. Immediately after weighing, the body weights of the embryos were evaluated and embryos were selected for inclusion in each part of this study.

Part I - Axon tracing with lipophilic dyes

Embryo selection, perfusion and fixation

In the evaluation of CC and HC axon growth using lipophilic dyes, embryos with body weights between .50 and .68 g were selected. This is the period in development after the HC has formed but before CC axons have crossed midplane in normal embryos (Ozaki and Wahlsten, 1992; Livy and Wahlsten, 1997). The number and weight range of embryos collected from each of the strains and providing useful data are shown in Table 6. In addition, a few older embryos (> 1.0 g) from RI strains 21 (normal) and 4 (acallosal) were collected to examine formation of the Probst's bundles and rerouting of HC axons.

Immediately after weighing, each embryo was perfused through the left ventricle with 3-5 ml of 10 mM phosphate-buffered saline followed by 10-15 ml of

Table 6: Number and weight range of embryos from RI strains examined using lipophilic dyes

Strain	Phenotype	N	Body Weights (g)
1	Acallosal	4	.517-.637
3	Acallosal	6	.560-.625
4	Acallosal	6	.544-.646
14	Variable	6	.544-.627
15	Variable	6	.540-.647
21	Normal	5	.579-.672
23	Normal	5	.525-.667

6% paraformaldehyde in 0.1 M phosphate buffer (pH 7.6) by means of a peristaltic perfusion pump, micropipettes and a stereomicroscope. Embryo heads were immersed in fresh fixative for 3-5 days. At this time the cerebral cortex of both hemispheres was exposed by removing the occipital bone with fine tooth forceps and the head was stored in fresh fixative and stored until the dye crystals were inserted.

Dye Insertion

Labelling of axonal membranes was achieved using crystals of the carbocyanine dye DiI (1,1'-dioctadecyl-3,3,3',3'-tetramethylindocarbocyanine perchlorate) and the aminostyryl probe DiA (4-(4-dihexadecylaminostryryl)-N-methylpyridinium iodide) (Molecular Probes, Eugene, Oregon). The brain was extracted from the skull and the caudal parts of the entorhinal and occipital cortices were removed to expose the hippocampal fimbria (Livy and Wahlsten, 1997). With the aid of a dissecting microscope and a graticule in the eyepiece, a 30-50 μm crystal of DiI was inserted into the area of each hippocampal fimbria using the tip of a fine dissecting pin. The frontal cortex was then labelled with a crystal of DiA placed in the centre of the anterior third of the cortex of each hemisphere. All brains were double-labelled. After insertion of dye crystals, the brains were placed in fresh fixative and stored in the dark at 37° C for 4-6 weeks.

Sectioning and viewing

Previous research has suggested that tissue at these young ages suffered

extensive damage because of sheer stress, especially in embryos where midline fusion was limited and only a few axons had crossed midplane (Livy and Wahlsten, 1997). Therefore, brains were infiltrated with gelatin in order to provide structural support before being sectioned. The brains were first rinsed in 0.1 M phosphate buffer for 2 h at 37° C. They were then infiltrated with 2% gelatin at 37° C for 6 h, 5% gelatin at 37° C for 12-24 h and then the gelatin was fixed with 4% paraformaldehyde for 48 h at 4%. Brains were sectioned in the coronal plane at 50 μm thickness using a microslicer (DSK-DTK 1500E) and a sapphire knife (Pelco). Sections were collected in serial order, soaked overnight in a 1:1 solution of 100% glycerol and 8% PFA (pH 10.0) at 4° C, then mounted on slides in the same solution and coverslipped. To provide staining of cell nuclei, 0.02% bis-benzimide was added to the overnight solution of all sections (Senft, 1990). Specimens were stored at 4° C in order to keep the dye labelling stable for longer periods.

Sections were viewed and photographed with a Leitz epifluorescence microscope equipped with rhodamine filter set (B2) for viewing the orange-red DiI florescence and a fluorescein filter set (I3) for viewing the yellow-green DiA fluorescence. Photographs were made with Kodak Ektachrome ASA 400 color print film.

Measurements and analysis

Several distances were estimated for each cortical dye injection site with the aid of a graticule in a 10x eyepiece: 1) distance between the centre of the dye

injection site and the front edge of the main bundle of growing CC axons; 2) distance from the front edge of the main bundle to the point at the midsagittal plane where the CC axons would eventually cross. In only a few cases were growth cones evident far ahead of the leading edge of the main bundle of growing axons; most of the leading growth cones were grouped together into what is described here as the main bundle. Where the axons were found in several consecutive sections, the measurement took account of both the growth along the curved path from the dye injection site to the front edge of the growing CC axons evident in a single section, and longitudinal growth across a series of sections. Longitudinal growth across a series of sections was estimated by calculating the number of sections between the centre of the dye injection site and the leading edge of the growing axons, and multiplying this number by the section thickness (50 μm). Multiple regression methods (Marascuilo and Serlin, 1988) were used to analyze the CC data in the same manner as for normal (Ozaki and Wahlsten, 1992) and acallosal fetuses (Ozaki and Wahlsten, 1993). The dorsal-ventral thickness of the hippocampal commissure was estimated from bis-benzimide labelled tissue.

Part II - Midline anatomy in the sagittal plane

The strains and number of mice examined in the sagittal plane are summarized in Table 7. Embryos between .54 and .90 grams were selected for this part of the study because this is the weight range during which the septal notch defect first

Table 7: Number and weight range of embryos from RI strains examined in the sagittal plane

Strain	Phenotype	N	Body Weights (g)
1	Acallosal	11	.543-.877
3	Acallosal	10	.641-.739
4	Acallosal	10	.622-.771
14	Variable	10	.627-.860
15	Variable	10	.627-.860
21	Normal	11	.623-.815
23	Normal	11	.624-.783

becomes evident and the first axons of the corpus callosum normally cross midplane. Approximately 10 embryos were examined from each strain, as this is the number required to detect the septal notch defect with 80% power, based on previous research indicating that this defect has a large effect size (d = 1.5) at .7 grams body weight (Wahlsten and Bulman-Fleming, 1994). Histology, correction for artifacts, sagittal reconstructions and measurements were made using standard procedures as described in Experiment 1.

Part III - Midline anatomy in the coronal plane

The strains and numbers of mice examined in this part of the experiment are presented in Table 8. Embryos to be examined in the coronal plane were selected to be between .45 and .80 g body weight. Because embryonic development of telencephalic midplane structures had not been quantified previously, embryos with a wide range of body weights during the period when CC and HC axons are normally crossing midplane were examined. Normal development in the coronal plane was quantified in a sample of 22 B6D2F_2 embryos between .40 and 1.00 g body weight.

Histology

Immediately after weighing, whole embryos were fixed by immersion in Bouin-Duboscq fixative for 48 hours. Shortly after being placed in fixative, each embryo had the scalp removed and small slits were cut in the skull lateral to midline

Table 8: Number and weight range of embryos from RI strains examined in the coronal plane

Strain	Phenotype	N	Body Weights (g)
1	Acallosal	9	.453 - .760
3	Acallosal	10	.615 - .752
4	Acallosal	10	.619 - .775
14	Variable	10	.604 - .807
15	Variable	9	.547 - .801
21	Normal	10	.514 - .807
23	Normal	8	.593 - .747

to aid in penetration of the fixative. Embryos were then transferred to several changes of 70% ethanol after which whole heads were embedded in paraffin for sectioning in the coronal plane. Serial sections were cut at 10 μm and stained with haematoxylin and eosin. Sections were cut carefully in order to ensure that the angle of cutting was perpendicular to the dorsal surface of the brain and symmetrical in the medial-lateral plane. Tracings were made with a Leitz tracing device and measurements were made with a Numonics 2200 graphics tablet and the Sigma Scan program from Jandel.

Dehydration shrinks neural tissue substantially and slicing the paraffin block dorsal to ventral compresses the section to some degree, which necessarily affects measures of area and distance. The magnitudes of the artifacts have previously been estimated for data collected at the University of Alberta (see Experiment 1). Distance and area measures were corrected by multiplying the raw measure by the appropriate correction factor.

Coronal landmarks

Examination of serial sections in the coronal plane rapidly made it evident that errors in cutting may cause structures to be in different sections in different brains. In order to control for the differences in cutting angle between brains, a careful survey was made of pertinent landmarks related to morphometry of midplane structures (Figure 15). In order to assess the accuracy of cutting in the medial-lateral plane, notes were made on the section numbers in which the first extension of the

Figure 15: Measurements made in the coronal plane. A) Sketch of the coronal plane at the anterior-posterior landmark in a B6D2F$_2$ mouse brain (approximately .70 g body weight), showing normal development of the CC and HC. B) Sketch of the midline region at the anterior-posterior landmark in a B6D2F$_2$ mouse brain (approximately .70 g body weight), showing structures measured. Abbreviations: AC = anterior commissure; ACA = anterior cerebral artery; CC = corpus callosum; CF = columns of the fornix; HC = hippocampal commissure; IG = indusium griseum; LF = longitudinal cerebral fissure; LV = lateral ventricle.

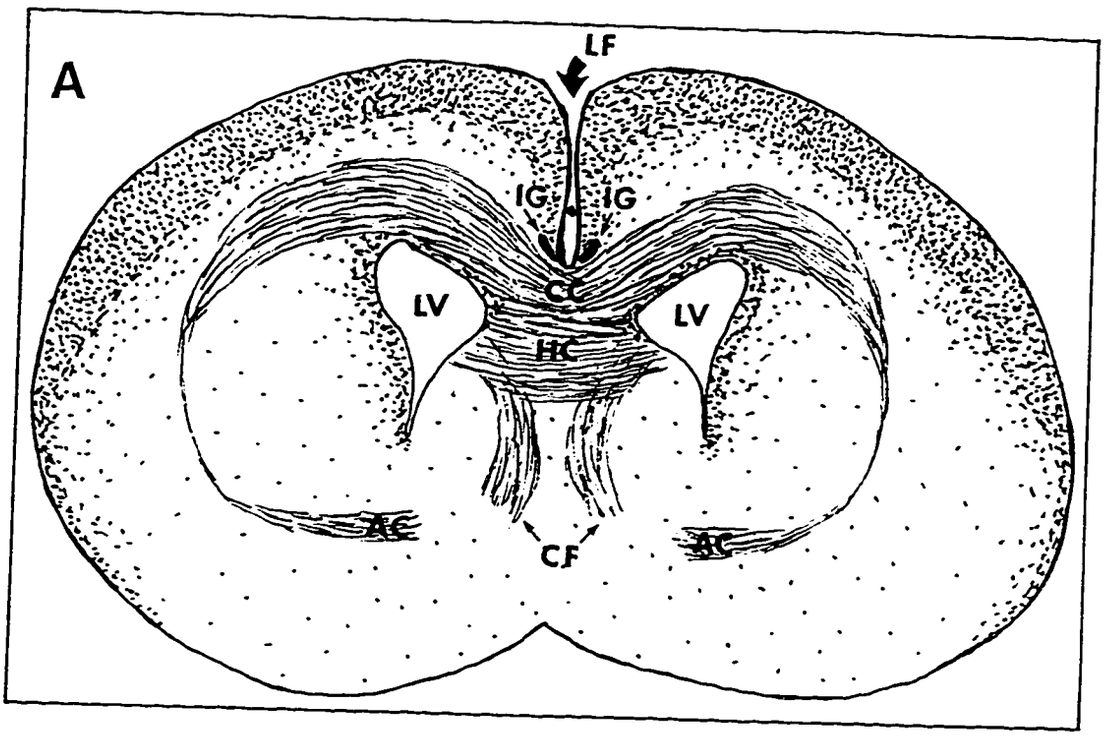
A
LF
IG
IG
CC
LV
LV
HC
AC
AC
CF

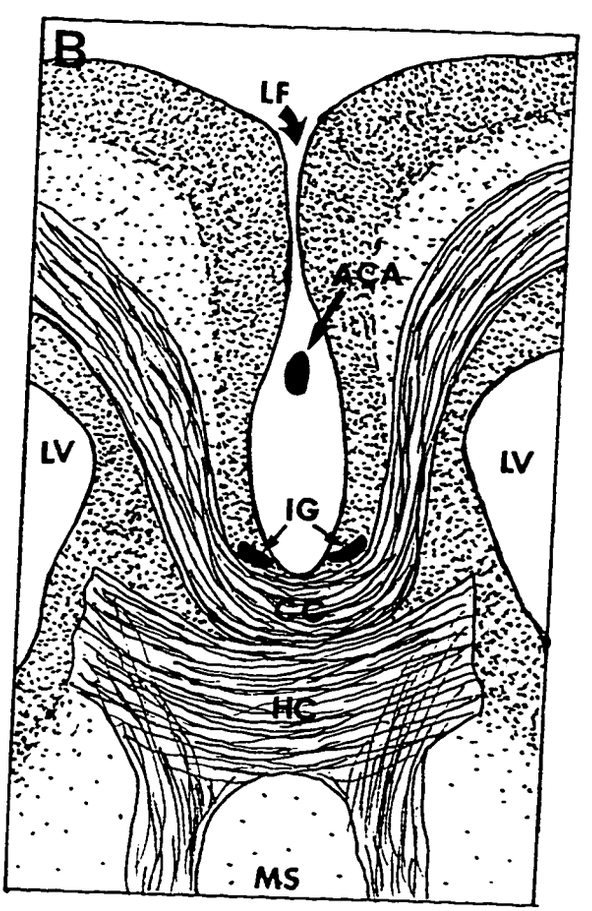
B
LF
ACA
LV
LV
IG
CC
HC
MS

anterior commissure arrived under the lateral portion of the third ventricle (see Figure 15A) and the interventricular foramen (foramen of Munro) first appeared in the left and right halves of the brain. The lateral cutting angle was very accurate in most brains because these structures occurred in the same section for the two hemispheres or only one or two sections apart (10-20 μm). After a detailed survey of landmarks that may be useful in identifying the midsagittal plane, it was decided that for the purposes of morphometric quantification of the development of midplane structures near where the CC and HC axons first cross, the section midway between where the columns of the fornix meet the fimbria and where they reach their most anterior position may provide the best indication of the central location of CC/HC defect in the RI lines. The fornix columns course ipsilateral to midline in the septal region and contain primarily fibres connecting the hippocampus with the mamilliary bodies and the septal nuclei (Swanson and Cowan, 1979). In the rostral-causal direction the fornix columns form a horseshoe shape and are closest to midplane coronally at their most anterior point. The first section where both left and right limbs of the columns of the fornix join the fimbria, such that distinct fornix columns can no longer be seen near midplane and the fimbria can be clearly seen on both right and left sides, was indicated for each brain. The most anterior section where both columns of fornix could be seen at their closest approach to midplane was also noted. Then the section midway between these two landmark sections was calculated and the interhemispheric fissure region of this section was traced at 100x for each brain (see Figure 15B). In addition, observations were made on several aspects of midplane development in

serial sections to gain a better understanding of the three-dimensional development of this region. The thickness of the CC and HC in serial sections was recorded in order to provide a measure of the area of this structure; the relationship between axons of the CC and HC was noted in serial sections to provide an indication of the early relationship between these structures in the rostral-caudal plane; and the appearance of cell bodies of the glial sling formation at or near midplane was observed through serial sections (see Figure 25). All brains were coded so that tracings and measurements were done without knowledge of the animals' age or pedigree.

Measurements

For each tracing, the distance from the ventral edge of the cells of the indusium griseum to the following points was measured: 1) the bottom of the longitudinal cerebral fissure; 2) the centre of the anterior cerebral artery; 3) the dorsal surface of the cortex (see Figure 15B). The distance between the cells of the indusium griseum on either side of midplane was measured, as was the maximum width of the longitudinal cerebral fissure and the distance between the edges of the lateral ventricles at their closest approach. The area of the intercerebral fissure within the pial membrane was also calculated. All measurements were corrected for tissue shrinkage and compression that occurred during processing.

Results

Body weight versus age

Chronological or embryonic age (e.g. E17) often is not the best indicator of stage of development. Significant differences in rate of development may exist between embryos at the same age within a litter or between strains. Stage of development or, for the range of ages in this study, body weight may be a more accurate estimate of maturity. By comparing brains of embryos at the same body weight rather than the same chronological age the confounding effects of differences in rates of development are avoided. The relationship between age and body weight (BW) has been found to be linear in hybrid B6D2F_2 embryos for the weight range .5 to 1.0 g body weight studied under equivalent conditions (Ozaki and Wahlsten, 1992) and is described by the equation E(Age) = 14.65 + 2.42 BW. For the recombinant inbred strains in this study the difference between the actual age of an embryo and the age expected from this equation was between 0.1 and 1.5 days and averaged more than 0.8 days. The developmental rate of the recombinant inbred embryos lagged about 1 day behind that of normal hybrids, a difference comparable to that for other inbred strains (e.g. 129/ReJ and BALB/cWah1) studied using these methods (Ozaki and Wahlsten, 1993; Livy and Wahlsten, 1997).

Possible differences in rate of development between acallosal, normal and variable strains of recombinant inbred mice were analyzed using litter means. Embryos within a litter are extracted at the same age and therefore analysis of individuals, rather than the litter mean, may inflate the size of effects. No significant

difference in overall rate of development was found between groups of RI strain embryos ($F = 2.49$; $p = .10$). However, because of the large differences in overall developmental rate between individual embryos, body weight rather than chronological age was used as the common measure for comparing different embryos (Wahlsten, 1987).

Part I - Axon tracing with lipophilic dyes

Clear growth cones could be visualized in all brains, indicating complete anterograde transmission of both dyes. The bis-benzimide gave a clear view of the nuclei of the pia membrane and other cells which were present in the midline region. Because the emission spectra of DiI and DiA overlap considerably with the fluorescein filter and the DiI emission is very bright, photographing the DiI and DiA labelling together at high magnifications was very difficult (see Figure 16A and B). Confocal imaging would provide better resolution of the double-labelling in these instances.

CC development

All embryos showed emergence of the CC axons from their cells of origin in the frontal cortex and substantial growth of axons toward the midplane crossing point (Figure 16A). Axons travelled laterally towards midplane, then ventrally and caudally along the edge of the cells of the ventricular zone until making a sharp

Figure 16: Growth of CC and HC axons in younger embryos. Corpus callosum axons from the frontal cortex had grown to within .50 mm of the putative midplane crossing point in all embryos. A) Growth cones (arrows) of callosal axons displayed a complex morphology as they approached the crossing point in this .60 g RI-23 embryo. Because of overlap in the emission spectra, HC axons labelled with DiI appear yellow-orange and CC axons labelled with DiA appear yellow in this photo. B) In a .63 g RI-23 embryo, the main bundle of CC axons was at midplane and one leading fibre (arrows) had crossed midplane. Because of overlap in the emission spectra, HC axons labelled with DiI appear yellow-orange and CC axons labelled with DiA appear yellow in this photo. C) and D) In one normal RI-21 strain embryo (.67 g) a corpus callosum and Probst bundles (asterisks) had formed. D) is a more posterior section than C) in which fewer frontal cortex axons are found. Fibres of the CC that have crossed midplane are between the bottom of the interhemispheric fissure and the dorsal surface of the hippocampal commissure. E) In this same embryo, the hippocampal commissure appeared to be of normal size. CC axons (arrows) do not stain with bis-benzamide. F) A .68 g acallosal RI-1 strain embryo in which only a small HC was evident at the bottom of the interhemispheric fissure (arrow). Scale bars = .05 mm.


A
HC
B
HC
C
D
E
F

lateral turn towards the point at the midsagittal plane where the axons would or did cross (Silver et al., 1982; Wahlsten, 1987; Ozaki and Wahlsten, 1993). All growth cones of CC axons for embryos in this weight range (.50 to .70 g) were found within .50 mm laterally and .015 mm caudally to the midplane crossing point and showed very little variability. This suggests that there may be a slowing of growth or a "waiting period" as the axons approach midplane. In almost all cases pioneers did not grow far in advance of the leading edge of the main bundle, consistent with previous observations of CC axons before they have crossed midplane (Ozaki and Wahlsten, 1992). In many of the older embryos (> .6 g) a few pioneer fibres could be seen at the edge of the midplane crossing point but not yet past midline (Figure 16A). These axons were consistently found either just on or slightly intermingled with the dorsal edge of the hippocampal commissure and directly in contact with the bottom of the pial membrane lining the interhemispheric cleft (Figure 16B).

In only one normal strain embryo (RI-21; .67 g) had the CC axons traversed midplane and was a well-formed callosum evident (Figure 16C). Double labelling of the CC and HC allowed the relative position of these structures to be visualized and it was evident that there was a large degree of intermingling between the two fibre systems. Again, the fibres at midplane were in contact with the bottom of the interhemispheric cleft and were found on the dorsal surface of the HC. It was surprising that in this normal RI strain embryo a substantial portion of the CC fibres did not cross midplane but instead travelled longitudinally and eventually swirled in a tight mass, forming a small Probst bundle on the dorsal edge of the CC (Probst,

1901; see Figure 16C). Probst bundles were also evident in a slightly smaller normal strain RI-21 embryo (.66 g), an acallosal strain RI-4 embryo (.64 g), and a variable strain RI-14 embryo (.63 g). It is not known whether in the .66 g RI-21 embryo later arriving CC axons would traverse midline or whether this embryo would have been acallosal as an adult, as happens in a few cases in this normal strain. However, the presence of Probst bundles and a CC in the normal strain embryo suggests that although adults of this strain usually exhibit normal commissural sizes, prenatal development may be retarded.

Multiple regression has been used to quantify normal growth of the CC axons from their cells of origin, across midplane and into the contralateral hemisphere for B6D2F_2 embryos (Ozaki and Wahlsten, 1992). Over the weight range .3 to 1.1 g, the distance from the dye injection site and the leading edge of the main bundle (ISMB) expected for a given body weight (BW) is given by the equation E(ISMB) = -3.944 + 9.936 BW for axons originating in the frontal cortex (Ozaki and Wahlsten, 1992). To compare axon growth in normal hybrids and recombinant inbred strains, the axon length expected from this equation was calculated for the RI embryos. Axon growth in RI embryos was significantly less than in hybrid embryos, averaging about .121 mm or .90 hours less ($t = -3.16$, $p = .002$), but the size of the effect was not large ($d = -.37$).

Comparisons between groups of recombinant inbred strains can be made using a multiple regression analysis in which axon length is predicted from body weight and then a dummy variable is added to represent the comparison of interest. The distance

from the dye injection site to the leading edge of the main bundle (ISMB) for a given body weight is best described by the equation: ISMB = -.683 + 4.234 BW (R^2 = .35) for the RI data. No difference was found in axon growth between acallosal and normal RI groups (p = .425). In addition, the variable group did not differ from either the acallosal (p = .515) or normal group (p = .066). As can be seen in Figure 17, body size is a reasonable predictor of CC axon growth to midplane in the RI embryos and large differences between acallosal, normal and variable strains of RI embryos are not evident. The slope of the line predicting axon length from body weight differs between B6D2F_2 and RI embryos because the value for B6D2F_2 hybrids was calculated over a much larger range of body sizes.

The distance of the main bundle of axons from the midplane crossing point (CPMB) allows the determination of when the CC axons first reach midplane, even when no single individual exhibits CC axon growth cones exactly at midplane (Ozaki and Wahlsten, 1992). Observation of the anatomy of many acallosal and normal embryos allowed the midplane crossing point to be defined as the point between the ventral edge of the cells of the indusium griseum and the dorsal surface of the hippocampal commissure or septal plate, when no HC had formed (Schambra et al., 1992). For prediction of body weight from CPMB, the Y-intercept is the body weight when axons would have just reached midplane (CPMB = 0; see Figure 18). Arrival of the axons from the frontal cortex is estimated to be at about .686 g body weight (E16.3) for normal hybrid B6D2F_2 mice (Ozaki and Wahlsten, 1992). The predicted body weight when CC axons cross midplane for the recombinant inbred

Figure 17: Growth of callosal axons from the frontal cortex to midplane. A plot of the distance from the injection site in the frontal cortex to the leading edge of the main bundle (ISMB) versus body weight for recombinant inbred embryos. Solid line indicates value expected for B6D2F$_2$ hybrid embryos (Ozaki and Wahlsten, 1992). Dashed line represents line of best fit for RI data (ISMB = -.683 + 4.234 BW; R^2 = .35). Symbols: circles = normal RI strain; squares = variable RI strains; triangles = acallosal RI strains.

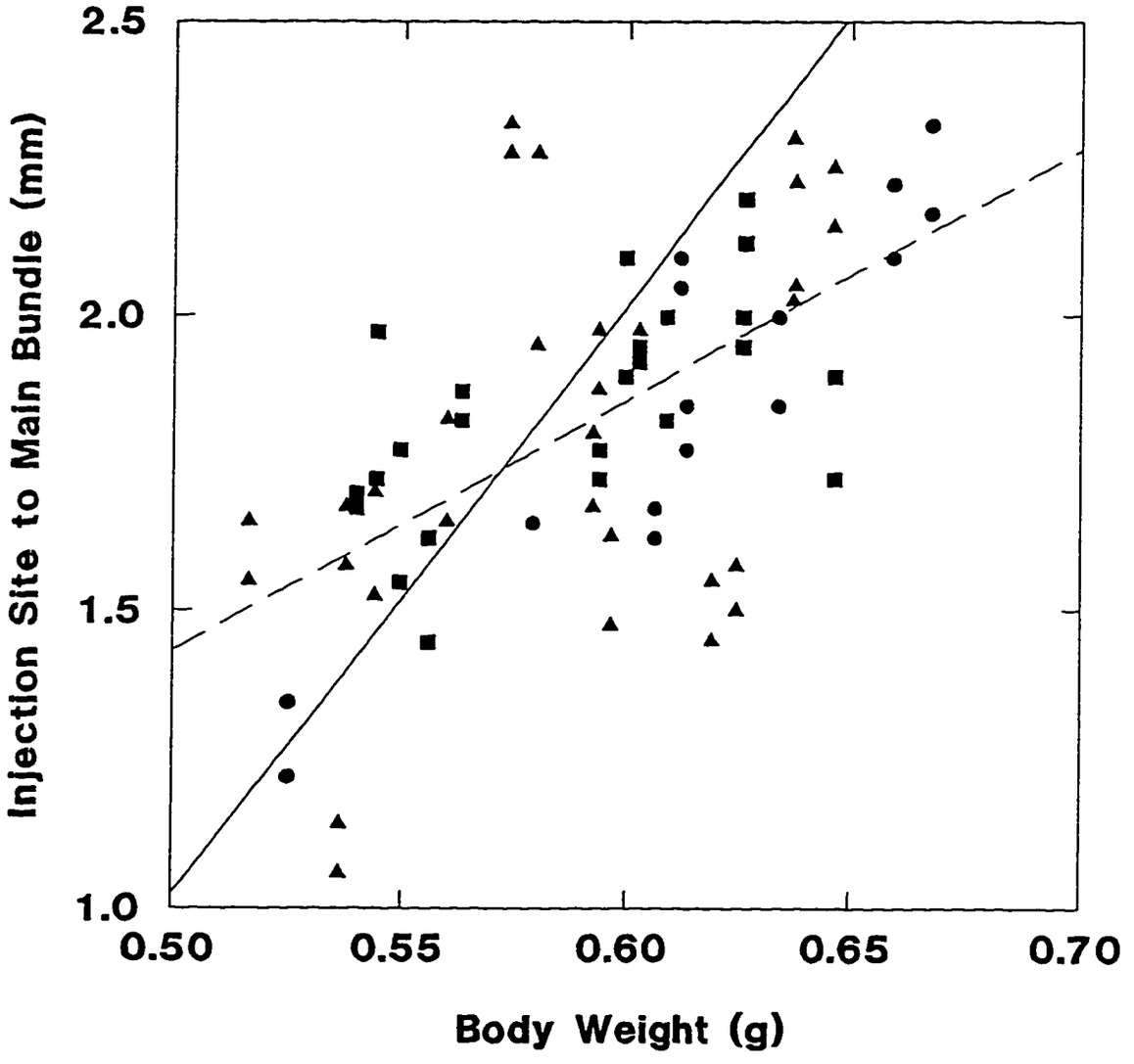
2.5
2.0
1.5
1.0
0.50
0.55
0.60
0.65
0.70
Injection Site to Main Bundle (mm)
Body Weight (g)

Figure 18: Predicted arrival of CC axons at the midplane crossing point. Distance from the leading edge of the main bundle of axons to the midplane crossing point (CPMB) versus embryonic body weight for axons from the frontal cortex. Solid line indicates the value expected for hybrid B6D2F_2 embryos (Ozaki and Wahlsten, 1992). Dashed line indicated line of best fit for RI embryos (CPMB = -1.239 + 1.903 BW; R^2 = .48). Analysis includes only brains in which no CC axons had crossed midplane or formed Probst bundles. Symbols: circles = normals RI strain; triangles = acallosal RI strains; squares = variable RI strains.

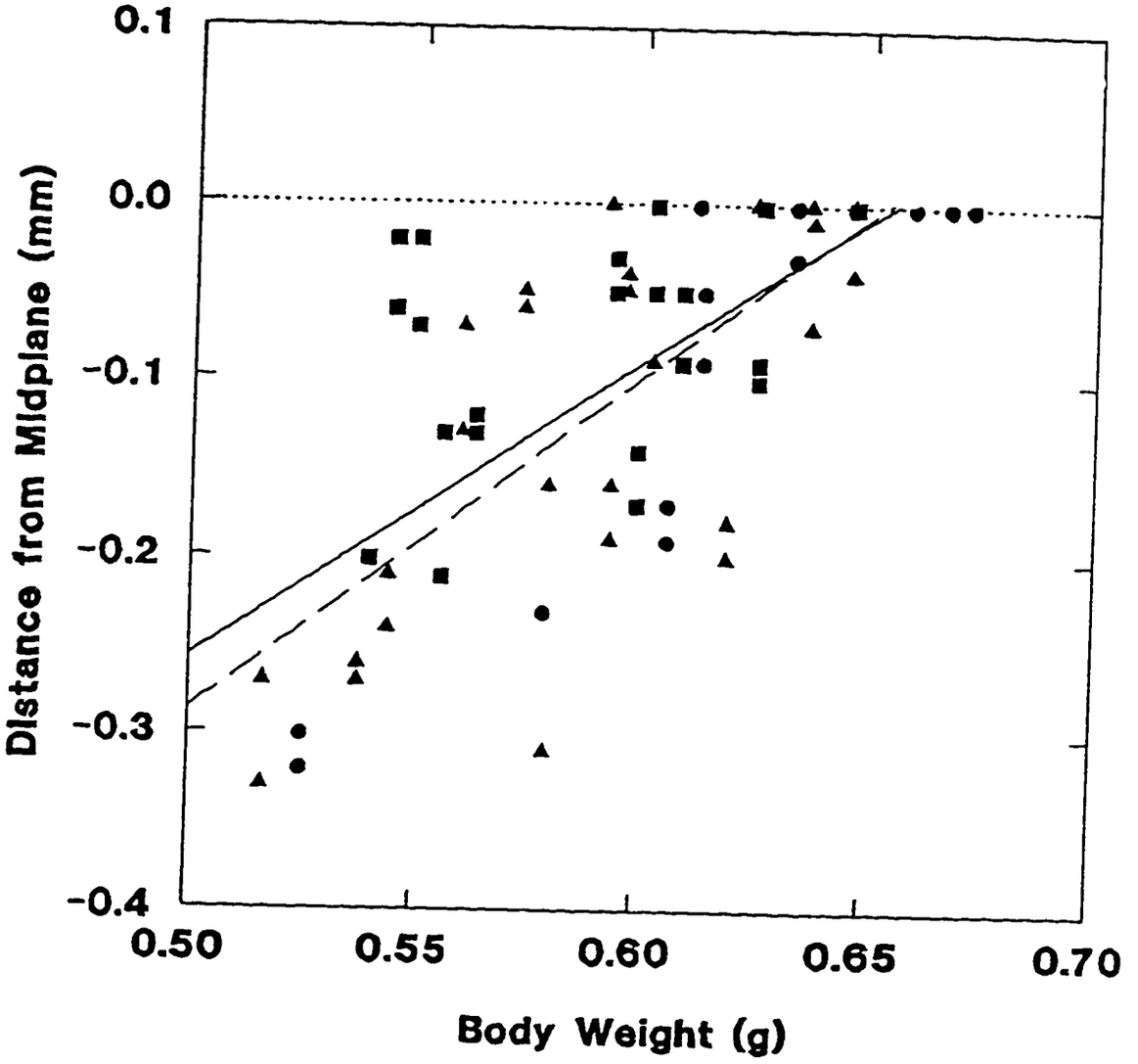
0.1
0.0
-0.1
-0.2
-0.3
-0.4
Distance from Midplane (mm)
0.50
0.55
0.60
0.65
0.70
Body Weight (g)

mice was earlier than for the hybrid mice, ($t = -37.54$; $p < .001$; see Figure 18). The predicted crossing weight was .650 g (E17.11) for the normal RI strains, .617 g (E17.09) in the acallosal RI strains, and .609 g (17.09) in the variable RI strains. Obviously, axon growth to midplane is not at all retarded in RI strains that usually exhibit agenesis of the corpus callosum. Groups of RI embryos differing in adult commissural morphology did not differ in CC axon growth or in time of arrival at the putative crossing point.

HC development

Formation of the hippocampal commissure at midline was clearly visualized using the dye labelling. The columns of the fornix coursed longitudinally parallel to midline in the septal region. In most of the embryos from the normal RI strains, axons of the hippocampal commissure could be seen to emerge from the columns and grow towards and across midplane. In most cases when a HC was present, it was large and contained many fibres emanating from the length of the fornix columns and connecting the two hemispheres (Figure 16E). In many embryos from the acallosal and variable strains the HC axons did not form interhemispheric connections but instead stopped at the walls of the interhemispheric fissure. Bis-benzimide staining showed a substantial space between the hemispheres in these embryos. In a few cases a small HC consisting of only a few axonal connections was visible, always located at the bottom of the pial membrane lining the fissure and coursing along the ventral outline of the fissure floor (Figure 16F).

The body weights of the recombinant inbred embryos in this study were carefully chosen to be greater than .40 g, the stage when the HC has formed in $B6D2F_2$ and $129XCF_2$ hybrid embryos (Livy and Wahlsten, 1997). Therefore, it is expected that a HC will be evident in normal strains of mice. A plot indicating whether a HC had formed in normal, acallosal, and mixed recombinant inbred strains by body weight (Figure 19) confirms this prediction and suggests that there is a relationship between development of the corpus callosum and formation of the hippocampal commissure in acallosal mice. In only two cases did any of the acallosal strain mice show a HC and in both cases it was very small (thickness < .03 mm). In contrast, all but one of the normal strain mice showed a substantial HC, in most cases being about .20 mm thick, the normal size for hybrid embryos at about .6 g (Livy and Wahlsten, 1997). The one normal strain embryo that did not have a HC was the same embryo that exhibited Probst bundles and no CC. As is expected if there is a relationship between HC and CC development, the strains with variable CC size as adults also showed the greatest amount of variability in HC development as embryos. Thus, there was considerable variability in formation of the hippocampal commissure in the recombinant inbred strains and this variability correlated with the degree of CC defect observed in adults of these strains.

Older embryos

A few older embryos (> 1.0 g body weight) from RI normal strain 21 and RI acallosal strain 4 were examined in order to obtain a description of CC and HC axon

Figure 19: Hippocampal commissure formation in RI embryos. Filled circles represent RI strain brains in which hippocampal commissure axons have crossed midplane and open circles indicate brains in which no HC axons have yet crossed midplane.

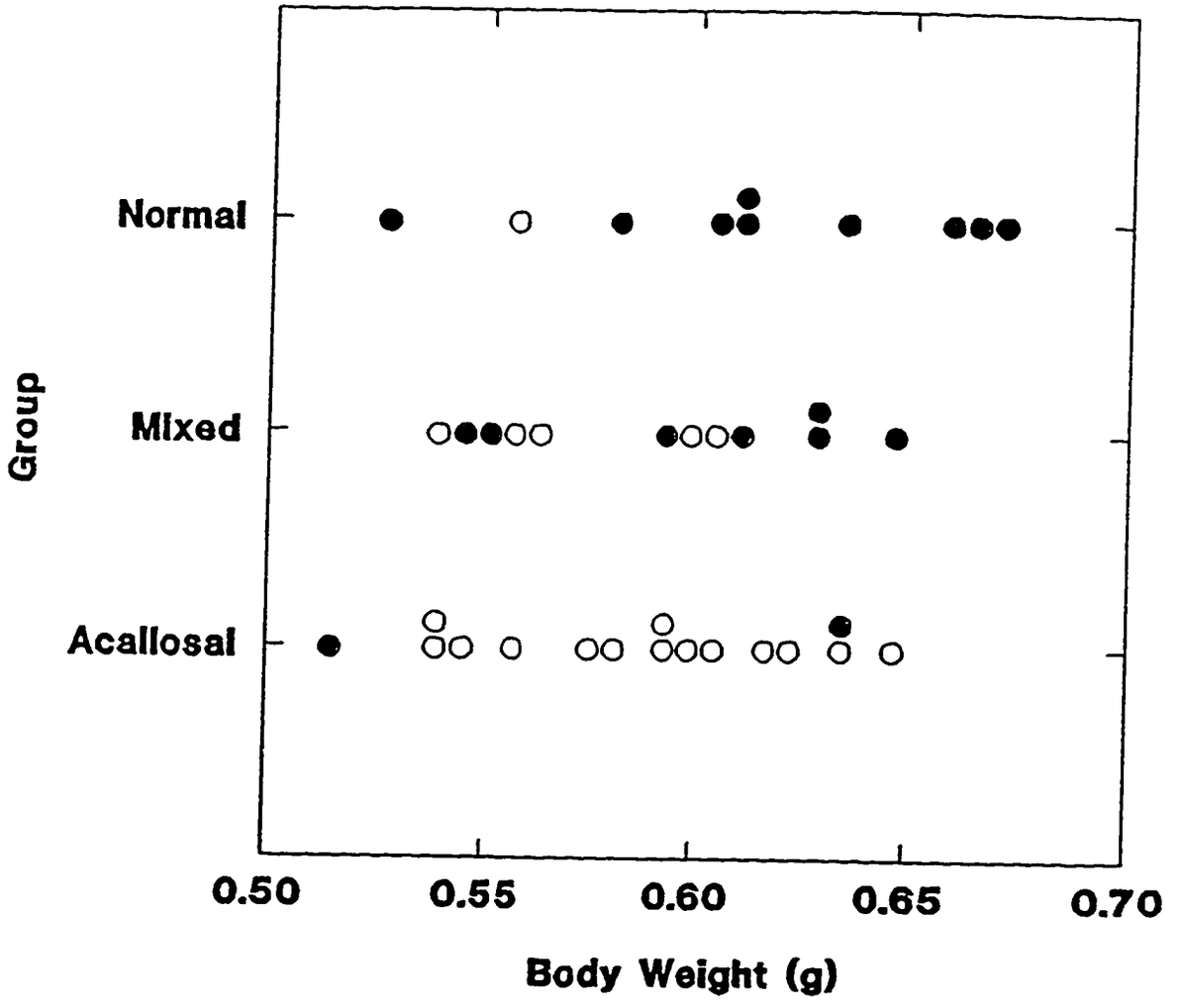
Normal
Mixed
Acallosal
Group
0.50
0.55
0.60
0.65
0.70
Body Weight (g)

pathways in the severely acallosal brain. In the normal strain embryo a very large CC was evident at midplane (Figure 20A) dorsal to the hippocampal commissure. Although a large CC was evident in bis-benzimide stained tissue, most of the labelling from the frontal cortex was found within Probst bundles on either side of midline and dorsal to the midplane CC (Figure 20A). However, morphology of the HC was normal in this brain (Figure 20B). The dorsal surface of the CC or, in more posterior sections, the HC, was consistently in close proximity to the bottom of the interhemispheric fissure.

Very large Probst bundles were observed in the acallosal strain embryo (Figure 20C), extending about .40 mm rostrally through several sections. However, the most interesting thing about this embryo was a novel axon route extending from the dorsal area of the columns of the fornix, around the Probst's bundles and then laterally to midplane ventral to the bundles (Figure 20D). These axons formed a heart shaped structure around the Probst bundles without extending into the area occupied by the bundles. This novel route was labelled with the dye injected into the hippocampal fimbria, suggesting that it may be the route taken by some hippocampal commissure axons that are not able to cross midplane. However, careful study of this novel axon tract in a larger sample is needed.

Part II - Midline anatomy in the sagittal plane

Corpus callosum and hippocampal commissure development

Figure 20: Growth of CC and HC axons in older embryos. A) .99 g RI-21 normal strain embryo in which the CC axons have formed both a large corpus callosum and Probst bundles (arrows). B) In a more posterior section the HC and CC (arrow) appear normal. C) 1.20 g RI-4 acallosal strain embryo in which the CC axons are unable to cross midplane because of an abnormally deep interhemispheric fissure (arrow) and instead form large Probst bundles. D) In this acallosal embryo some of the hippocampal commissure axons (arrows) reroute around the Probst bundles to the edge of the interhemispheric fissure dorsal to the Probst bundles. Scale bars = .05 mm.

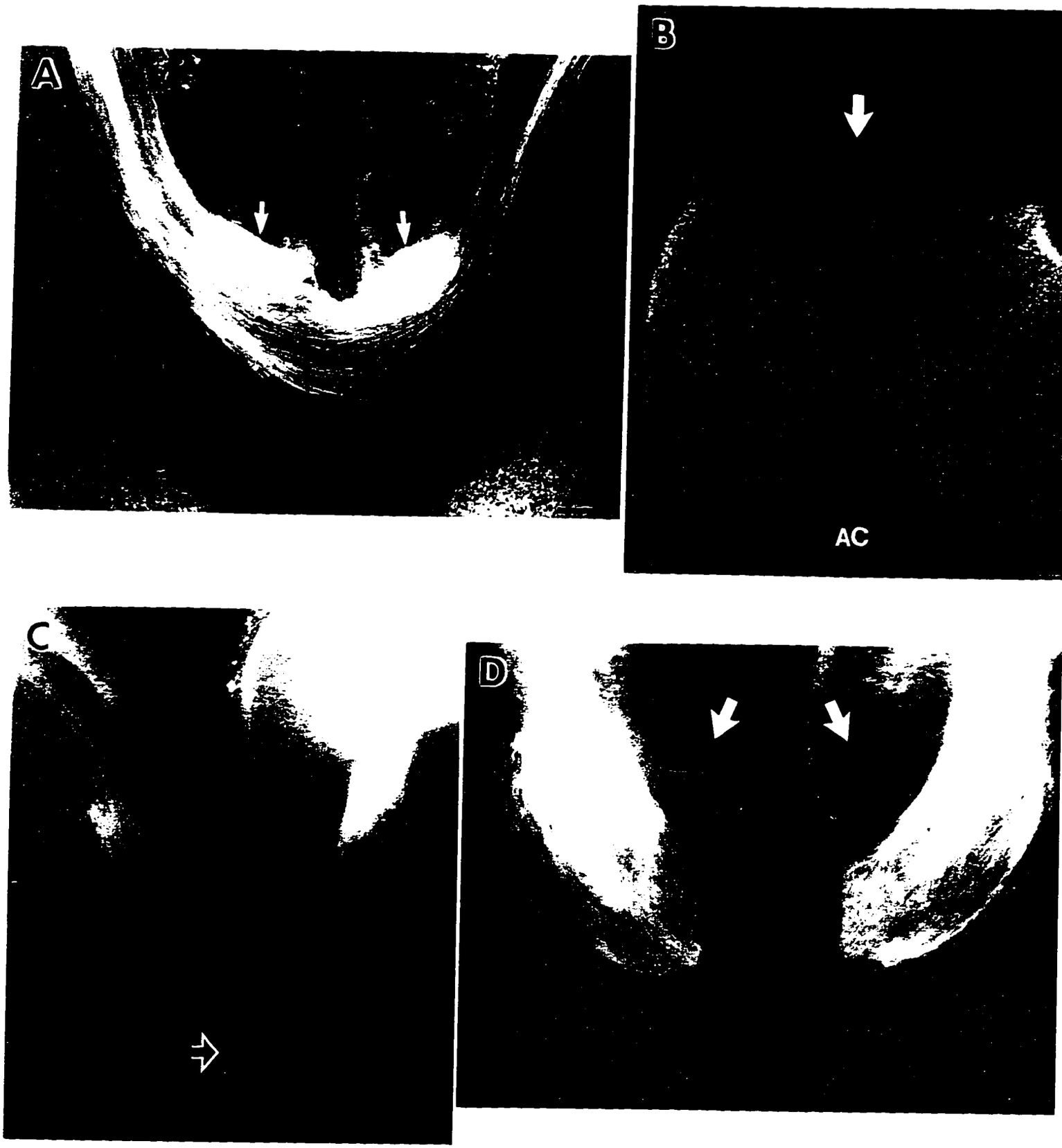
A
B
AC
C
D

Normal growth of the cerebral commissures has previously been described and quantified for B6D2F$_2$ hybrid embryos (Wahlsten and Bulman-Fleming, 1994; see Experiment 1 for description); hybrid mice provide a useful reference group for analysing development of the commissures in the midsagittal plane. CCHC areas for the RI embryos are plotted against body weight in Figure 21A, where the dashed line indicates the values expected from normal hybrids of the same body weight. It is obvious that all the RI embryos exhibit substantial retardation of corpus callosum and hippocampal commissure development, even in those strains that exhibit normal commissure sizes as adults. The CCHC size expected for an embryo of a given body weight (BW) can be calculated from the equation CCHC = -.0375 + .0956*BW + .296*BW^2, based on data from the normal hybrid embryos (Wahlsten and Bulman-Fleming, 1994). The commissure sizes for the RI embryos were, on average, more than .15 mm^2 smaller than expected from their body weights ($t = -30.9$, $p < .000001$). An examination of RI strain commissures indicated that in almost all cases either no axons from either the CC or HC had crossed midplane or that only a small group of axons (presumably HC) was evident at midplane (see Figure 22A and B). In normal hybrid embryos the CC usually had extended dorsal and anterior to the developing HC by this age but in only four RI embryos from normal strains RI-21 and 23 was this evident (Figure 22D). CCHC development was remarkably retarded in all of the RI embryos and very few axons from either commissure had crossed midplane by .80 g body weight (Figure 22C).

Differences in commissure growth between the RI strains can be tested using a

Figure 21: Growth of midplane structures in RI embryos. Body weight plotted against A) CCHC area B) AC area C) MS area for recombinant inbred strain embryos. Dashed line indicates the expected value for B6D2F_2 embryos. Symbols: circles = normal RI strains; triangles = acallosal RI strains; squares = variable RI strains.

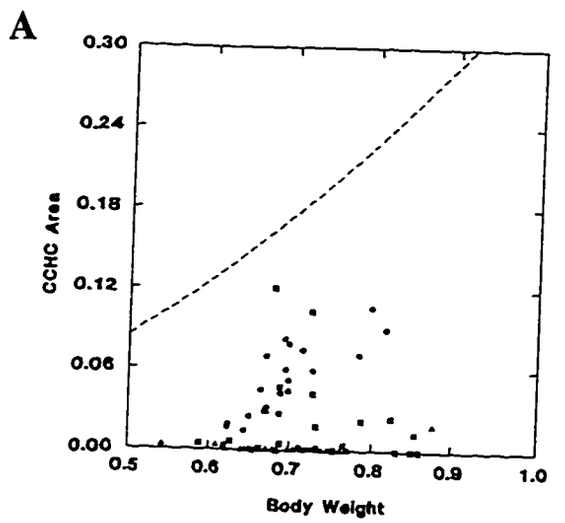
A
0.30
0.24
0.18
0.12
0.06
0.00
CCHC Area
0.5
0.6
0.7
0.8
0.9
1.0
Body Weight

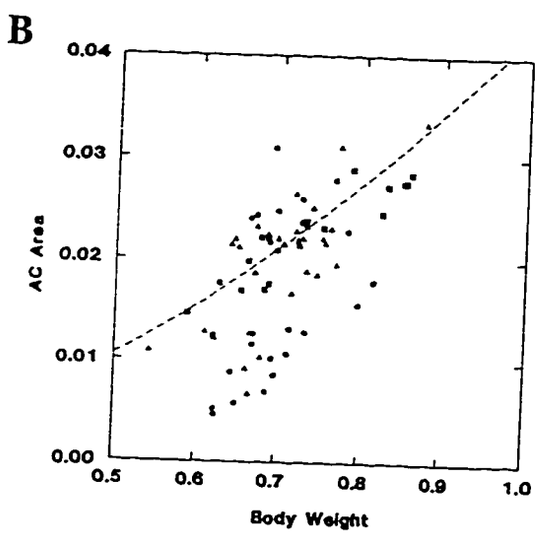
B
0.04
0.03
0.02
0.01
0.00
AC Area
0.5
0.6
0.7
0.8
0.9
1.0
Body Weight

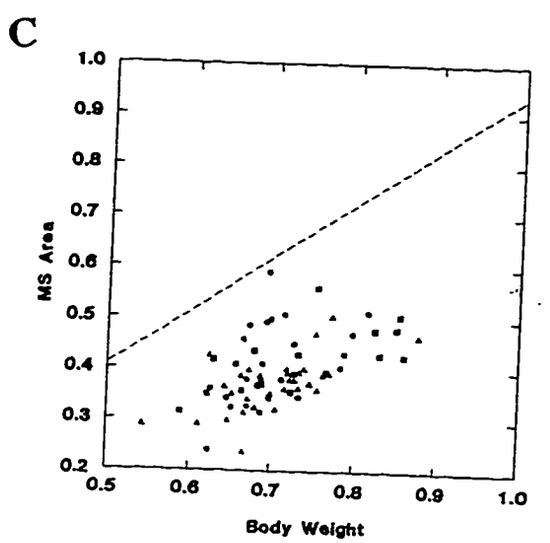
C
1.0
0.9
0.8
0.7
0.6
0.5
0.4
0.3
0.2
MS Area
0.5
0.6
0.7
0.8
0.9
1.0
Body Weight

Figure 22: Development of the midsagittal region in RI embryos. A) Acallosal strain RI-3 embryo in which no axons of the CC or HC have crossed midplane at .64 g body weight and the dorsal medial septal (MS) region remains "notched" (arrows). B) A normal RI-21 strain embryo at .67 g body weight, showing a small HC and a "rounded" dorsal medial septum. C) .77 g strain RI-4 acallosal embryo with no CC or HC, a large anterior commissure (AC) and retarded development of the dorsal medial septal region. D) By .81 g body weight a substantial CC is evident and the dorsal medial septal region has started to fuse in this normal RI-21 strain embryo. Scale bar = .2 mm.

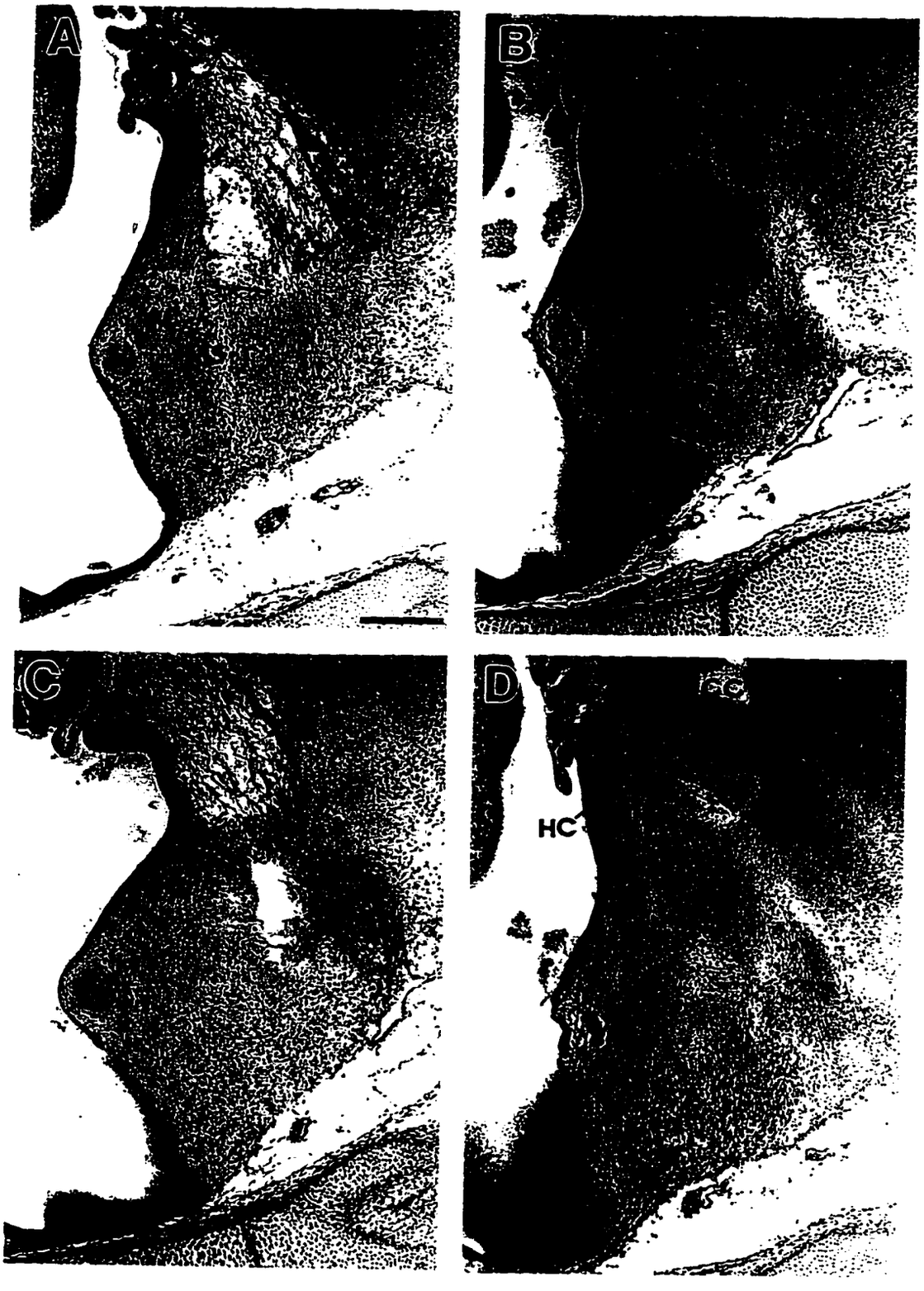
A
B
C
D
HC

regression analysis in which commissure size is predicted from body weight and dummy variables are then added to the equation to represent the comparison between groups. Comparisons between strains within the same group indicate that there was no significant difference in commissure development between the two normal strains (RI-21 vs. RI-23, $p = .650$) or between the three acallosal strains (RI-1 vs RI-3, $p = .113$; RI-1 vs. RI-4, $p= .150$; RI-3 vs RI-4, $p = 1.0$). Therefore, data can be justifiably pooled within these groups. However, the two variable strains (RI-14 and RI-15) differed in prenatal commissure development ($p = .018$), with strain 15 exhibiting more retarded commissures than strain 14, as for adults of these two strains.

Differences were found in embryonic CC and HC development between the groups of recombinant inbred strains that exhibit differences in CC and HC anatomy in adulthood. Frequency distributions for CCHC indices for the embryos in these groups are presented in Figure 23. All but one of the embryos in the acallosal group had indices below .15 (the threshold for normal development of the CC) and the majority of the embryos in this group had indices of zero (the threshold for normal development of the HC), indicating that no axons from either the CC or HC have crossed midline at this stage. Based on the embryonic distribution of CCHC sizes, the threshold model predicts that almost all of the adult animals from RI strains 1, 3 and 4 will have no CC and an abnormally small HC and that occasionally an adult will be found that has a normal HC and a small CC. This is exactly what has been found in adults of these RI strains (Table 5; see also Wahlsten, Sparks and Bishop,

Figure 23: Development of the CC and HC in individual RI strain embryos in the sagittal plane. Frequency distributions for CCHC index values (CCHCI) plotted separately for RI strain groups (see Experiment 1 for method of calculating CCHCI).

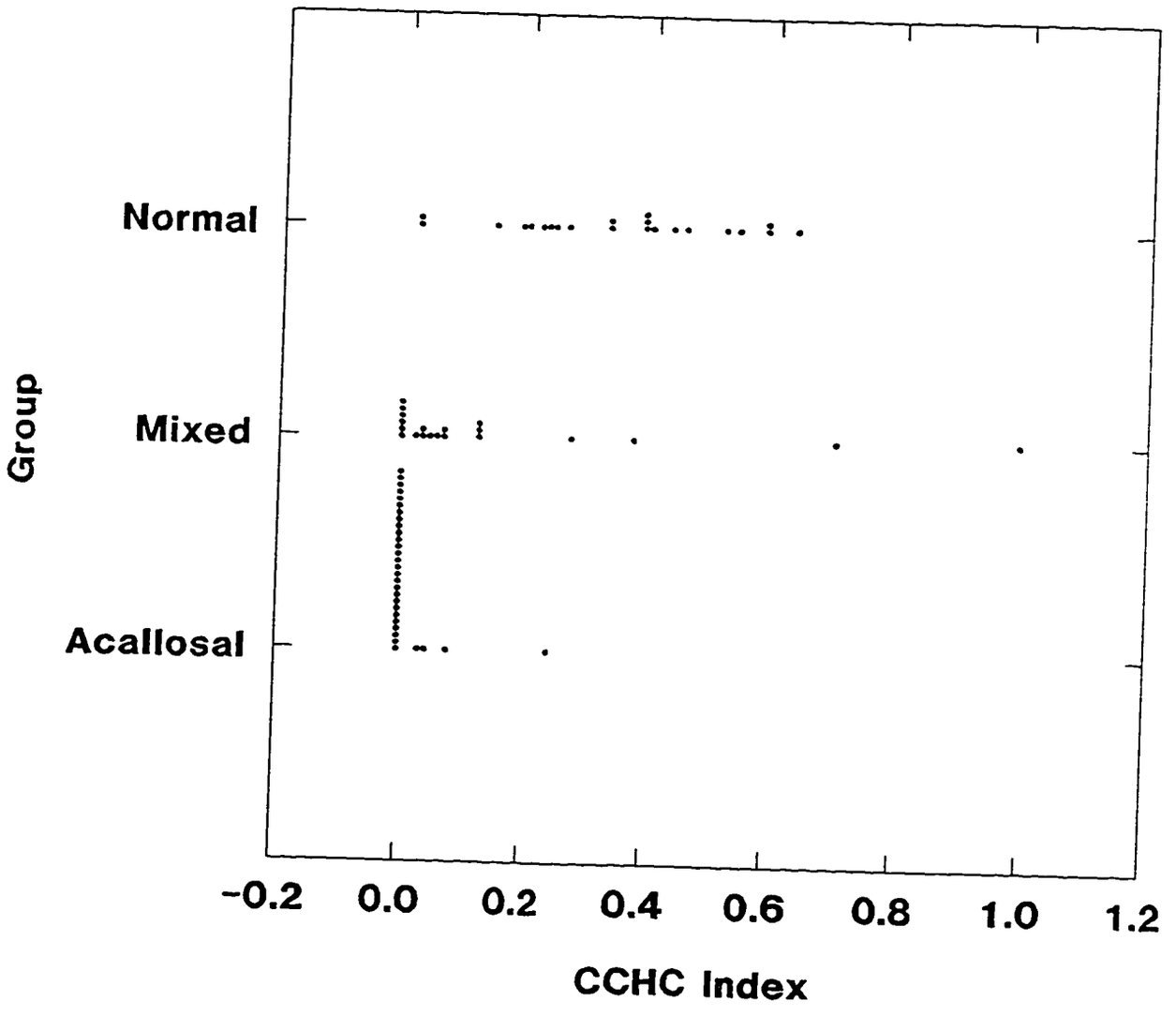
Normal
Mixed
Acallosal
Group
-0.2
0.0
0.2
0.4
0.6
0.8
1.0
1.2
CCHC Index

1997). Almost all of the embryos in the normal strains have index values above .15, the threshold for normal development of the CC, although there are two embryos that have index values below .15 but above zero. This pattern predicts that almost all adults in these strains will have a normal CC and HC, that occasionally an animal will be found that has a normal HC and an abnormally small CC but that no adults in these strains will have a small HC. Again, this predicted pattern of adult callosal sizes matches what has been observed (Table 5). The mean index values for the normal strains are significantly below 1, the mean expected for normal development of the CC and HC (see Table 9). Prenatal formation of the commissures is retarded in these strains and compensation for this early defect must occur before adulthood. The variable RI lines show a wide range of index values from zero to one, consistent with the range of defects observed in adults of these strains. Thus, when the proposed developmental thresholds are imposed on the distribution of CCHC sizes in embryos from the RI strains the pattern of defects observed in adults is accurately predicted, supporting the threshold model.

Anterior commissure development

Development of the anterior commissure was close to that observed for hybrid B6D2F$_2$ embryos (Figure 22B), although an analysis of RI embryonic anterior commissure areas compared to areas expected based on the relationship with body size in the normal hybrid sample ($AC = -.00341 + .0101*BW + .0357*BW^2$) indicated that AC formation was retarded in RI embryos ($t = -4.09$, $p = .0001$;

Table 9: Mean and SD of CCHC Index values for RI embryos examined in the sagittal plane

		z-score		CCHCI	
Strain	Phenotype	Mean	SD	Mean	SD
1	Acallosal	-6.037	0.454	.036	.072
3	Acallosal	-6.175	0.021	0	0
4	Acallosal	-6.200	0.047	0	0
14	Variable	-4.532	2.077	.278	.327
15	Variable	-6.168	0.184	.022	.026
21	Normal	-3.935	1.151	.365	.187
23	Normal	-4.210	1.066	.320	.171

effect size d = .54). Comparison of the RI groups suggests that development of the anterior commissure in one or both of the normal strains may be slightly retarded. Examination of anterior commissure formation in the normal RI strains confirms this impression and indicates that the defect is specific to RI-23 embryos, which often exhibit extremely small anterior commissures ($<.01$ mm^2). This is the same RI strain that has a high frequency of collisions between the anterior commissure and columns of the fornix in adults (Wahlsten et al., 1997).

Growth of the Medial Septum

Almost all of the RI embryos exhibited retarded development of the medial septal region. As illustrated in Figure 21C, the area of the medial septum was well below what is expected for this stage in development of B6D2F$_2$ animals. Analysis of this difference indicates that the growth of the medial septal region in RI animals was, on average, a substantial .23 mm^2 ($t = 30.3$, $p < .000001$) less than what is expected from the equation MS = -.115 + 1.05*BW (Wahlsten and Bulman-Fleming, 1994). The dorsal region of the medial septum undergoes an abrupt transition in form from being notched to rounded normally at about .7 g body weight (Experiment 1). The RI sample contained many embryos larger than this, but the transition in form was consistently absent. Only two of the RI embryos exhibited fusion of the dorsal medial septal region; all other embryos exhibited the notched phenotype (see Figure 24). The two embryos that had made this transition were both from the normal strain RI-23 at the body weight when this transition is normally made (.7 g; see Figure

Figure 24: Development of the medial septum in individual RI strain embryos. Frequency distributions for mean width of the dorsal medial septum plotted separately for RI strain groups.

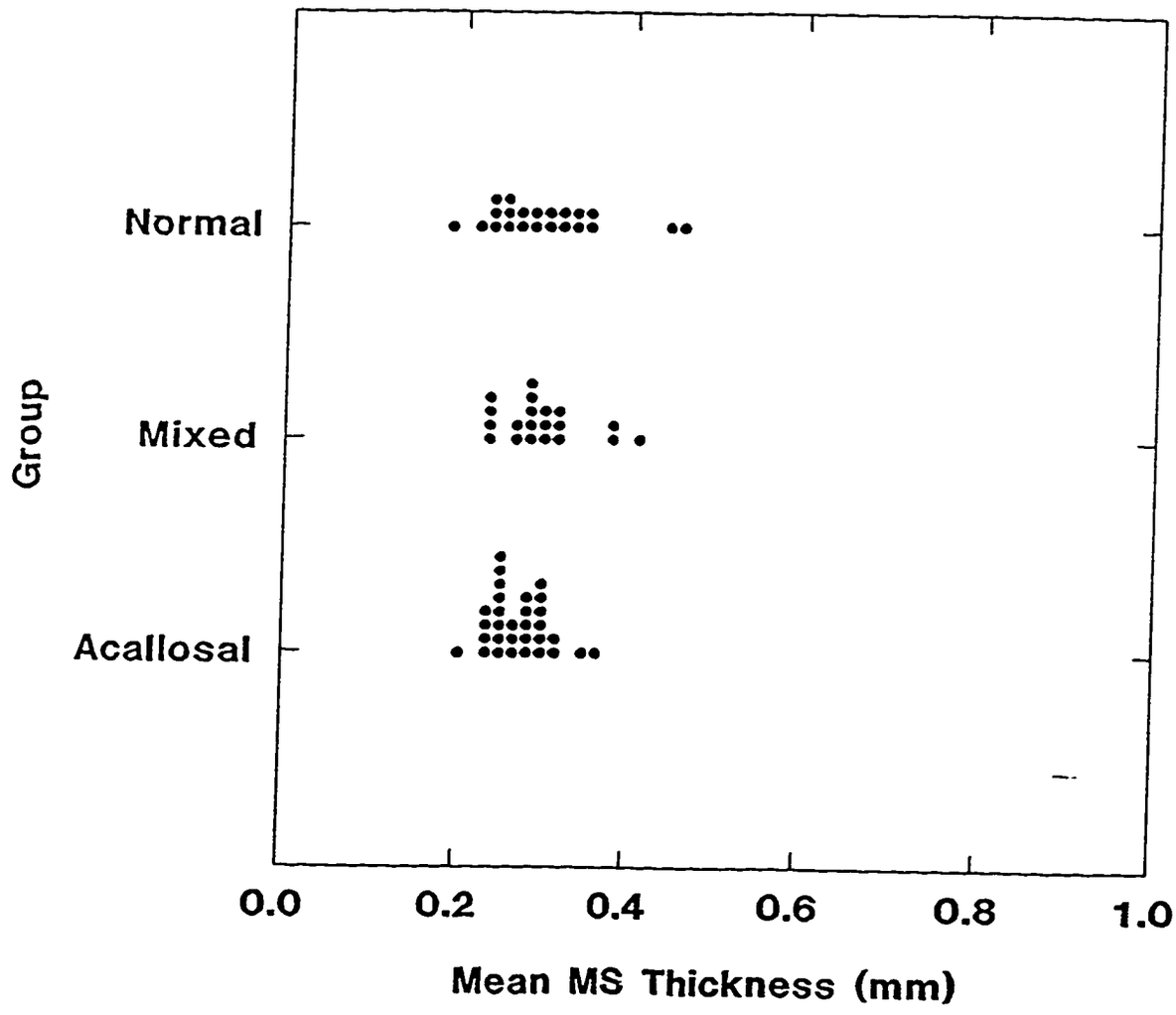
Normal
Mixed
Acallosal
Group
0.0
0.2
0.4
0.6
0.8
1.0
Mean MS Thickness (mm)

23B). No significant differences between RI groups were found for the area or dorsal thickness of the medial septal region (t-tests; p's > .05). Because development of the medial septum was retarded in all of the recombinant inbred embryos, irrespective of group membership, this defect probably is not the cause of retarded development of the CC and HC. It is possible, however, that the narrow weight range examined in this study obscured recovery from slight retardation in dorsal MS development or that development of the medial septum is necessary for recovery from earlier callosal defects.

Part III - Midline anatomy in the coronal plane

Normal development of the midplane region

Before attempting to identify structures in the midplane region related to development of the corpus callosum and hippocampal commissure, it was important that development of this region be quantified in a sample of normal embryos. Normal development of the midplane region in the coronal plane was examined in a standard sample of 22 B6D2F_2 mice between .40 and 1.00 g body weight. At the landmark section in the youngest embryo (.40 g body weight), a substantial HC was already evident, being about .16 mm in thickness (Figure 25A). The HC in this young embryo extended about .19 mm in the anterior-posterior dimension and thus was substantially formed at this stage. The dorsal surface of the HC was in direct contact

Figure 25: Normal development of the midplane region shown in the coronal plane. Normal hybrid B6D2F$_2$ embryos at approximately A).4 g body weight; B) .5 g body weight; C) .6 g body weight; D) .7 g body weight; E) .8 g body weight and F) .9 g body weight. Commissural axons (CCHC) have crossed midplane already at .4 g body weight, but a small cleft is evident in the bottom of the interhemispheric fissure (IF). As the embryo grows, axons are added to the dorsal surface of the CCHC and the bottom of the fissure moves dorsally. At about .6 g body weight a wedge of glial cells emanate from the lateral ventricles (arrows) but do not span midplane until about .7 - .8 g body weight when a substantial CC is clearly evident. Scale bar = .2 mm.

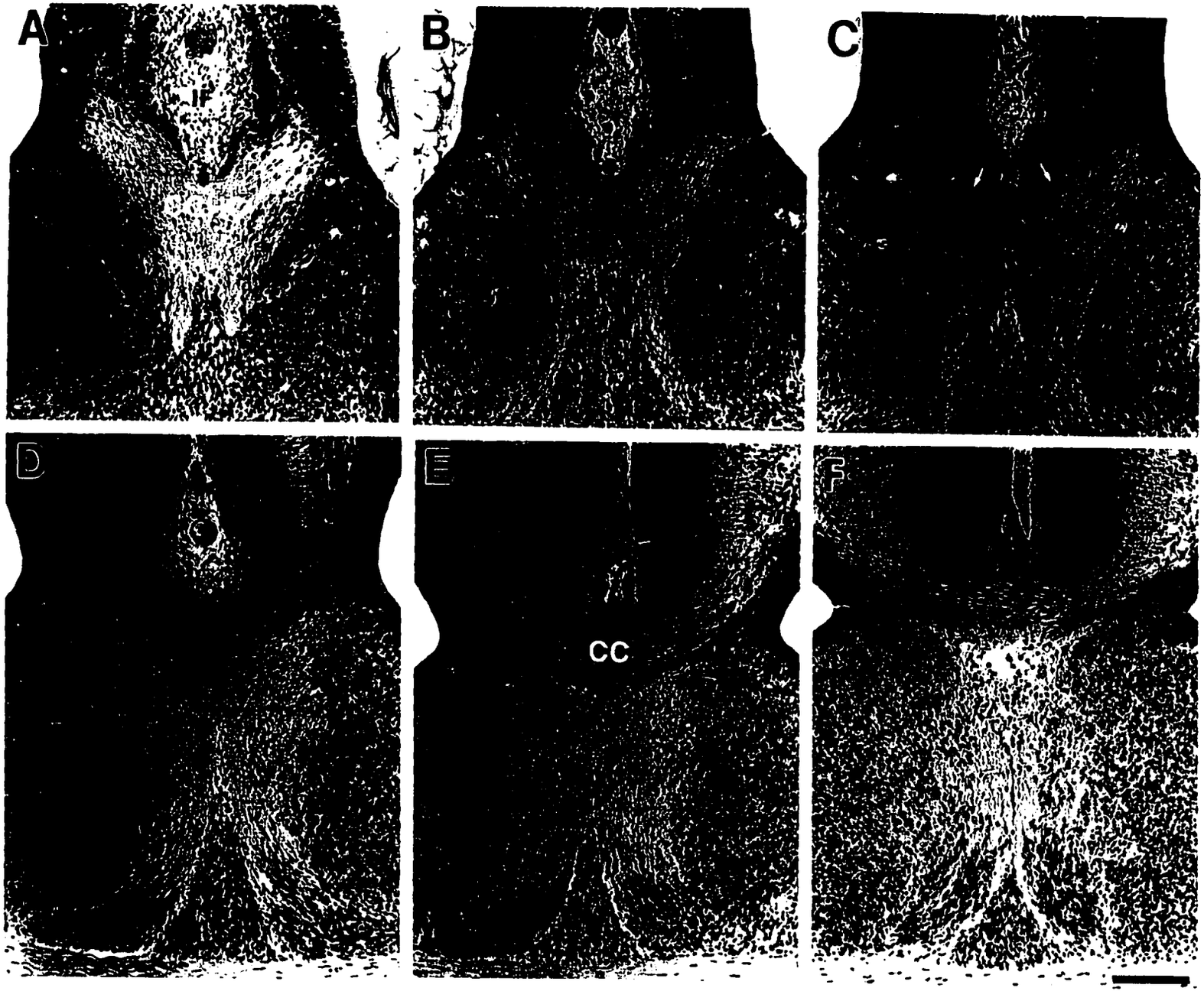
A
IF
B
C
D
E
CC
F

with the bottom of the longitudinal fissure, which extended well below thebottom of the indusium griseum, creating a small cleft at the bottom of the fissure (Figure 25A). A few glial cell bodies were evident within the area of the axons of the HC but these were arranged haphazardly and were sparsely distributed. Growth of the area of the CC and HC was rapid in normal embryos between .4 and 1.0 g body weight (Figure 26) and overall growth as measured by body weight accounted for about 80% of the variance in CCHC size. The relationship with brain weight was approximately linear in this restricted body weight range. Axons were added to the combined area of the CC and HC in both the dorsal-ventral and rostral-caudal dimensions. However, growth in the rostral-caudal dimension was much more rapid (approximately 1.05 mm/g body weight) than in the dorsal-ventral dimension (approximately .42 mm/g). Along the rostral-caudal axis, growth of the CC and HC anterior to the landmark section was estimated to be about .18 mm/g while growth posterior to the landmark section was much more rapid (about .66 mm/g). CCHC thickness reached a value equivalent to the maximum thickness of the HC alone (.20 mm) at about .50 g body weight. The areas of the CC and HC could be distinguished from each other in stained sections based on a difference in textural perception (Figure 25). Whereas the HC area appeared somewhat grainy, the area of the CC appeared to consist of laterally coursing fibres. This perceptual difference may be due to differences in orientation of oligodendroglia in the two structures.

Axons of the CC could be first seen crossing midplane in a .48 g embryo; these axons most likely originated in the cingulate cortex (Koester and O'Leary,

Figure 26: Development of the CCHC and interhemispheric fissure in B6D2F$_2$ normal hybrid embryos. Plot of body weight against A) CCHC area and B) depth of the interhemispheric fissure (LFD). C) CCHC area plotted against depth of the interhemispheric fissure indicates a relationship between these two structures in normal development. Dashed lines indicate the lines of best fit, A) CCHC = -.136 + .398 BW (R^2 = .79); B) LFD = .165 - .183 BW (R^2 = .65).

A

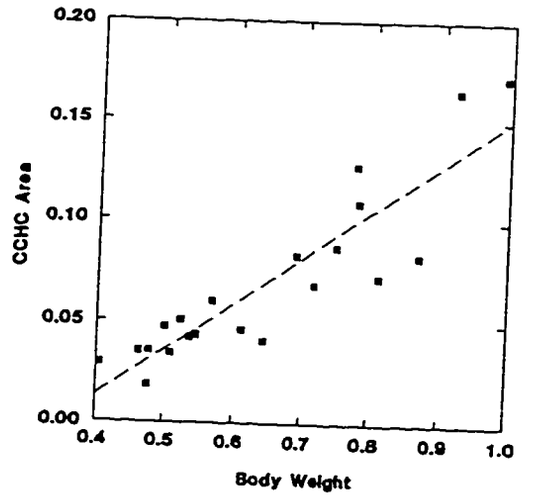
0.20
0.15
0.10
0.05
0.00
CCHC Area
0.4
0.5
0.6
0.7
0.8
0.9
1.0
Body Weight

B

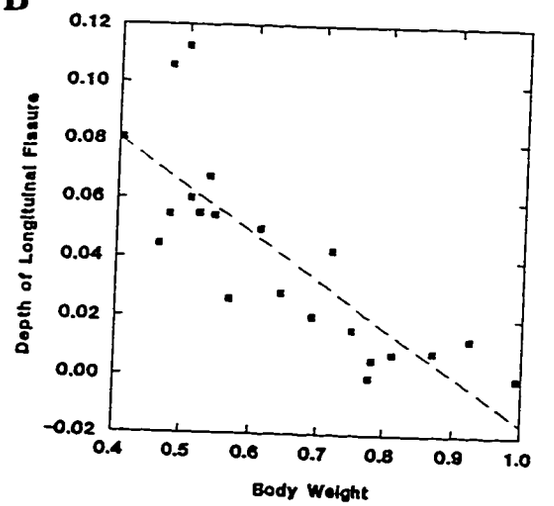
0.12
0.10
0.08
0.06
0.04
0.02
0.00
-0.02
Depth of Longitudinal Fissure
0.4
0.5
0.6
0.7
0.8
0.9
1.0
Body Weight

C

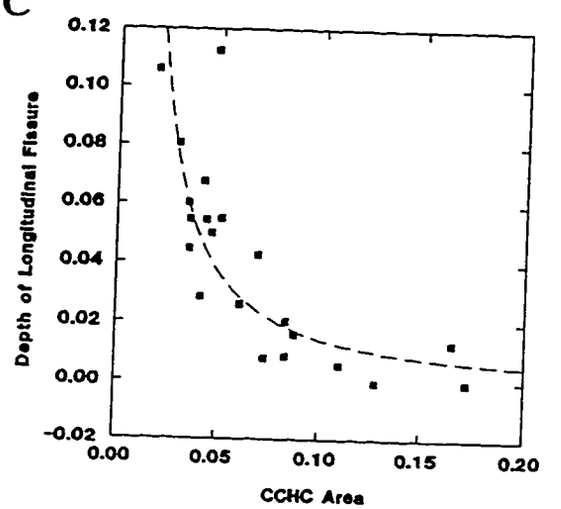
0.12
0.10
0.08
0.06
0.04
0.02
0.00
-0.02
Depth of Longitudinal Fissure
0.00
0.05
0.10
0.15
0.20
CCHC Area

1992). A distinct row of cells extending from the medial edge of each lateral ventricle towards midplane was clearly evident at about .54 g body weight, although these cells did not extend across midplane at this stage (Figure 25). These lateral structures are cells of the glial sling described by Silver et al. (1982). Cell bodies of the sling cells did not extend across midplane until about .78 g body weight when they appeared to separate a well-formed CC (approximately .11 mm thick) from the dorsal surface of the HC. The bottom of the lateral fissure moved dorsally rapidly and linearly during this period in development (Figure 26B) and reached the level of the cells of the indusium griseum by about .68 g body weight. At this point the bottom of the fissure was level; the small cleft in the bottom of the fissure had disappeared. In all brains the dorsal surface of the CCHC was always in close contact with the bottom of the fissure. Growth of the CCHC in the dorsal direction appeared to occur in synchrony with movement of the bottom of the fissure towards the surface of the cortex. However, it is not clear whether the addition of axons on the dorsal surface of the CCHC pushes the fissure floor dorsally or whether movement of the fissure floor itself somehow permits or stimulates axons of the CC and HC to cross midplane. CCHC area plotted against fissure depth (Figure 26C) reveals that the relationship between these two events is nonlinear. It appears as though the bottom of the fissure must be within about .02 mm of the indusium griseum before axons of the HC and CC are able to cross midplane. Before this, the fissure floor moves dorsally rapidly without substantial growth of the CC and HC, suggesting that fusion of the hemispheres occurs prior to commissural development.

Most other structures measured in the landmark coronal section developed in a linear relationship with body weight of the embryo over this restricted weight range (Table 10). The only exception to this was the distance between the indusium griseum in either hemisphere, which remained constant. These findings justify the use of body weight as an indication of overall development of the embryo and support the choice of the indusium griseum as a stable dorsal-ventral landmark.

Development of the midplane region in recombinant inbred embryos

Development of the corpus callosum and hippocampal commissure

The combined area of the corpus callosum and hippocampal commissure is plotted against body weight for each embryo in Figure 27, where the dashed line represents the value expected from analysis of B6D2F_2 hybrid embryos. It is evident that CCHC development is retarded in all the RI embryos because only a few of the CCHC sizes are within range of the normal values for their body weight (see Figure 28). The expected CCHC area for each RI embryo based on its body weight (BW) was calculated using the equation: E(CCHC) = -.078 + .229*BW. The CCHC sizes of the RI embryos averaged .03 mm^2 behind what was expected ($t = -16.4$, $p < .001$). The mean CCHC index values for all of the RI strains were significantly less than 1 (Table 11). The CCHC index values calculated for the coronal measurements were very close to what was found using sagittal plane measurements. Thus, delay in CCHC growth in the RI mice has been confirmed in two samples

Table 10: Development of midline structures in normal hybrid B6D2F$_2$ embryos.

Measurement	B_0	B_1	Adj. R^2	p
CCHC Area	-.078	.229	.79	<.001
LF Depth	.145	-.161	.65	<.001
Distance to ACA	.307	-.260	.64	<.001
Distance to DSC	1.006	-.488	.74	<.001
IG Width	.190	-.110	.11	.078
LF Width	.245	-.222	.59	<.001
LV Width	-.047	1.578	.72	<.001
LF Area	.058	-.060	.65	<.001

B_0 is the Y-intercept and B_1 the slope of the linear regression equation predicting measurement from body weight. For area measurements the units of B_0 are mm^2 and of B_1 are mm^2/g; for distance measurements the units of B_0 are mm and of B_1 are mm/g. Abbreviations: CCHC = corpus callosum and hippocampal commissure; LF = longitudinal fissure; ACA = anterior cerebral artery; DSC = dorsal surface of the cortex; IG = indusium griseum; LV = lateral ventricles; see text and Figure 15 for a description of the measurements made. using both the sagittal and coronal planes for measuring the area of the corpus callosum and hippocampal commissure at midplane.

Figure 27: Development of the CCHC and interhemispheric fissure in RI embryos. Plot of body weight against A) CCHC area and B) depth of the interhemispheric fissure. C) CCHC area plotted against depth of the interhemispheric fissure. Lines indicate values expected from hybrid B6D2F_2 embryos. Symbols: circles = normal RI strains; triangles = variable RI strains; squares = acallosal RI strains.

A

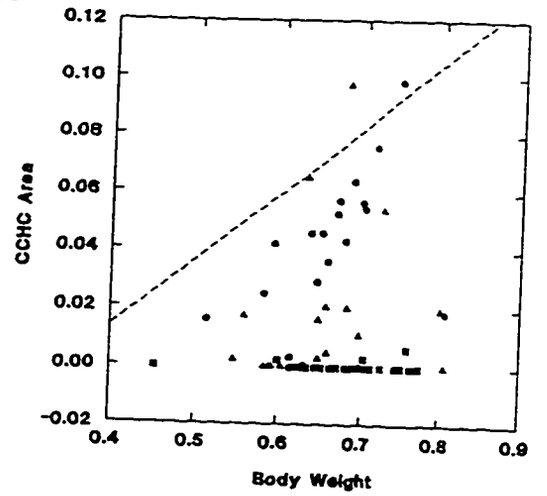
0.12
0.10
0.08
0.06
0.04
0.02
0.00
-0.02
CCHC Area
0.4
0.5
0.6
0.7
0.8
0.9
Body Weight

B

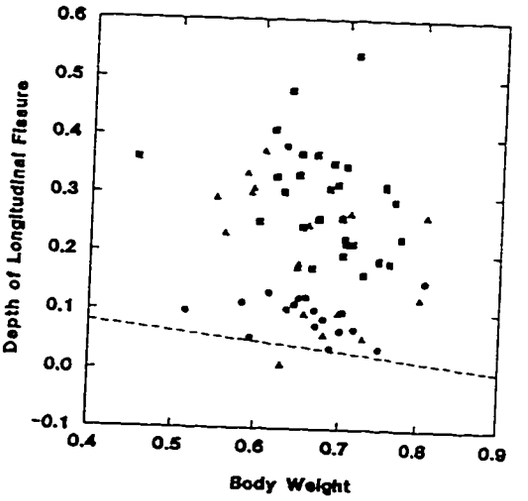
0.6
0.5
0.4
0.3
0.2
0.1
0.0
-0.1
Depth of Longitudinal Fissure
0.4
0.5
0.6
0.7
0.8
0.9
Body Weight

C

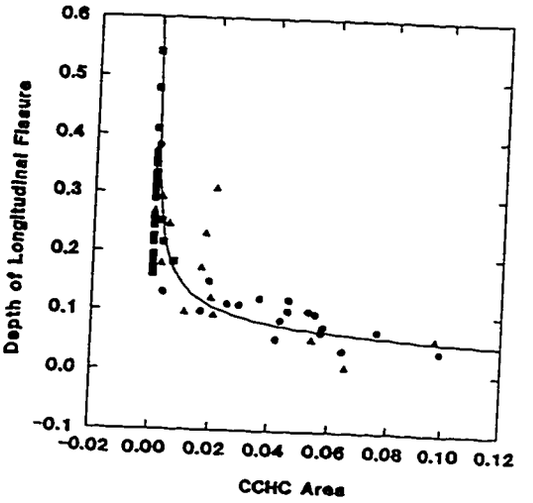
0.6
0.5
0.4
0.3
0.2
0.1
0.0
-0.1
Depth of Longitudinal Fissure
-0.02
0.00
0.02
0.04
0.06
0.08
0.10
0.12
CCHC Area

Figure 28: Development of the CC and HC in the coronal plane in individual RI strain embryos. Frequency distributions for CCHC index values plotted separately for groups of RI strains for measurements made in the coronal plane.

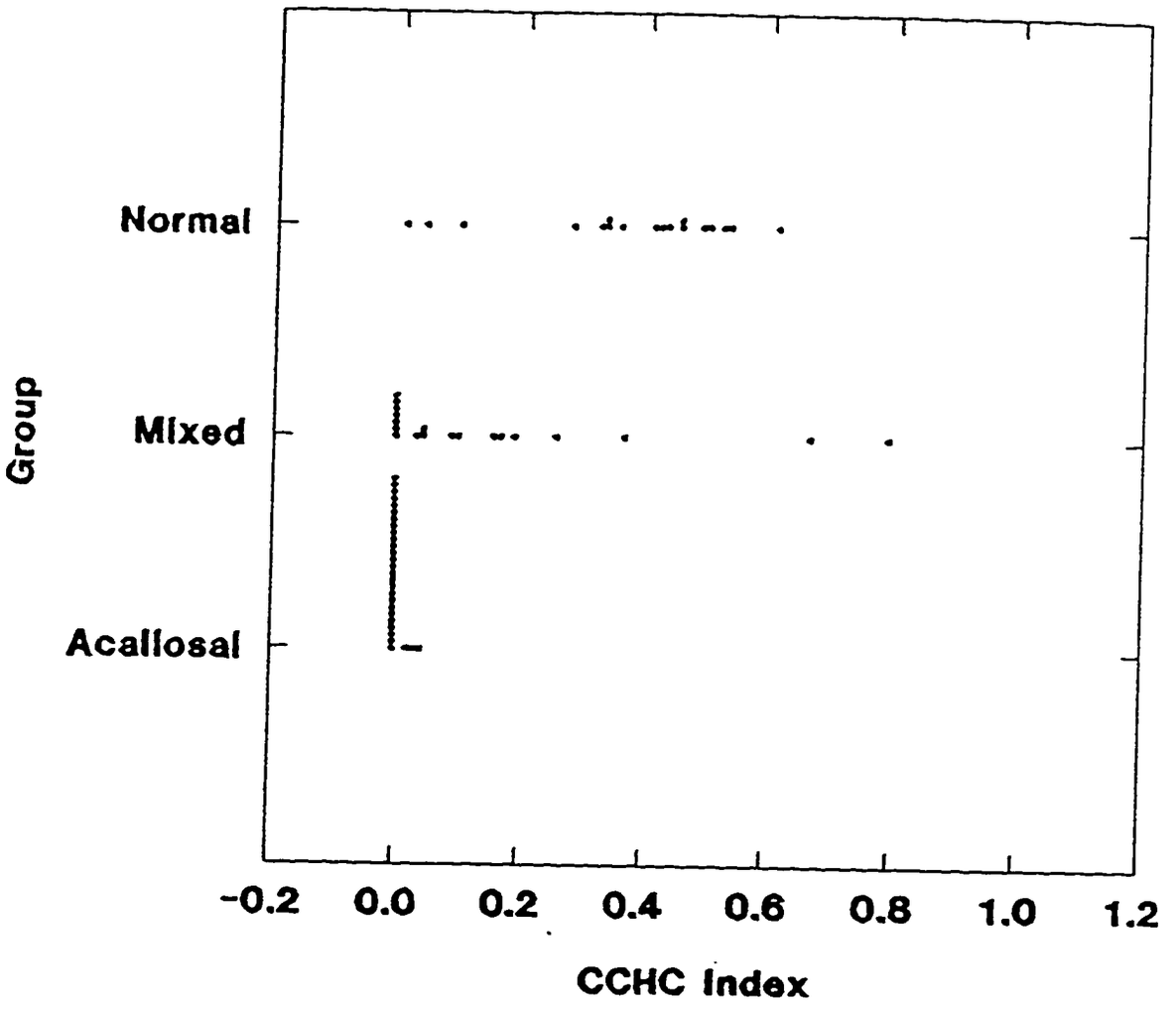
Normal
Mixed
Acallosal
Group
-0.2
0.0
0.2
0.4
0.6
0.8
1.0
1.2
CCHC Index

Table 11: Mean and SD of CCHC Index values for RI embryos examined in the coronal plane

		z-score		CCHCI	
Strain	Phenotype	Mean	SD	Mean	SD
1	Acallosal	-5.889	0.732	.010	.016
3	Acallosal	-6.187	0.048	0	0
4	Acallosal	-6.201	0.054	0	0
14	Variable	-4.799	1.815	.228	.290
15	Variable	-5.953	0.567	.065	.089
21	Normal	-4.102	1.082	.345	.165
23	Normal	-3.794	1.145	.389	.184

Differences in commissure growth between the RI strains can be tested using a regression analysis in which commissure size is predicted from body weight and a dummy variable is then added to the equation to represent the comparison between groups. Using this approach to evaluate differences between strains within the same group, it was found that CCHC area did not differ between the two normal strains (RI-21 and RI-23, $p = .56$), between the two mixed strains (RI-14 and RI-15, $p = .13$) or between the acallosal strains (RI-1 vs RI-3, $p = .05$; RI-3 and RI-4, $p = 1$; RI-1 and RI-4, $p = .06$). The use of these strains classifications is therefore supported.

Differences were found in CCHC area between the acallosal, normal and variable RI strain groups (Figure 28). Index values for embryos from acallosal RI strains all fall below the threshold for normal CC size and all but three of the embryos have index values of zero, the threshold for normal adult HC size. Therefore, the adult pattern of defects in the acallosal RI strains (Wahlsten et al., 1997; also see Table 5) is correctly predicted by the embryonic thresholds for commissure development. Almost all of the index values for embryos from normal RI strains fall above .15, the threshold for normal CC development, predicting that the majority of mice in these strains will exhibit normal CC and HC sizes. Two of the normal strain RI embryos have index values below .15 but above zero, predicting that occasionally a normal strain RI adult will be found that has a smaller than normal CC but a normal HC. Again, the embryonic thresholds correctly predict the adult pattern of defects (Wahlsten et al., 1997; also see Table 5). The distribution of

CCHC index values in the variable RI strains ranges from zero to almost one, consistent with the variability in CC and HC sizes seen in adult mice of these strains. Out of the 19 variable strain embryos examined, seven had CCHC index values of zero, five had index values between zero and .15, and another seven had values greater than .15. Therefore, the threshold model correctly predicts that the full range of CC and HC defects will be observed in adults from these strains. Overall, the thresholds proposed for normal development of the HC and CC have been confirmed in samples of embryos from the 9XC recombinant inbred strains examined in both the sagittal and coronal planes.

In RI embryos that exhibited agenesis of the corpus callosum and hippocampal commissure, CC axons formed large Probst bundles and the interhemispheric fissure was well below where the CC and HC axons normally cross midplane (Figure 29A). In all of the RI embryos that exhibited CC or HC axons crossing midplane, the dorsal edge of the CCHC area was consistently found to be in close contact with the pial membrane lining the bottom of the cerebral fissure. This was true even in embryos that had only a small number of HC axons crossing midplane (Figure 29B). For embryos that had formed only a small HC, the ventral surface of the area of the CCHC either passed over the medial septum, or, in about an equal number of cases, crossed over an open space at midline. In one particularly interesting brain (strain RI-14, .68 g body weight) a very small group of HC axons was observed extending just past midline (but not across it) on one side only. At midline these axons were closely associated with pial membrane lining the bottom of the interhemispheric

Figure 29: Midline development in acallosal embryos in the coronal plane. A) .76 g RI-1 embryo with very large Probst bundles (asterisks) and a deep interhemispheric fissure (IF). B) A few axons of the hippocampal commissure have crossed midplane at the bottom of the interhemispheric fissure in this .66 g RI-1 acallosal strain embryo (arrow). C) and D) when only a few axons are crossing or have crossed midplane, they are found in close apposition to the pial membrane lining the bottom of the interhemispheric fissure (arrows). C) RI-14, .65 g embryo D) RI-4, .80 g embryo. Scale bars = .2 mm.

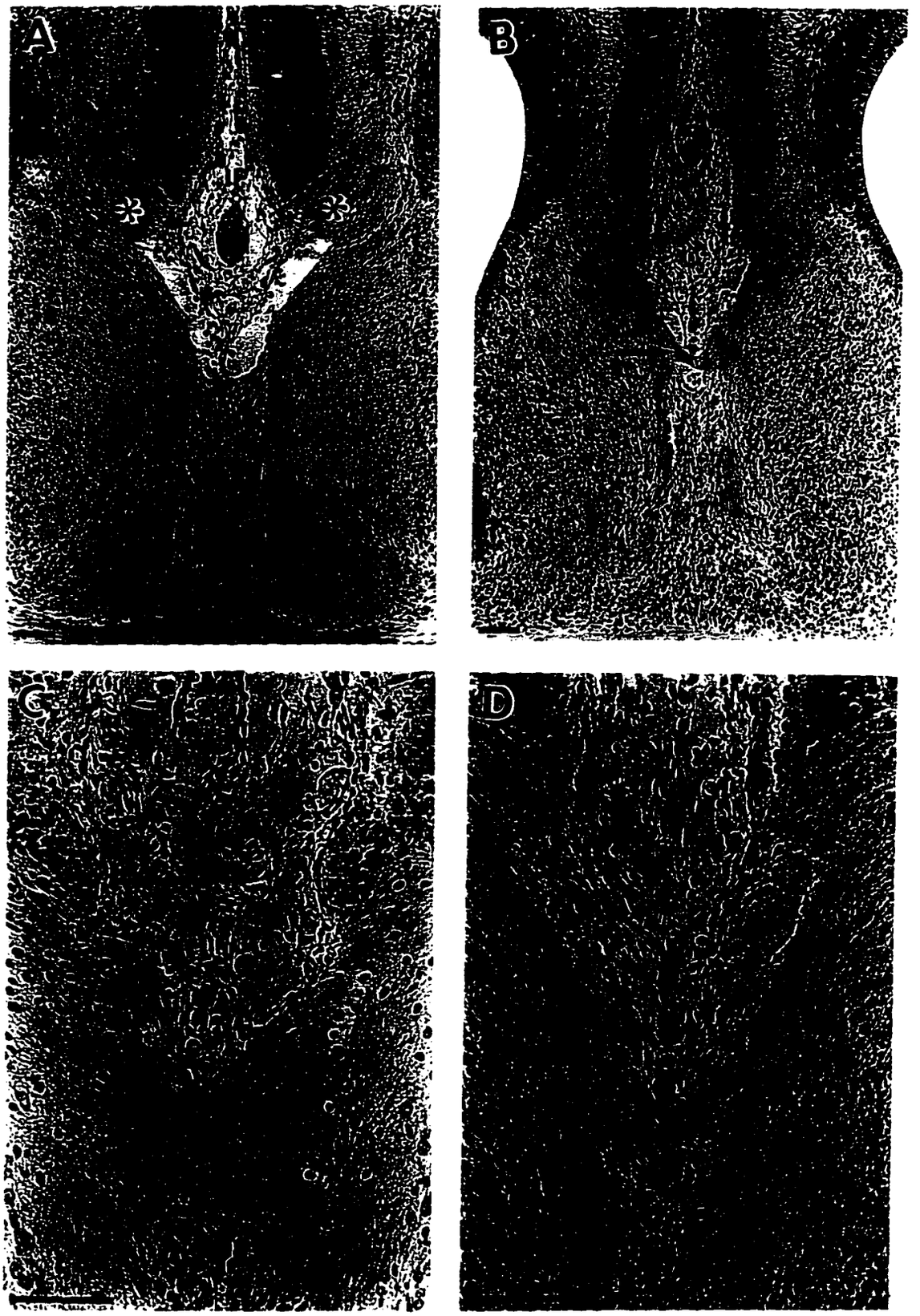
A
B
C
D

fissure (see Figure 29C and D). It is possible that cells associated with the bottom of the pial membrane lining the longitudinal fissure play a role in guiding the first axons to cross to midplane.

Development of midplane structures

The development of structures at the cerebral midplane was assessed in embryos from normal, acallosal and variable RI strains in an attempt to identify structures that may be implicated in agenesis of the corpus callosum. Midplane development in RI embryos can be compared with development in the standard $B6D2F_2$ hybrid embryos by calculating the expected value for each structure, based on an embryo's body weight using the regression values presented in Table 11. Development of every one of the midplane structures was retarded in the RI mice compared to the $B6D2F_2$ embryos (p's $< .03$). This result indicates that there is overall retardation in the midplane region, independent of overall body development. Whether the developmental delay extends to all regions of the brain, some regions, or if it is specific to the midplane remains to be investigated.

RI group differences in development of midplane structures can be tested using a regression analysis in which commissure size is predicted from body weight and dummy variables are added to the equation to represent the comparison between groups. Surprisingly, only the depth of the longitudinal fissure differed significantly between normal, acallosal and variable RI embryos ($F = -26.5$; $p < .001$). Figure

27B plots fissure depth against body weight for the RI embryos, with the dashed line indicating the values expected from the B6D2F_2 hybrid sample. Shortening of the interhemispheric fissure is clearly retarded in the majority of RI brains, whereas only embryos from the normal RI strains (represented by circles) exhibit values close to normal. The group differences can be seen more clearly in Figure 30, a frequency distribution of fissure depths for the acallosal, normal and variable RI strains. The distributions of fissure depths for normal and acallosal groups do not overlap much. The one normal group embryo with an abnormally deep fissure is important because it suggests that the occasional unexpected adult defect seen in this group is also related to fissure formation. The mixed RI strains exhibit a very wide range of fissure depths, maybe because these strains have not yet fixed for the alleles related to agenesis of the corpus callosum and shortening of the interhemispheric fissure. A plot of the depth of the interhemispheric fissure against CCHC area (Figure 27C) confirms the relationship between these two structures found in the B6D2F_2 hybrid sample. Axons from the CC and HC only start to cross midplane when the bottom of the interhemispheric fissure has grown close to the level of the indusium griseum. Once the bottom of the fissure has reached this critical height, commissural formation is rapid. Therefore, quantification of midplane development in the coronal plane identified a severe and specific defect (retarded closure of the interhemispheric fissure) that correlated with development of the corpus callosum and hippocampal commissure in normal and acallosal mice.

Figure 30: Depth of the interhemispheric fissure in RI embryos. Frequency distribution plotted separately for RI strain groups shows clearly that interhemispheric fissure development differs in normal and acallosal strain mice. Distributions for acallosal and normal RI strains show very little overlap. The distribution for variable RI strains shows greater variability than the strains with more consistent commissural formation.

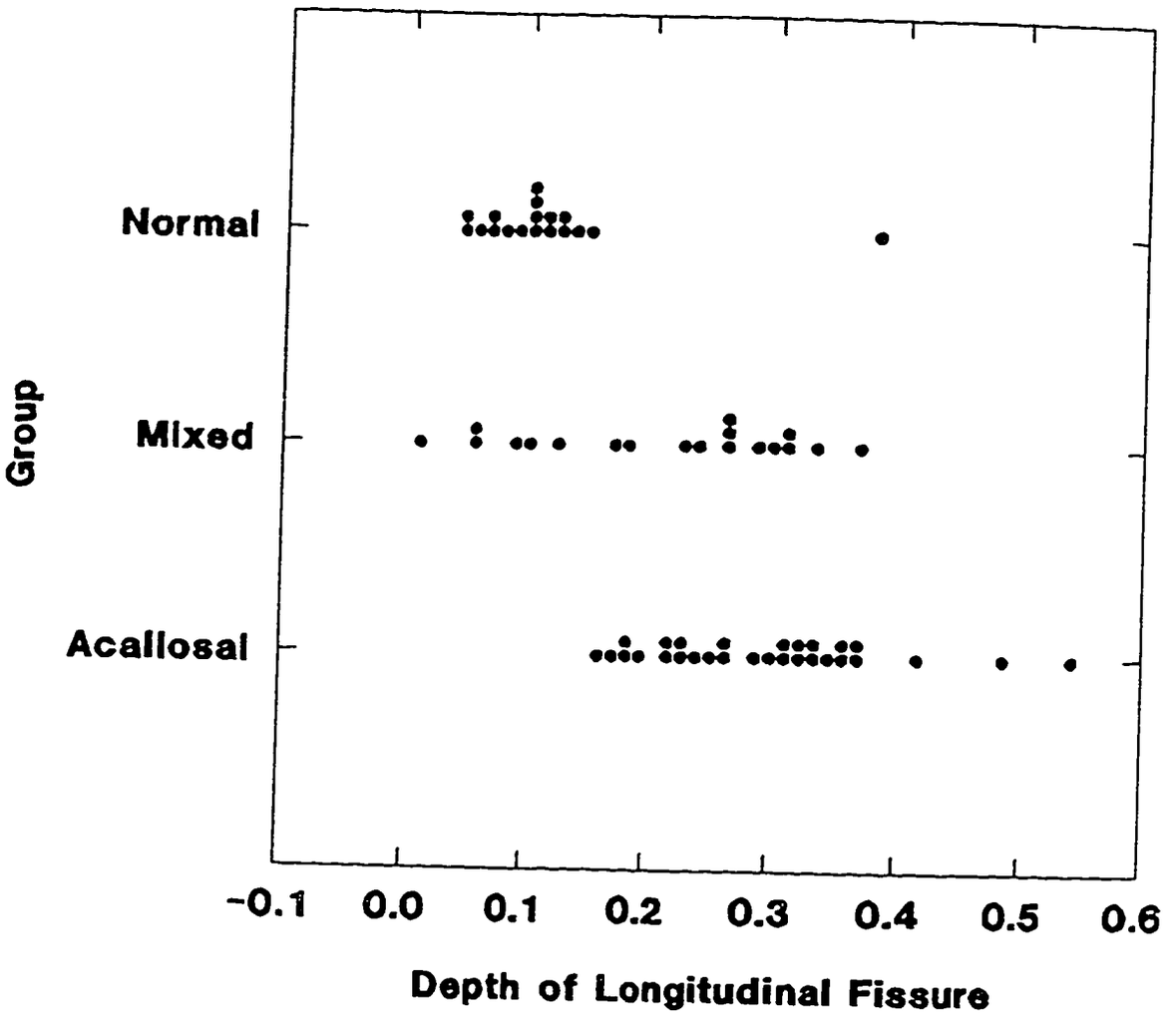
Normal
Mixed
Acallosal
Group
-0.1
0.0
0.1
0.2
0.3
0.4
0.5
0.6
Depth of Longitudinal Fissure

Discussion

Results indicate that corpus callosum and hippocampal axon growth to midplane is normal in acallosal recombinant inbred embryos. There was no difference in axon growth rate or timing of CC axon arrival at the midplane crossing point between normal, acallosal and variable recombinant inbred strains. In addition, the predicted body weight at which the axons from the frontal cortex reached the midplane crossing point was the same in recombinant inbred as in hybrid B6D2F_2 animals (Ozaki and Wahlsten, 1992). However, because of an overall slower rate of development (about 1 day) in recombinant inbred embryos compared to hybrid mice, the age at which the first frontal axons crossed midplane was somewhat later (about .8 day). Normal growth of callosal axons to midplane was expected for the RI strains because previous research has shown that CC axon growth to midplane is normal in the 129/ReJ and BALB/cWah1 progenitor strains (Ozaki and Wahlsten, 1993). These results suggest that agenesis of the corpus callosum and hippocampal commissure in the RI strains is due to a problem in the substrates for axon guidance across midplane, not a property of the callosal cells or axons themselves.

Previous research has suggested that the axons of the corpus callosum may use the dorsal surface of the hippocampal commissure as a substrate for crossing midplane (Wahlsten, 1989; Livy and Wahlsten, 1997). Differential labelling with lipophilic dyes confirmed a relationship between embryonic development of the hippocampal commissure and adult anatomy of the corpus callosum; large differences were

observed for hippocampal commissure formation, and the degree of retardation in prenatal formation of the HC correlated with the pattern of callosal defects observed in adults of these strains. In acallosal strain embryos that showed only a very small HC, the axons were always found to be in close contact with the bottom of the longitudinal fissure, suggesting that this area may provide cues for axon guidance across the midplane. Examination of older acallosal embryos suggested a novel pathway for the HC axons that do not cross midplane, in which they travel from the columns of the fornix, around the lateral surface of the Probst bundles, and then to midline on the dorsal surface of the Probst bundles in the cingulate cortex (Schambra et al., 1992).

Surprisingly, several of the older, usually normal strain embryos were found with Probst bundles, suggesting that although CC size is normal in adults from these strains, prenatal CC development may be retarded. Just as 129XCF$_1$ embryos recover from an early defect in commissural formation (see Experiment 1), so must the normal RI strain embryos. Although the embryonic callosal defect may be related to delayed formation of the hippocampal commissure in these embryos, the possibility remains that both CC and HC development are delayed because of some other defect in the midplane region.

Examination of the midplane region in the sagittal plane did not reveal a defect correlated with the pattern of commissural morphologies in adults of these strains. Almost all of the RI embryos showed the notched phenotype for the dorsal region of the medial septum: there were no differences between groups of RI strains. It is

expected that between .5 - .9 g body weight the distribution of dorsal medial septum sizes is normally bimodal (see Experiment 1). Unimodal distributions for all three groups of the RI strains suggests that the putative major gene responsible for the septal notch defect does not differ between RI strains. The thresholds proposed for normal development of the CC and HC in experiment 1 were confirmed in the RI sample. Imposition of the proposed thresholds on the distribution of CC and HC sizes in the embryos correctly predicted the adult pattern of defects. Most importantly, the threshold model allowed for the possibility that occasionally a normal strain embryo is found with a CC defect and an acallosal strain embryo has a normal HC and a small CC. Embryos found in the extreme tails of the distributions for CCHC size crossed the threshold values and were predicted to develop a CC and HC that was anomalous for their group. As hypothesized based on the severe defects observed in adults, the embryonic defect in CCHC size was more extreme in the acallosal RI strains than in the 129 and BALB/cWah1 inbred strains. Retarded development of the CC and HC in normal RI strains was confirmed, although development was not so retarded as to be below threshold in most cases so that recovery was possible.

Examination of the midline region in the coronal plane was successful in identifying a severe defect in midplane development that strongly correlated with the adult pattern of callosal morphology. Fusion of the interhemispheric fissure was severely delayed in acallosal embryos, normal in normal embryos and extremely variable in the variable RI strains. A defect in interhemispheric fissure development

has been proposed by several researchers (Silver et al., 1982; Wahlsten, 1984; Silver et al., 1993; Wahlsten and Bulman-Fleming, 1994) but this is the first study to quantify development of this region and correlate it with the development of the corpus callosum and hippocampal commissure. The timing of interhemispheric fissure development coincided with crossing of the midline by axons of the CC and HC in both normal hybrids and RI embryos. Surprisingly, no other midplane measurements showed a relationship with development of the CC and HC, although the entire midplane region was slightly delayed compared to hybrid embryos. In a study of midline defects in human infants, Martínez-Frías (1995) reported that fusion (closure) defects were the most frequently observed midline anomaly. Opitz and Gilbert (1982) have proposed that the midline is a primary developmental field and that the effectiveness of developmental buffering systems in this field is compromised, resulting in a high proportion of midline developmental anomalies. Agenesis of the corpus callosum may be an indirect consequence of the vulnerability of the midline region to developmental defects in both mouse and human.

The relationship between CC formation and development of the interhemispheric fissure is supported by findings from humans with holoprosencephaly, a condition in which the interhemispheric fissure does not form and the hemispheres remain undivided. Agenesis of the corpus callosum is associated with holoprosencephaly, suggesting that presence of a normal hemispheric fissure is required for callosal formation (Rubenstein et al., 1996; Oba and Barkovitch, 1995). It is also interesting that in marsupials, which lack a CC, the hemispheres also do not

fuse in the dorsal region of midline and the major pathway between the two hemispheres, the hippocampal commissure, is found at the bottom of the interhemispheric fissure (Heath and Jones, 1971; Silver et al., 1982).

Examination of a developmental series of hybrid embryos in the coronal plane also allowed for observation of the spatial and temporal positioning of cells of the glial sling. The glial sling has previously been identified in the cat (Silver et al., 1985) and rat (Katz et al., 1983), but not in rhesus monkeys (LaMantia and Rakic, 1990). However, Valentino and Jones (1982) were unable to identify organized glial cells at midplane associated with CC axon migration in the rat and suggested instead that the first callosal axons to cross midplane may do so over the dorsal surface of the hippocampal commissure. In this study, a row of sling cells was evident emanating from either lateral ventricle toward midplane at about .54 g body weight. However, it was clear that in normal B6D2F_2 hybrid embryos, the cell bodies of the sling cells did not form a bridge across midplane until well after a substantial number of callosal axons had crossed. This observation is consistent with a barrier function for the glial sling cells (see also Livy and Wahlsten, 1997), rather than a role in callosal axon guidance across the midplane (Silver et al., 1982). The glial sling cells may prevent callosal axons from entering the septal region and guide them in making a sharp turn towards the midplane crossing point, in preparation for crossing. The glial sling cells may move to midplane later in development to separate the corpus callosum from the hippocampal commissure, as glial cells separate CNS midplane commissures in invertebrates (Jacobs and Goodman, 1988; Klambt et al., 1991).

It is proposed instead that cells at the bottom of the rapidly fusing hemispheric fissure are associated with a molecular signal important for axon guidance across the midplane. CC and HC axons crossing midplane are consistently found in close apposition to the bottom of the fissure, new axons to cross midplane do so between the dorsal surface of the existing commissure and the bottom of the fissure (Silver et al., 1982), and in the few cases in which the first HC axons to cross have been observed, the leading edge of the axon bundle has been found right at the bottom of the fissure (Experiment 2; Livy and Wahlsten, 1997).

Axon guidance and growth are generally thought to be directed by molecular cues in the environment (for reviews see Dodd and Jessell, 1988; Goodman, 1996; Nieto, 1996). Molecules controlling axon guidance and growth can be either substrate-bound molecules that provide guidance through physical contact (Dodd and Jessell, 1988; Hynes and Lander, 1992) or chemotropic factors that establish diffusible gradients (Tessier-Lavigne and Placzek, 1991; Tessier-Lavigne, 1991; Tessier-Lavigne, 1994). Contact mediated guidance may be either permissive (Rauvala and Pihlaskari, 1987; Mendez-Otero et al., 1988) or repulsive (Raper and Kapfhammer, 1990; Stahl et al., 1990). Similarily, both attractive (Placzek et al., 1990; Zheng et al., 1994) and repulsive (Fitzgerald et al., 1993; Pini, 1993) chemotropism have been observed. A single molecule may in fact have both attractive and repulsive roles, as has been observed for netrin-1, which is released by the floor plate (Serafini et al., 1994; Kennedy et al., 1994; Shirasaki et al., 1995; Colamarino and Tessier-Lavigne, 1995). The distinct axonal trajectories of individual

neurons are most likely controlled by the coordinated actions of systems of guidance cues.

It is possible that cells at the bottom of the longitudinal cerebral fissure are associated with molecular signals that attract corpus callosum and hippocampal commissure axons towards and then away from midplane into the contralateral hemisphere. Hippocampal commissure outgrowth toward midline suggests chemoattractive factors in this region. Netrin-1 provides a good candidate molecule for this function, as netrin-1 deficient mice exhibit defects in the corpus callosum, hippocampal commissure, and anterior commissure and netrin-1 is distributed along the paths of these axons and at the point where they cross midplane (Serafini et al., 1996). Callosal axons may also be repelled from midplane as they travel parallel to the interhemispheric fissure, and midline cells at the bottom of the fissure may be associated with a permissive molecular signal that represses this repellant, allowing the axons to travel towards and across midplane. Similar repression functions of midplane structures have been proposed for commissural axon tracts of the spinal cord and optic chiasm (Snow et al., 1990; Snow et al., 1991).

Results obtained from morphological examination of the RI embryos can be used to further elucidate the threshold model for development of the corpus callosum and hippocampal commissure. It is proposed that the primary genetic defect in acallosal animals of these strains is closure of the interhemispheric fissure; axons of the corpus callosum and hippocampal commissure can not cross midplane until the bottom of the fissure rises to a critical point. The region at the bottom of the fissure

may contain molecular signals stimulating axon guidance across the midplane using permissive and/or attractive mechanisms. The relative timing of shortening of the fissure, HC axon arrival at midplane, and CC axon arrival at midplane creates thresholds for development of the cerebral commissures. If shortening of the interhemispheric fissure is severely delayed, the fissure floor will not arrive at the level of the HC axons until after most of them are available to cross, and reduced adult HC will result. If movement of the fissure floor is only slightly delayed, it will arrive in time for axons of the HC to cross midplane, but some or all of the CC axons will not cross because of the delay in HC formation.

SUMMARY AND CONCLUSIONS

Agenesis of the corpus callosum was used as a model system to examine axon growth and guidance across the midplane and the plasticity evident in development of the cerebral commissures. Several discoveries regarding axon guidance across the cerebral midplane made in the course of the present research suggest a threshold model for development of the corpus callosum and hippocampal commissure.

In Experiment 1, large samples of inbred mouse strains and classical crosses with varying defects in the corpus callosum were examined and substantial plasticity in development of the commissures was observed. Recovery from retarded development of the commissures starts at about embryonic day 18 and is almost complete by the time of birth (approximately E20). However, there are prenatal thresholds of abnormality beyond which recovery does not occur. An embryonic CCHC index of .15 is the threshold for normal development of the corpus callosum and an index of 0 is the threshold for normal development of the hippocampal commissure. Therefore, if no axons of the hippocampal commissure have crossed midplane by about .9 g body weight, the HC will never attain a normal adult size and the corpus callosum will be completely absent. If the area of the HC has not grown to about .005 mm^2 by about .9 g body weight, then the hippocampal commissure may appear normal but the corpus callosum will be abnormally small. The thresholds proposed for normal development of the CC and HC in experiment 1 were confirmed in the RI sample in experiment 2. These thresholds correctly predicted that

occasionally a normal RI strain embryo is found with a CC defect and an acallosal RI strain embryo has a normal HC and a small CC (Wahlsten et al., 1997). The abrupt thresholds for normal development of the corpus callosum and hippocampal commissure mean that small variations in the embryo are magnified into macroscopic differences in the anatomy of the adult brain.

The first axons of the hippocampal commissure to cross midline do so over the dorsal medial septal region (Livy and Wahlsten, 1997) and it has been suggested that the septal notch defect plays a role in retardation of the cerebral commissures. Although Wahlsten and Bulman-Fleming (1994) found a medial septal defect in BALB/cWah1 mice that also exhibit agenesis of the corpus callosum, results from this study provide only weak support for a relationship between these two midline defects. Development of the CC and HC was retarded in all embryos and neonates that exhibited the notched defect, but some axons were able to cross midplane in these brains. The delay in prenatal commissural formation may be associated with retarded development of the dorsal medial septum, and/or growth of the septal region may be important for recovery from retarded growth of the commissures. However, development of the medial septal region was equally retarded in acallosal and normal strains of recombinant inbred embryos, but the sample size and age range of RI embryos examined in the sagittal plane may have been inadequate to detect a difference between these groups. Growth of the dorsal medial septum occurred by an abrupt transition in form from a notched shape to a fully rounded one, and this transition corresponded with fusion between the dorsal region of the septum and a

mass of cells lying caudal to this region in the midsagittal plane. Results of these experiments also provided support for a single-gene model for delayed growth of the dorsal medial septal region, but these results can also be explained by a polygenic threshold model, and proof of a single gene effect for this defect was not provided.

Results from Experiment 2 indicated that corpus callosum and hippocampal axon growth to midplane is normal in acallosal recombinant inbred embryos, as was expected from previous research on acallosal mouse strains (Ozaki and Wahlsten, 1993). These results further confirm that agenesis of the corpus callosum and reduced hippocampal commissure in genetically acallosal mouse strains result from a problem in the substrates for axon guidance across midplane, not a defect of the callosal cells or axons themselves. Differential labelling with lipophilic dyes confirmed a relationship between embryonic development of the hippocampal commissure and adult anatomy of the corpus callosum that had been suggested in previous research (Wahlsten, 1987; Livy and Wahlsten, 1997). Large differences were observed for HC formation, and the degree of retardation in prenatal formation of the HC correlated with the pattern of callosal defects observed in adults of these strains. Preliminary evidence was provided for a novel pathway for some of the hippocampal commissure axons that can not cross midplane but instead course lateral to the Probst bundles to the edge of the interhemispheric fissure dorsal to the bundles.

A severe defect in fusion of the interhemispheric fissure was identified that strongly correlated with the adult pattern of callosal morphology. A defect in interhemispheric fissure development had been proposed by several researchers (Silver

et al., 1982; Wahlsten, 1987; Silver et al., 1993; Wahlsten and Bulman-Fleming, 1994), but this is the first study to quantify development of this region and correlate it with the development of the corpus callosum and hippocampal commissure. It is proposed that the primary genetic defect in acallosal mouse strains with agenesis of the corpus callosum is delayed fusion of the interhemispheric fissure. The floor of the hemispheric fissure must rise to a critical level near the cells of the indusium griseum before HC and CC axons may cross midplane. The region at the bottom of the fissure may contain molecular signals stimulating axon guidance across the midplane using permissive and/or attractive mechanisms.

These results may be integrated in a threshold model for development of the cerebral commissures in which agenesis of the corpus callosum and reduced hippocampal commissure result from an interaction between genetic influences, relative structural growth, and chance. The relative timing of shortening of the interhemispheric fissure, HC axon arrival at midplane, and CC axon arrival at midplane creates the thresholds for development of the cerebral commissures. Genetic differences between inbred strains determine the degree of interhemispheric fissure development, such that the time during which the axons may successfully traverse midline is altered. In addition, the inherently random nature of development means that individual differences exist in axon growth and development of the interhemispheric fissure, even in embryos from inbred strains raised in a controlled environment. The general scheme of this threshold model is presented in Figure 31, where the critical events are presented relative to each other in time and the

Figure 31: Developmental threshold model for agenesis of the corpus callosum in the mouse. Critical events identified in development of the corpus callosum and hippocampal commissure are placed on a developmental time scale in relation to each other. Shaded regions correspond to thresholds for development of the CC and HC and these thresholds are broad, rather than sharply defined, to represent the inherent variability in developmental processes.

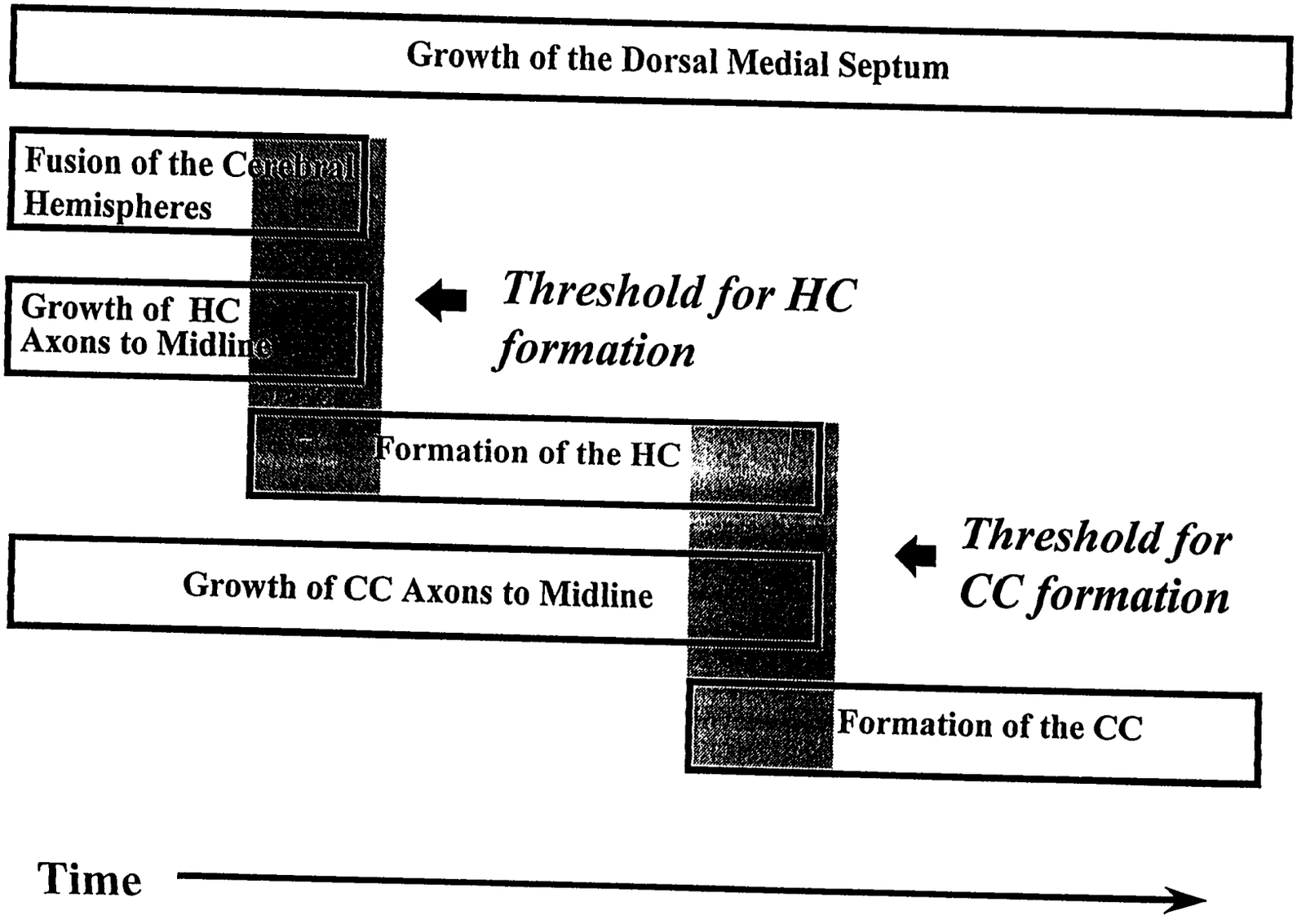
Growth of the Dorsal Medial Septum
Fusion of the Cerebral Hemispheres
Growth of HC Axons to Midline
Threshold for HC formation
Formation of the HC
Growth of CC Axons to Midline
Threshold for CC formation
Formation of the CC
Time

developmental thresholds are broad, representing the variability in timing of these events due to the inherently random nature of development. Future research may refine the timing of the events presented in this model. For example, although the "windows" for CC and HC development are the same size in this model, a general impression is that the "window" for HC formation may be much wider than for the CC.

The unexpectedly high incidence of commissural defects in 129xCF_2 animals found in neonates (Experiment 1) and adults (Wahlsten et al., 1997) is not consistent with the two-gene model with developmental thresholds, however. The two-gene model predicts that defects in the hippocampal commissure should be observed in approximately 4% of F_2 animals (Wahlsten et al., 1997). Results from embryos are consistent with this frequency, and the developmental threshold model predicts that about 2% of F_2 animals should exhibit HC defects (Experiment 1). However, the frequency of this severe defect is 12% for neonates (Experiment 1) and 14% for adults (Wahlsten et al., 1997). Hybrid F_2 mice do not seem to recover from prenatal retardation of the commissures as well as inbred strains do, maybe because of reduced phenotypic variance in the F_2 population.

Observations from the two recombinant inbred strains of mice that exhibit continued variability in morphology of the cerebral commissures also can not be accounted for by the two-gene model with developmental thresholds. Progeny of two mice that exhibit complete absence of the corpus callosum and reduced hippocampal commissure may be found with a range of callosal sizes, some even with a corpus

callosum within the normal range of sizes. The model predicts that mice with a deficient HC should never produce offspring with a normal corpus callosum. Results from these strains may be explained, however, if genetic segregation in these strains is incomplete at this point. These strains were last examined at about generation 13 of inbreeding, so continuing genetic segregation is a possibility. Continued monitoring of the phenotypes in these variable strains as inbreeding progresses will provide a test of this hypothesis. As inbreeding progresses, phenotypic variability should become reduced.

Although the developmental threshold model is useful for explaining the etiology of agenesis of the cerebral commissures, the genes and developmental defects that are critical for commissural formation in these mice remain to be identified. Mapping and identification of the genes involved and analysis of the functions of those genes in development of the midline region and callosal formation are required. The recombinant inbred strains derived from 129 and BALB/cWah1 examined in this experiment provide excellent material to map the two genetic loci associated with agenesis of the corpus callosum that differ between these strains (Wahlsten et al., 1997). RI strains 1, 3 and 4 should possess only the BALB-like allele at one locus and the 129 allele at the other locus. The opposite pattern of alleles should be found in the normal strains 21 and 23. Analysis of microsatellite markers that span the mouse genome (Dietrich et al, 1995) in the acallosal and normal recombinant inbred strains should yield evidence of linkage to two or more candidate loci. False positives may be eliminated with data from an F_2 hybrid cross.

Genes having effects on forebrain development and/or axon guidance provide especially good candidates for loci correlated with forebrain commissural defects. Results from genetic knockouts engineered so far provide evidence that *Emx-1*, *Pax-6*, *Sek4*, *Nuk*, and *Macs* might provide excellent candidates for the two genes associated with agenesis of the corpus callosum in BALB and 129 inbred strains of mice. MARCKS deficient mice produced by knock-out of the *Macs* gene exhibit agenesis of the corpus callosum associated with failure of fusion of the hemispheres, although the defects are much more severe than observed in inbred strains of mice (Stumpo et al., 1995; Blackshear et al., 1996). *Emx-1* and *Pax-6* are transcription factors known to be expressed in the forebrain during prenatal development (Qiu et al., 1995; Schmahl et al., 1996). *Sek4* and *Nuk* are members of the Eph-family of receptor protein-tyrosine kinases and these receptors are thought to have cell fusion functions, specifically in promoting fusion of the midline epithelial cells of the palate (Orioli et al., 1996). However, development of the forebrain commissures is a complicated process and it is likely that many other genes and molecules are important for formation of the corpus callosum and hippocampal commissure.

Examination of development of the cerebral commissures in normal and acallosal mouse strains provides evidence that genes are a necessary but not sufficient component of ontogenesis. Positional relationships, threshold values and the inherently random nature of development are all important. From this standpoint, it is not expected that a mutation has a consistent phenotypic outcome. Instead, plasticity in development of the cerebral commissures is to be expected.

REFERENCES

Aboitiz, F., Scheibel, A.B., Fisher, R.S. and Zaidel, E. (1992). Fiber composition of the human corpus callosum. Brain Research, 598, 143-153.

Aggoun, D. and Innocenti, G.M. (1994). Juvenile visual callosal axons in kittens display origin- and fate-related morphology and distribution of arbors. European Journal of Neuroscience, 6, 1846-63.

Barr, M. Jr., Jensh, R. P., and Brent, R.L. (1970). Prenatal growth in the albino rat: Effects of number, intrauterine position and resorptions. American Journal of Anatomy, 128, 413-428.

Berrebi, G.M., Fitch, R.H., Ralphe, D.L., Denenberg, J.O., Friedrich, V.L. and Denenberg, V.H. (1988). Corpus callosum: region-specific effects of sex, early experience and age. Brain Research, 438, 216-224.

Biddle, F.G. (1980). Palate development in the mouse: a quantitative method that permits the estimation of time and rate of palate closure. Teratology, 22, 239-246.

Biddle, F.G. and Eales, B.A. (1996). The degree of lateralization of paw usage (handedness) in the mouse is defined by three major phenotypes. Behavior Genetics, 26, 391-406.

Biddle, F.G., Jung. J.D. and Eales, B.A. (1991). Genetically determined variation in the azygous vein in the mouse. Teratology, 44, 675-683.

Bishop, K.M., Kruyer, A. and Wahlsten, D. (1996). Agenesis of the corpus

callosum and voluntary wheel running in acallosal mice. Psychobiology, 24, 187-194.

Bishop, K. M. and Wahlsten, D. (1997). Sex differences in mouse and rat forebrain commissures: Relationship with brain size. Submitted.

Blackshear, P.J., Lai, W.S., Tuttle, J.S., Stumpo, D.J., Kennington, E., Nairn, A.C. and Sulik, K.K. (1996). Developmental expression of MARCKS and protein kinase C in mice in relation to the exencephaly resulting from MARCKS deficiency. Developmental Brain Research, 96, 62-72.

Bulman-Fleming, B. and Wahlsten, D. (1991). The effects of intrauterine position on the degree of corpus callosum deficiency in two substrains of BALB/c mice. Developmental Psychobiology, 24, 395-412.

Bulman-Fleming, B., Wainwright, P.E., and Collins, R.L. (1992). The effects of early experience on callosal development and functional lateralization in pigmented BALB/cCF mice. Behavioral Brain Research, 50, 31-42.

Carpenter, S. (1994). The pathology of the Andermann syndrome. In Lassonde, M. and Jeeves, M.A. (Eds.), Callosal Agenesis: A Natural Split Brain? New York: Plenum.

Casaubon, L.K., Melanson, M., Lopes-Cendes, I., Marineau, C., Andermann, E., Andermann, F., Weissenbach, J., Prévost, C., Bouchard, J.-P., Mathieu, J. and Rouleau, G.A. (1996). The gene responsible for a severe form of peripheral neuropathy and agenesis of the corpus callosum maps to chromosome 15q. American Journal of Human Genetics, 58, 28-34.

Colamarino, S.A. and Tessier-Lavigne, M. (1995). The axonal chemoattractant netrin-1 is also a chemorepellant for trochlear motor axons. Cell, 81, 621-629.

Coleclough, C. (1983). Chance, necessity, and antibody gene dynamics. Nature, 303, 23-26.

Conti, F. and Manzoni, T. (1994). The neurotransmitters and postsynaptic actions of callosally projecting neurons. Behavioral Brain Research, 64, 37-53.

Cowell, P.E., Allen, L.S., Zalatimo, N.S. and Denenberg, V.H. (1992). A developmental study of sex and age interactions in the human corpus callosum. Developmental Brain Research, 66, 187-192.

Crabbe, J. C, Belknap, J.K. and Buck, K.J. (1994). Genetic animal models of alcohol and drug abuse. Science, 264, 1715-1723.

Dennis, M. (1981). Language in a congenitally acallosal brain. Brain and Language, 12, 33-53.

Dietrich, W.F., Copeland, N.G., Gilbert, D.J., Miller, J.C., Jenkins, N.A. and Lander, E.S. (1995). Mapping the mouse genome: Current status and future prospects. Proceedings of the National Academy of Sciences U.S.A., 92, 10849-10853.

Dobyns, W.B. (1996). Absence makes the search grow longer. American Journal of Human Genetics, 58, 7-16.

Dodd, J. and Jessell, T.M. (1988). Axon guidance and the patterning of neuronal projections in vertebrates. Science, 242, 692-699.

Elberger, A.J. (1992a). Transitory corpus callosum axons projecting throughout developing rat visual cortex revealed by DiI. Cerebral Cortex, 4, 279-99.

Elberger, A.J. (1992b). The corpus callosum provides a massive transitory input to the visual cortex of cat and rat during early postnatal development. Behavioural Brain Research, 64, 15-33.

Elberger, A.J. (1993). Distribution of transitory corpus callosum axons projecting to developing cat visual cortex revealed by DiI. Journal of Comparative Neurology, 333, 326-342.

Fitch, R.H., Berrebi, A.S., Cowell, P.E., Schrott, L.M. and Denenberg, V.H. (1990). Corpus callosum: effects of neonatal hormones on sexual dimorphism in the rat. Brain Research, 515, 111-116.

Fitzgerald, M., Kwait, G.C., Middleton, J. and Pini, A. (1993). Ventral spinal cord inhibition of neurite outgrowth from embryonic rat dorsal root ganglion. Development, 117, 1377-1384.

Fransen, E., Lemmon, V., Van Camp, G., Vits, L., Coucke, P. and Willems, P.J. (1995). CRASH syndrome: clinical spectrum of corpus callosum hypoplasia, retardation, adducted thumbs, spastic paraparesis and hydrocephalus due to mutations in one single gene, L1. European Journal of Human Genetics, 3, 273-284.

Fraser, F.C. (1980). Evolution of a palatable multifactorial threshold model. American Journal of Human Genetics, 32, 796-813.

Gärtner, K. (1990). A third component causing random variability beside environment and genotype. A reason for the limited success of a 30 year long effort

to standardize laboratory animals? Laboratory Animals, 24, 71-77.

Gärtner, K. and Baunack, E. (1981). Is the similarity of monozygotic twins due to genetic factors alone? Nature, 292, 646-647.

Geoffrey, G. (1994). Other syndromes frequently associated with callosal agenesis. In Lassonde, M. and Jeeves, M.A. (Eds.), Callosal Agenesis: A Natural Split Brain? New York: Plenum.

Glas, P. (1975). Onderzoek naar de vroege ontwikkeling van de commissuren in het mediane gebied van het telencephalon bij de witte muis. Groningen: Drukkerij Van Denderen B.V.

Godement, P., Vanselo, J., Thanos, S. and Bonhoeffer, T. (1987). A study in developing visual systems with a new method of staining neurones and their processes in fixed tissue. Development, 101, 697-713.

Goodman, C.S. (1996). Mechanisms and molecules that control growth cone guidance. Annual Review of Neuroscience, 19, 341-377.

Green, E.L. (1981). Genetics and Probability in Animal Breeding Experiments. New York: Oxford UP.

Grobstein, P. (1988). From the head to the heart: Some thoughts on similarities between brain function and morphogenesis, and on their significance for research methodology and biological theory. Experientia, 44, 960-971.

Gruber, D., Waanders, R., Collins, R.L., Wolfer, D.P. and Lipp, H-P. (1991). Weak or missing paw lateralization in a mouse strain (I/LnJ) with congenital absence of the corpus callosum. Behavioral Brain Research, 46, 9-16.

Gupta, J.K. and Lilford, R.J. (1995). Assessment and management of fetal agenesis of the corpus callosum. Prenatal Diagnosis, 15, 301-312.

Gusella, J., Geller, R., Clarke, B., Weeks, V. and Housman, D. (1976). Commitment to erythroid differentiation by friend erythroleukemia cells: a stochastic analysis. Cell, 9, 221-229.

Hankin, M.H., Schneider, B.F. and Silver, J. (1988). Death of the subcallosal sling is correlated with formation of the cavum septi pellucidi. Journal of Comparative Neurology, 272, 191-202.

Heath, C.J. and Jones, E.G. (1971). Interhemispheric pathways in the absence of the corpus callosum: An experimental study of commissural connections in the marsupial phalanger. Journal of Anatomy, 109, 253-270.

Henkemeyer, M., Orioli, D., Henderson, J.T., Saxton, T.M., Roder, J., Pawson, T. and Klein, R. (1996). Nuk controls pathfinding of commissural axons in the mammalian central nervous system. Cell, 86, 35-46.

Honig, M.G. and Hume, R.I. (1989). DiI and DiO: versatile fluorescent dyes for neuronal labelling and pathway tracing. Trends in Neuroscience, 12, 337-341.

Hynes, R.O. and Lander, A.I. (1992). Contact and adhesive specificities in the associations, migrations, and targeting of cells and axons. Cell, 68, 303-322.

Innocenti, G.M., Fiore, L. and Caminiti, R. (1977). Exuberant projections into the corpus callosum from the visual cortex of newborn cats. Neuroscience Letters, 4, 237-242.

Ivy, G.O. and Killacky, H.P. (1982). Ontogenic changes in the projections of

neocortical neurons. Journal of Neuroscience, 2, 735-743.

Jacobs, J.R. and Goodman, C.S. (1988). Embryonic development of axon pathways in the *Drosophila* CNS. I. A glial scaffold appears before the first growth cones. Journal of Neuroscience, 9, 2402-2411.

Jeeves, M.A. (1986). Callosal agenesis: neuronal and developmental adaptation. In Lepore, F., Ptito, M. and Jasper, H. (Eds.), Two Hemispheres - One Brain. New York: Liss.

Jeret, J.S., Serur, D., Wisniewski, K.E. and Lubin, R.A. (1987). Clinicopathological findings associated with agenesis of the corpus callosum. Brain and Development, 9, 255-264.

Juriloff, D.M. (1995). Genetic analysis of the construction of the AEJ.A congenic strain indicates that nonsyndromic CL(P) in the mouse is caused by two loci with epistatic interaction. Journal of Craniofacial Genetics and Developmental Biology, 15, 1-12.

Katz, M.J., Lasek, R.J. and Silver, J. (1983). Ontophyletics of the nervous system: Development of the corpus callosum and evolution of axon tracts. Proceedings of the National Academy of Sciences U.S.A., 80, 5936-5940.

Kaufman, M.H. (1992). The Atlas of Mouse Development. Academic Press: San Diego, CA.

Keeler, C.E. (1933). Absence of the corpus callosum as a Mendelizing character in the house mouse. Proceedings of the National Academy of Sciences U.S.A., 19, 609-611.

Kennedy, T.E., Serafini, T., de la Torre, J.R. and Tessier-Lavigne, M. (1994). Netrins are diffusible chemotropic factors for commissural axons in the embryonic spinal cord. Cell, 78, 425-435.

King, L.S. (1936). Hereditary defects of the corpus callosum of the mouse *Mus musculus*. Journal of Comparative Neurology, 64, 337-363.

Klambt, C., Jacobs, J.R. and Goodman, C.S. (1991). The midline of the *Drosophila* nervous system: A model for the genetic analysis of cell fate, cell migration, and growth cone guidance. Cell, 64, 801-815.

Koester, S.E. and O'Leary, D.D.M. (1992). Functional classes of cortical projection neurons develop dendritic distinctions by class specific sculpting of an early common pattern. Journal of Neuroscience, 12, 1382-1393.

Koester, S.E. and O'Leary, D.D.M. (1994). Axons of early generated neurons in cingulate cortex pioneer the corpus callosum. Journal of Neuroscience, 14, 6608-6620.

Knudson, A.G. Jr. (1971). Mutation and cancer: statistical study of retinoblastoma. Proceedings of the National Academy of Sciences U.S.A., 68, 820-823.

Kurnit, D.M., Layton, W.M. and Matthysse, S. (1987). Genetics, chance, and morphogenesis. American Journal of Human Genetics, 41, 979-995.

Kurnit, D.M., Matthysse, S, Papayannopoulou, T. and Stamatoyannopoulos, G. (1985). Stochastic branching model for hemopoietic progenitor cell differentiation. Journal of Cellular Physiology, 123, 55-63.

LaMantia, A.-S. and Rakic, P. (1990a). Cytological and quantitative characteristics of four cerebral commissures in the rhesus monkey. Journal of Comparative Neurology, 291, 520-537.

LaMantia, A.-S. and Rakic, P. (1990b). Axon overproduction and elimination in the corpus callosum of the developing rhesus monkey. Journal of Neuroscience, 10, 2156-75.

Lassonde, M., Bryden, M.P. and Demers, P. (1990). The corpus callosum and cerebral speech lateralization. Brain and Language, 38, 195-206.

Lassonde, M. and Jeeves, M.A., Eds. (1994). Callosal Agenesis. New York: Plenum.

Lefkowitz, M., Durand, D., Smith, G. and Silver, J. (1991). Electrical properties of axons within Probst bundles of acallosal mice and callosa that have reformed upon glial-coated polymer implants. Experimental Neurology, 113, 306-314.

Lent, R. and Schmidt, S.L. (1993). The ontogenesis of the forebrain commissures and the determination of brain asymmetries. Progress in Neurobiology, 40, 249-76.

Lipp H.-P., Bechel, C., Wolfer, D.E. and Scheffrahn, H. (1991). Variations in size of corpus callosum, eye color and hippocampal mossy fibres: their relations to swimming navigation learning of mice. Third IBRO World Congress of Neuroscience Abstracts, 169.

Lipp, H.-P and Waanders, R. (1990). The acallosal mouse strain I/Ln:

behavioral comparisons and effects of cross-breeding. Behavior Genetics, 20, 728-729.

Lipp, H.-P. and Wahlsten, D. (1992). Absence of the corpus callosum. In P. Driscoll (Ed.), Genetically Defined Animal Models of Neurobehavioral Dysfunction. Boston: Birkhauser.

Livy, D.J., Schalomon, P. M., Roy, M., Zacharias, M.C., Pimenta, J., Lent, R. and Wahlsten, D. (1997). Increased axon number in the anterior commissure of mice lacking a corpus callosum. Experimental Neurology, 146, 491-501.

Livy, D.J. and Wahlsten D. (1991). Tests of genetic allelism between four inbred mouse strains with absent corpus callosum. Journal of Heredity, 82, 459-464.

Livy, D.J. and Wahlsten, D. (1997). Retarded formation of the hippocampal commissure in embryos from mouse strains lacking a corpus callosum. Hippocampus, 7, 2-14.

Lomber, S.G., Payne, B.R. and Rosenquist, A.C. (1994). The spatial relationship between the cerebral cortex and fiber trajectory through the corpus callosum. Behavioral Brain Research, 64, 25-35.

Lyon, G., Arita, F., Le Galloudec, E., Vallée, L., Misson, J.-P. and Ferriére, G. (1990). A disorder of axonal development, necrotizing myopathy, cardiomyopathy, and cataracts: a new familial disease. Annals of Neurology, 27, 193-199.

McClearn, G.E., Wilson, J.R. and Meredith, W. (1970). The use of isogenic and heterogenic mouse stocks in behavioral research. In G. Lindzey and D.D.

Thiessen (Eds.), Contributions to Behavior Genetic Analysis: The Mouse as a Prototype. New York: Appleton.

McLaren, A. and Michie, D. (1960). Control of pre-natal growth in mammals. Nature, 187, 363-365.

Marascuilo, L.A. and Serlin, R.C. (1988). Statistical methods for the Social and Behavioral Sciences. Freeman: New York.

Martínez-Fríaz, M-L. (1995). Primary midline developmental field. I. Clinical and epidemiological characteristics. American Journal of Medical Genetics, 56, 374-381.

Mendez-Otero, R., Schlosshauer, B., Barnstable, C.J. and Constantine-Paton, M. (1988). A developmentally regulated antigen associated with neural cell and process migration. Journal of Neuroscience, 8, 564-579.

Milleret, C. and Buser, P. (1993). Reorganization processes in the visual cortex also depend on visual experience in the adult cat. Progress in Brain Research, 95, 257-69.

Morin, C.L., Dolina, S., Robertson, R.T. and Ribak, C.E. (1994). An inbred epilepsy-prone substrain of BALB/c mice shows absence of the corpus callosum, an abnormal projection to the basal forebrain, and bilateral projections to the thalamus. Cerebral Cortex, 4, 119-128.

Nadeau, J.H., Davisson, M.T., Doolittle, D.P., Grant, P., Hillyard, A.L., Kosowsky, M.R. and Roderick, T.H. (1992). Comparative map for mice and humans. Mammalian Genome, 3, 480-356.

Neumann, P.E. and Collins, R.L. (1991). Genetic dissection of susceptibility to audiogenic seizures in inbred mice. Proceedings of the National Academy of Sciences U.S.A., 88, 5408-5412.

Newman, T.B. (1985). Etiology of ventricular septal defects: an epidemiological approach. Pediatrics, 76, 741-749.

Nieto, M.A. (1996). Molecular biology of axon guidance. Neuron, 17, 1039-1048.

Oba, H. and Barkovich, J. (1995). Holoprosencephaly: An analysis of callosal formation and its relation to development of the interhemispheric fissure. American Journal of Neuroradiology, 16, 453-460.

Olavarria, J., Serra-Oller, M.M., Yee, K.T. and Van Sluyters, R.C. (1988). Topography of interhemispheric connections in neocortex of mice with congenital deficiencies of the callosal commissure. Journal of Comparative Neurology, 270, 575-590.

O'Leary, D.D.M., Stanfield, B. and Cowan, W.M. (1981). Evidence that the early postnatal restriction of the cells of origin of the corpus callosal projections is due to the elimination of axon collaterals rather than to the death of neurons. Developmental Brain Research, 1, 607-617.

Opitz, J.M. and Gilbert, E.F. (1982). Editorial comment: CNS anomalies and the midline as a "developmental field". American Journal of Medical Genetics, 12, 443-455.

Orioli, D., Henkenmeyer, M., Lemke, G., Klein, R. and Pawson, T. (1996).

Sek4 and Nuk receptors cooperate in guidance of commissural axons and in pathway formation. EMBO Journal, 15, 6035-6049.

Ozaki, H.S., Murakami, T.H., Toyoshima, T. and Shimada, M. (1984). Agenesis of the corpus callosum in ddN strain mouse associated with unusual facial appearance (flat face). Neuroscience Research, 1, 81-87.

Ozaki, H.S., Murakami, T.H., Toyoshima, T. and Shimada, M. (1987). The fibers which leave the probst's longitudinal bundle seen in the brain of an acallosal mouse: a study with the horseradish peroxidase technique. Brain Research, 400, 239-246.

Ozaki, H.S. and Wahlsten, D. (1992). Prenatal formation of the normal mouse corpus callosum: a quantitative study with carbocyanine dyes. Journal of Comparative Neurology, 323, 81-90.

Ozaki, H.S. and Wahlsten, D. (1993). Cortical axon trajectories and growth cone morphologies in fetuses of acallosal mouse strains. Journal of Comparative Neurology, 336, 595-604.

Payloor, S.T. and Seyfried, T.N. (1984). Genetic study of cationic ATPase activities and audiogenic seizure susceptibility in recombinant inbred and congenic strains of mice. Journal of Neurochemistry, 42, 529-533.

Pini, A. (1993). Chemorepulsion of axons in the developing mammalian central nervous system. Science, 261, 95-98.

Placzek, M., Tessier-Lavigne, M., Jessell, T. and Dodd, J. (1990). Orientation of commissural axons *in vitro* in response to a floor plate-derived

chemoattractant. Development, 110, 19-30.

Pujol, J., Vendrell, P., Junque, C., Marti-Vilalta, J.L. and Capdevilla, A. (1993). When does human brain development end? Evidence of corpus callosum growth up to adulthood. Annals of Neurology, 34, 71-75.

Qiu. M.-S., Anderson, S., Chen, S.D., Meneses, J., Hevner, R., Kuwana, E., Pedersen, R.A. and Rubenstein, J.L.R. (1996). Mutation of the *Emx-1* homeobox gene disrupts the corpus callosum. Developmental Biology, 178, 174-178..

Raper, J.A. and Kapfhammer, (1990). The enrichment of a neuronal growth cone collapsing activity from embryonic chick brain. Neuron, 4, 21-29.

Rauvala, H. and Pihlaskari, R. (1987). Isolation and some characteristics of an adhesive factor of brain that enhances neurite outgrowth in central neurons. Journal of Biological Chemistry, 262, 16625-16635.

Rubinstein, D., Cajade-Law, A.G., Youngman, V., Hise, J.M. and Baganz, M. (1996). The development of the corpus callosum in semilobar and lobar holoprosencephaly. Pediatric Radiology, 26, 839-844.

Sauerwein, H.C. and Lassonde, M. (1994). Cognitive and sensori-motor functioning in the absence of the corpus callosum: neuropsychological studies in callosal agenesis and callosotomized patients. Behavioral Brain Research, 64, 229-240.

Schalomon, P.M. and Wahlsten, D. (1997). Manual motor coordination in congenitally acallosal and split brain mice, submitted.

Schambra, U.B., Lauder, J.M. and Silver, J. (1992). Atlas of the Prenatal

Mouse Brain. Academic Press: San Diego, CA.

Schmahl. W., Knoedlseder, M., Favor, J. and Davidson, D. (1993). Defects of neuronal migration and the pathogenesis of cortical malformations are associated with Small eye (Sey) in the mouse, a point mutation at the Pax-6-locus. Acta Neuropathologia, 86, 126-135.

Schmidt, S.L. and Caparelli-Dáquer., E.M. (1989). The effects of total and partial callosal agenesis on the development of morphological brain asymmetries in the BALB/cCF mouse. Experimental Neurology, 104, 172-180.

Schmidt, S.L., Manhães, A.C. and de Moráes, V.Z. (1991). The effects of total and partial callosal agenesis on the development of paw preference performance in the BALB/cCF mouse. Brain Research, 545, 123-130.

Senft, S.L. (1990). Prenatal central vibrissal pathways labelled with DiI and DiA. Society for Neurosciences Abstracts, 16, 1215.

Serafini, T., Colamarino, S.A., Leonardo, E.D., Wang, H., Beddington, R., Skarnes, W.C. and Tessier-Lavigne, M. (1996). Netrin-1 is required for commissural axon guidance in the developing vertebrate nervous system. Cell, 87, 1001-1014.

Serafini, T., Kennedy, T.E., Galko, M.J., Mirzayan, C., Jessell, T. and Tessier-Lavigne, M. (1994). The netrins define a family of axon outgrowth-promoting proteins homologous to C. elegans UNC-6. Cell, 78, 409-425.

Shirasaki, R., Tamada, A., Katsumata, R. and Murakami, F. (1995). Guidance of cerebellofugal axons in the rat embryo: Directed growth toward the floor

plate and subsequent elongation along the longitudinal axis. Neuron, 14, 961-972.

Sidman, R.L. and Rakic, P. (1982). Development of the human central nervous system. In Haymaker, W. and Adams, R.D. (Eds.), Histology and Histopathology of the Central Nervous System. Springfield, Illinois: Charles C. Thomas.

Silver, J., Edwards, M.A. and Levitt, P. (1993). Immunocytochemical demonstration of early appearing astroglial structures that form boundaries and pathways along axon tracts in the fetal brain. Journal of Comparative Neurology, 328, 415-436.

Silver, J. Lorenz, S.E., Wahlsten, D. and Coughlin, J. (1982). Axonal guidance during development of the great cerebral commissures: descriptive and experimental studies, in vivo, on the role of preformed glial pathways. Journal of Comparative Neurology, 210, 10-29.

Smith, J.A. and Martin, L. (1972). Do cells cycle? Proceedings of the National Academy of Sciences U.S.A., 70, 1263-1267.

Smith, J.R. and Whitney, R.G. (1979). Intraclonal variation in proliferative potential of human diploid fibroblasts: stochastic mechanism for cellular aging. Science, 207, 82-84.

Snow, D.M., Steinler, D. and Silver, J. (1990). Molecular and cellular characterization of the glial roof plate of the spinal cord and optic tectum: A possible role for proteoglycan in development of an axon barrier. Developmental Biology, 138, 359-376.

Snow, D.M., Watanabe, M., Letourneau, P.C. and Silver, J. (1991). A chondroitin sulfate proteoglycan may influence the direction of ganglion cell outgrowth. Development, 113, 1473-1485.

Sperry, R.W. (1982). Some effects of disconnecting the cerebral hemispheres. Science, 217, 1223-1226.

Stahl, B., Mueller, B., von Boxberg, Y., Cox, E.C. and Bonhoeffer, T. (1990). Biochemical characterization of a putative axonal guidance molecule of the chick visual system. Neuron, 5, 733-743.

Stumpo, D.J., Bock, C.B., Tuttle, J.S. and Blackshear, P.J. (1995). MARCKS deficiency in mice leads to abnormal brain development and perinatal death. Proceedings of the National Academy of Sciences USA, 92, 944-948.

Sturrock, R.R. (1980). Myelination of the mouse corpus callosum. Neuropathology and Applied Neurobiology, 6, 415-420.

Swanson, L.W. and Cowan, W.M. (1979). The connections of the septal region in the rat. Journal of Comparative Neurology, 186, 621-656.

Temple, C.M., Jeeves, M.A. and Villarroya, O. (1989). Ten pen men: rhyming skills in two children with callosal agenesis. Brain and Language, 37, 548-564.

Tessier-Lavigne M. (1991). Axon guidance by molecular gradients. Current Opinion in Neurobiology, 2, 60-65.

Tessier-Lavigne M. (1994). Axon guidance by diffusible repellents and attractants. Current Opinion in Genetics and Development, 4, 596-601.

Tessier-Lavigne M. and Placzek, M. (1991). Target attraction: are developing axons guided by chemotropism? Trends in Neuroscience, 7, 303-310.

Tomasch, J. (1954). Size, distribution and number of fibres in the human corpus callosum. Anatomical Record, 119, 119-135.

Usuki, T., Iwahashi, K., Tanaka, K., Murakami, T., Kugoh, T. and Hosokawa, K. (1992). Bilateral interhemispheric synchrony and amygdaloid kindling in congenitally acallosal and corpus callosum bisected mice. Japanese Journal of Psychiatry and Neurology, 46, 498-500.

Valentino, K.L. and Jones, E.G. (1982). The early formation of the corpus callosum: A light and electron microscopic study in foetal and neonatal rats. Journal of Neurocytology, 11, 583-609.

Vekemans, M.J.J. and Biddle, F.G. (1984). Genetics of palate development. Current Topics in Developmental Biology, 19, 165-192.

Wahlsten, D. (1974). Heritable aspects of anomalous myelinated fibre tracts in the forebrain of the laboratory mouse. Brain Research, 1, 461-473.

Wahlsten, D. (1981). Prenatal schedule of appearance of mouse brain commissures. Developmental Brain Research, 1, 461-473.

Wahlsten, D. (1982). Mode of inheritance of deficient corpus callosum in mice. Journal of Heredity, 73, 281-285.

Wahlsten, D. (1984). Growth of the mouse corpus callosum. Developmental Brain Research, 15, 59-67.

Wahlsten, D. (1987). Defects of the fetal forebrain in mice with hereditary

agenesis of the corpus callosum. Journal of Comparative Neurology, 262, 227-241.

Wahlsten, D. (1989). Deficiency of the corpus callosum: incomplete penetrance and substrain differentiation in BALB/c mice. Journal of Neurogenetics, 5, 61-76.

Wahlsten, D. and Bulman-Fleming, B. (1994). Retarded growth of the medial septum: a major gene effect in acallosal mice. Developmental Brain Research, 77, 203-214.

Wahlsten, D. and Jones, G.B. (1983). Structural changes in brains of mice with agenesis of the corpus callosum. Society for Neuroscience Abstracts, 9, 494.

Wahlsten, D. and Ozaki, H.S. (1994). Defects of the fetal forebrain in acallosal mice. In Lassonde, M. and Jeeves, M.A. (Eds.), Callosal Agenesis: A Natural Split Brain? New York: Plenum.

Wahlsten, D. and Schalomon, P.M. (1994). A new hybrid mouse model for agenesis of the corpus callosum. Behavioral Brain Research, 64, 111-117.

Wahlsten, D. and Smith, G. (1989). Inheritance of retarded forebrain commissure development in fetal mice: results from classical crosses and recombinant inbred strains. Journal of Heredity, 80, 11-16.

Wahlsten, D. and Sparks, V. (1996). New recombinant inbred strains expressing 100% total absence of the corpus callosum. Society for Neuroscience Abstracts, 21, 796.

Wahlsten, D., Sparks, V. and Bishop, K.M. (1997). Rapid emergence of absent corpus callosum in recombinant inbred lines derived from the 129 and BALB/c

mouse strains: support for a two-locus model. Submitted.

Wahlsten, D. and Wainwright, P. (1977). Application of a morphological time scale to hereditary differences in prenatal mouse development. Journal of Embryology and Experimental Morphology, 42, 79-92.

Wainwright, P. and Deeks, S. (1984). A comparison of corpus callosum development in BALB/cCF and C57BL/6J inbred mouse strains. Growth, 48, 192-197.

Wang, K-Y., Juriloff, D.M. and Diewert, V.M. (1995). Deficient and delayed primary palatal fusion and mesenchymal bridge formation in cleft lip-liable strains of mice. Journal of Craniofacial Genetics and Developmental Biology, 15, 99-116.

Ward, R. Tremblay, L. and Lassonde, M. (1987). The relationship between callosal variation in mice is genotype-dependent. Brain Research, 424, 84-88.

Wimer, R.E. (1965). Mouse News Letter No. 33, 32.

Wisniewski, K.E. and Jeret, J.S. (1994). Callosal agenesis: review of clinical, pathological and cytogenic features. In Lassonde, M. and Jeeves, M.A. (Eds.), Callosal Agenesis: A Natural Split Brain? New York: Plenum.

Zheng, J.Q., Felder, M., Conner, J.A. and Poo, M.M. (1994). Turning of nerve growth cones induced by neurotransmitters. Nature, 368, 140-144.